

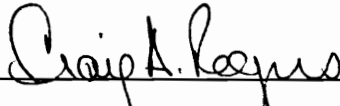
OPTIMIZATION OF PIEZOELECTRIC ACTUATOR SYSTEMS
FOR VIBRATION CONTROL OF FLEXIBLE STRUCTURES


by

Jianhu Jia


Dissertation submitted to the Faculty of the
Virginia Polytechnic Institute and State University
in partial fulfillment of the requirements for the degree of
Doctor of Philosophy
in
Mechanical Engineering


APPROVED:



Dr. C. A. Rogers, Chairman


Dr. C. R. Fuller


Dr. O. H. Griffin


Dr. J. R. Mahan


Dr. H. H. Robertshaw


R. Burdisso

July, 1990

Blacksburg, Virginia

OPTIMIZATION OF PIEZOELECTRIC ACTUATOR SYSTEMS FOR VIBRATION CONTROL OF FLEXIBLE STRUCTURES

by

Jianhu Jia

Committee Chairman: C. A. Rogers

Mechanical Engineering

Abstract

Actuator placement is a major concern in control system designs. Utilizing piezoelectric actuators increases the complexity of actuator designs, because both actuator location and dimensions need to be considered. A comprehensive study was conducted in this dissertation on the optimization of piezoelectric actuator designs for vibration suppression of flexible structures.

The investigation on the optimal piezoelectric actuator designs were grouped into two parts. Part one covered actuator designs when the same number of actuators as the controlled modes are used. Approaches were formed to optimally design piezoelectric actuators which requires least control efforts.

In part two of this dissertation, a method named the *Weighted Pseudoinverse Method* was introduced to deal with the cases in which fewer actuators than the controlled modes are utilized. The weighted pseudoinverse method yields an optimal transformation from modal control forces into the actuator-moments in physical space. Based on the Weighted pseudoinverse method, the piezoelectric actuator designs were optimized to ensure least-control-effort actuator designs.

A simply-supported beam was used as an example to demonstrate the effectiveness of the design methods proposed in this dissertation. However, the design methods are applicable to general cases.

ACKNOWLEDGEMENT

I would like to thank Dr. C. A. Rogers, my advisor, for his guidance and encouragement during this work. His encouragement, enthusiasm, and generosity during my study as a graduate student will have influence throughout my life. I also wish to thank Dr. J. R. Mahan, Dr. H. H. Robertshaw, Dr. C. Fuller, Dr. O. H. Griffin, and Dr. R. Burdisso for serving on my advisory committee.

Dr. R. Burdisso has given me much advice and help during the course of the study. Author would like to express his deep gratitude to Dr. Burdisso.

I would express my deepest appreciation to Mr. Jeff Paine for his excellent work in proof reading the dissertation.

I want to thank my parents and my friends for their all kinds supports. I am very grateful to my wife for her understanding and support.

Author would like to acknowledge the financial support from ONR/DARPA under contract number ONR-00014-88-k-0721.

Contents

1	INTRODUCTION	1
1.1	Control Theory	2
1.2	Actuator Placement	7
1.3	Actuators	9
1.4	Optimization	11
1.5	Scopes of Study	12
2	INDEPENDENT MODAL SPACE CONTROL	13
3	SUBSTRUCTURE MODELLING OF PIEZOELECTRIC ACTUA- TOR SYSTEMS	21
3.1	Piezoelectric Materials	21
3.2	Mechanical Model	26
3.3	Determination of Modal Control Forces	37
4	OPTIMAL PIEZOELECTRIC ACTUATOR LOCATIONS AND DI- MENSIONS	42
4.1	Introduction	43
4.2	Minimization of Control Effort	48
4.2.1	Objective Function	48
4.2.2	Constraints	53

4.2.3	Optimization Method	54
4.2.4	Structure Parameters	55
4.2.5	Actuator Locations and Dimensions	56
4.3	Minimization of Control Effort With Spillover Consideration	65
5	FEWER ACTUATORS THAN CONTROLLED MODES	81
5.1	Introduction	82
5.2	Pseudoinverse Method	86
5.2.1	Introduction to Pseudoinverse Method	86
5.2.2	Essence of Pseudoinverse Method	88
5.2.3	Problems of the Pseudoinverse Solution	91
5.2.4	Analysis of the Problem	99
5.3	Weighted Pseudoinverse Method	100
5.3.1	Essence of Weighted Pseudoinverse Method	102
5.3.2	Determination of Q Matrix	104
5.4	Optimal Actuator Designs	105
5.5	Results and Analysis	107
5.5.1	Actuator Designs	107
5.5.2	Closed-Loop Eigenvalues	113
5.5.3	Modal Control Forces Domains	119
6	CONCLUSIONS AND RECOMMENDATIONS	124
6.1	Conclusions	124
6.2	Discussions and Recommendations	124
	REFERENCES	127
	APPENDIX A: EIGENVALUES OF DAMPED SYSTEMS	133

List of Figures

2.1	Open-loop and closed-loop eigenvalues of a controlled system	19
3.1	Coordinate system of piezoelectric elements	25
3.2	Geometry of the piezoelectric actuators bonded to an elastic substructure	27
3.3	Strain profile by assuming linear Bernoulli-Euler strain distribution .	28
3.4	Shear Stress distribution along the bonding layer	36
3.5	Mechanical model of piezoelectric actuators	39
3.6	Beam structure with piezoelectric actuators	40
4.1	Controlled modal vibrations and optimal modal control forces	45
4.2	Transformation of modal control forces into control moments	47
4.3	Demonstration of modal control force domain and probability distribution	52
4.4	Optimal actuator designs: one actuator controlling one mode	57
4.5	Optimal actuator designs: two actuators controlling two modes	58
4.6	Optimal actuator designs: three actuators controlling three modes . .	59
4.7	Modal forces transformed into actuator moments when different actuator designs are chosen	61
4.8	Comparison between different actuator designs using two actuators to control 1st and 2nd modes	62

4.9	Comparison between volumes of domains of actuator moments for different three actuator designs	64
4.10	Time history of actuator moment when using one actuator to control first mode for different designs	66
4.11	Time history of control moments for optimal and non-optimal designs (when two actuators control first two modes)	67
4.12	Spillover into the third mode when using one actuator, (0.5,0.5), to control the first mode	68
4.13	Spillover into the third mode when using two actuators to control the first two modes; actuator design: (0.25,0.25), (0.75,0.25)	69
4.14	The actuator designs with different weighting factor when one actuator controlling first mode with second and third modes as residual	72
4.15	The actuator designs with different weighting factor when two actuators controlling first two modes with third and forth modes as residual	73
4.16	The actuator designs with different weighting factor when two actuators controlling first two modes with third mode as residual	74
4.17	Residual mode vibrations before and after spillover consideration of one actuator design	76
4.18	Comparison between control moments with and without spillover consideration of one actuator design	77
4.19	Residual mode vibrations with and without spillover considerations for two actuator system	78
4.20	Comparison of control moment between designs with and without spillover consideration for two actuators	79

5.1	Designed modal control force domain and the realized modal control force domain by using pseudoinverse method; one actuator, (0.177,0.177), controlling two modes	92
5.2	Vibrations of the first two modes when one actuator is used to control two modes, based on pseudoinverse method; actuator design (0.25,0.25)	93
5.3	Vibrations of the first three modes when one actuator is used to control three modes based on pseudoinverse method; actuator design (0.177,0.177)	94
5.4	Vibrations of the first three modes when two actuators are used to control three modes based on pseudoinverse method; actuator design (0.233,0.233), (0.767,0.233)	95
5.5	Comparison between the designed closed-loop eigenvalues and the realized closed-loop eigenvalues	98
5.6	Program structure for finding the optimal Q and actuator designs . .	106
5.7	One actuator controlling several modes	108
5.8	Two actuators controlling several modes	110
5.9	Controlled vibrations of weighted pseudoinverse and pseudoinverse methods	111
5.10	Comparison of actuator applied control moments by using weighted pseudoinverse and pseudoinverse methods	112
5.11	Controlled vibrations when weighted pseudoinverse and pseudoinverse methods are used under the same initial conditions	114
5.12	Comparison of actuator applied control moments by using weighted pseudoinverse and pseudoinverse methods	115
5.13	Controlled modal vibrations when weighted pseudoinverse and pseudoinverse are used in two actuator designs	116

- 5.14 Comparison of actuator applied control moments according to weighted
pseudoinverse and pseudoinverse methods 117
- 5.15 Comparison between the designed closed-loop eigenvalues and the closed-
loop eigenvalues by using weighted pseudoinverse 118
- 5.16 Designed modal control force domain and the realized modal control
forces domain by using weighted pseudoinverse 120
- 5.17 The control over each of the modes will spillover into the other modes
when weighted pseudoinverse or pseudoinverse is used 121
- 5.18 The spillover excited vibrations when fewer actuators are used 122

Nomenclature

A_1, A_2, A_3, A_4	constants
a_i	mid point location of i th actuator
b	beam width
B	modal participation matrix
$B_i()$	linear operator
B^+	pseudoinverse
c_i	half length of i th actuator
$\{e\}$	error vector
E_p	Young's modulus of piezoelectric actuators
E_s	Young's modulus of structure material
f_i	modal forces
$\{f\}$	vector of modal control forces
g_i	optimal gain factor
G	shear modulus (in Chapter 2)
G	weighted pseudoinverse (in Chapter 5)
h_i	optimal gain factor
I	unit matrix
$\text{Im}()$	imaginary part of a complex variable
J	quadratic cost function
$L()$	linear operator
$\{M\}$	vector of actual moment
Q	weighting matrix
$\text{Re}()$	real part of a complex variable

t	time
t_b	thichness of bonding layer
t_p	thichness of structure
t_s	thichness of piezoelectric actuator
u	displacement
U	unitary orthogonal matrix
V	unitary orthogonal matrix
ϕ_i	eignfunction
Φ	eignfunction
ω_i	eigenvalue of structure
ϵ	strain
ϵ_p	strain at a point in the piezoelectric actuator
ϵ_s	strain at a point in the structure
ϵ_s^s	strain on the structural surface
γ	shear strain in the bonding layer
τ	shear stress in the bonding layer
Λ	induced strain

Chapter 1

INTRODUCTION

“Human beings, guided and influenced by their natural surroundings, almost instinctively perform all functions in a manner that economizes energy or minimizes discomfort and pain. The motivation is to exploit the available limited resources in a manner that maximizes output or profit”(Haftka and Kamat, 1985). In engineering terms, this process may be described as seeking a design which is “the best feasible design according to a preselected quantitative measure of effectiveness”(Wilde, 1978). In the current engineering design process, decisions are made based on the best choice among the various various design parameters, such as weight, cost, safety, etc. This decision-making process in structural design is called structural optimization. While the development of structural optimization techniques dates back to the eighteenth century, the recent applications to the automotive and aerospace industries demonstrate the modern potential of mathematical optimization methods. Tremendous increases in computational power now available allows the time-consuming optimization algorithms to be more feasible. In the study presented here, the developments in the field of structural optimization are utilized in treating the piezoelectric actuator design of vibration suppression systems, which are often required in large space structures and many other applications.

Large flexible structures are found more and more frequently in the age of space. The advent of a space transportation system makes it possible to design very large satellites and spacecraft which could be carried into space and be deployed, assembled, or constructed there for various purposes. These structures involve a higher mechanical flexibility than those which have been previously considered. Often this is combined with extremely accurate pointing and shape requirements (Balas, 1982). Another characteristic of these structures is that they must be treated as distributed-parameter systems, which adds to the degree of the problem complexity. Due to the precision requirements of these large flexible structures, requirements for suppression of vibrations are often very stringent. In the course of solving vibration suppression problems, the concept of actively controlled large space structures has been developed. In these structures, a variety of sensors and actuators are located and operated through an on-line computer to control the performance and behavior of the system. Along with the space structures application, the concept of actively controlled systems has been used in other applications, such as active structural acoustic transmission loss control (Fuller, Rogers, and Robertshaw, 1989). Many studies have been conducted on various aspects of flexible structural control (Meirovich, *et al.*, 1983 and Balas, 1982). This study will try to explore an optimization solution to the design of these systems. More specifically, based on the control theory and actuator-structure interaction model presented by many researchers, the question of how to place and dimension the actuators is addressed.

1.1 Control Theory

Distributed-parameter-systems usually do not admit closed-form solutions. Therefore, besides control system design and implementation, modeling is an important concern of distributed-parameter-system control problems. Many different approaches

are available for modelling and control system design. One approach has been to first discretize the system geometrically to obtain the eigenfunctions. Then the distributed dependent variable can be expanded into a finite series of eigenfunctions and then control the discretized system. A reduced number of modes are retained for control, with the balance of modes left uncontrolled. The two classes of modes are referred to as controlled and residual modes, respectively. Together, the two classes comprise the so-called modelled modes. In addition, because discretization implies that only a finite number of modes are considered, there exist an infinite number of unmodelled modes. When a distributed-parameter system admits a closed-loop solution, no discretization is necessary. Moreover, because all modes are modelled, there are no unmodelled modes. However, in this case, there will be an infinite number of residual modes. In this study, the closed-loop solutions for the eigenvalues and eigenfunctions are available, and because there are no unmodelled modes, the residual modes will be the only concern with the modelling aspect. The approaches to be discussed here are applicable in more complicated distributed parameter systems which may require discretized models.

Control strategy design follows system modelling. Control theory of distributed-parameter systems is available in many forms, all of which are one form or another of modal control. One method of control is the Independent Modal Space Control(IMSC)(Meirovich, 1977, 1981a,1981b, 1983). As the name indicates, the various modes are controlled independently. Essentially, a set of independent second order systems are controlled in parallel. The modal vibrations are obtained by transforming the vibrations of a distributed-parameter system into the modal space. The modal vibrations are decoupled from each other, as they are orthogonal, which enables control laws to be generated for each of the one degree-of-freedom modal vibrations instead

of the distributed-parameter system.

Because the control design is conducted in the modal space independently for each mode, the control forces obtained in the modal space are abstract forces. The physical control forces can be obtained by an inverse transformation. The result is a set of physical control forces which are always distributed forces. However, when the control system is implemented, the designed control forces are realized in this study by actuating piezoelectric actuators. Because the control forces of actuators are not distributed and the number of the actuators is usually limited, the physical control forces may not be exactly the same as the continuously distributed forces required. Therefore, the control forces applied by the discrete actuators will not only control the "designed" modes but they will also disturb the modes which the control force should not affect. This problem is the so-called spillover problem. Another characteristic of Independent Modal Space Control is that implementing the IMSC requires the number of actuators to be equal to the number of the controlled modes. Without this requirement, when transformed into the modal control forces, the physical control forces cannot produce the optimal modal control forces for the controlled modes. The number of actuators required will pose a limitation if the objective is to reduce number of actuators due to economical considerations, or physical constraints. For example, in the case of piezoelectric actuators, the number of actuators used may be dictated by the structure's design, i.e., none of the actuators should lay on top of each other. This problem has received a great deal of attention recently(Lindberg, 1982; Baz and Poh, 1985).

Lindberg(1982) noted that the principal disadvantage of the Independent Modal Space Control is the requirement that the number of actuators be the same as the

number of modes in the control system model. To counter this disadvantage, Lindberg used the least-squares approach, which is called pseudoinverse to transform the design modal control forces into the physical space. The key issue is that the transformation between the designed optimal modal control forces and the actual control forces cannot be exact without a full rank transformation matrix or modal participation matrix. A full rank modal transformation matrix can only be produced by using the same number of actuators as the controlled modes. By applying the least-squares approach, an actual control force can be synthesized from the optimal modal control forces. The results thus obtained will only be approximations to the optimal ones. It is argued by Lindberg(1982) that by doing this, the fundamentals of the optimal control design were not violated, and the actuator number requirement can be largely relaxed. This argument is true. However, as will be discussed later, the use of the pseudoinverse approach in IMSC does have some problems. As mentioned earlier, this approach is an approximate one. By only using the pseudoinverse method, there is not much control over how close the results are to the corresponding optimal modal control forces. As will be shown later, the control effort obtained by using the pseudoinverse approach could be concentrated on certain modes, leaving other modes only slightly controlled. It is the author's understanding that this phenomenon is dependent on the inherent characteristic of each structure such as its mode shapes.

In another study (Baz and Poh, 1988), a different approach was taken to diminish the actuator number requirement by Independent Modal Space Control. The scenario of the method is that the modal vibrations of the flexible system are, first, ranked according to their modal energy levels. The actuators are secondly dedicated to control the modes which possess the highest modal energy levels. After a certain period of time, the initial controlled modes have been suppressed and their energy levels fall

below the levels of other modes. At this time, the actuators are then directed to control a new set of modes which now have the highest modal energy levels. Baz and Poh have referred to this method as Modified Independent Modal Space Control. The key to this method is the ‘time sharing’ of the actuators between the different modes by switching the actuator control signals according to the modal energy levels. The difference between the Modified Independent Modal Space Control(MIMSC) and IMSC is that MIMSC requires extra control logic to determine which modes to control to compensate for the actuator number requirement. However, we are still faced with the problem that the effective control of the system over vibration modes is structurally dependent. It will require different actuator designs to control different modes efficiently. The MIMSC does not offer the bases for dealing with this problem.

It is one of the purposes of this study to comprehensively study the flexible vibration control system design and develop a design methodology. That is to take various aspects of the system design into consideration, and to find an optimal solution among the conflicting aspects. The advantageous feature of IMSC should be retained, i.e., to do the optimal control design in modal space independently. This feature is vital for solving a large system. Then the cases, in which fewer actuators than the modes controlled are used, are dealt with. The weighted pseudoinverse method is introduced to synthesize the modal control forces into the physical space. The synthesized actual control forces can then be used in an optimization process to determine the best actuator designs. The goal is to achieve a economical system design under all the constraints.

The introduction of the weighting matrix is a new method to converting the optimal modal control forces into actual forces. The IMSC method is used to introduce modal

damping into the system. By doing this, the closed-loop eigenvalues of the system are controlled, i.e., the eigenvalue positions of the system are relocated. The IMSC controller will give a new set of locations of the system's eigenvalues. The locations are optimal according to index built in optimal control. However, when the pseudoinverse method is used, the implemented system will deviate from the design by IMSC. Each closed-loop eigenvalue of the system will have a distance from its counterpart in original IMSC design. The pseudoinverse method does very poorly in controlling the discrepancies between the designed and the realized closed-loop eigenvalues. The pseudoinverse method may give a very large eigenvalue discrepancy to one mode and a small eigenvalue discrepancy to another mode. The large discrepancies will result in poorer controls over the related modes than it has been designed. The weighted pseudoinverse method introduced in this research uses an optimization procedure to search for a set of values for the newly introduced weighting matrix, which will guarantee equal control over all the controlled modes.

1.2 Actuator Placement

Determining the actuator locations and the sizes(i.e, shapes) is a very important issue. The actuator locations can influence the efficiency of the control system. They also determine if the system is stable or not. Some efforts (Kissel and Lin, 1982; Longman and Lingberg, 1981; and Viswanathan, *et al.*, 1979) have attempted to address the problem with very diverse approaches. By eliminating all interaction between the control system and a set of known residual modes which have been truncated from the control system model, it is found that a large number of actuators are constrained to achieve the desired isolation. A small number of actuators are then left available for realizing the control objective(Kissel and Lin, 1982). In treating the general prob-

lems, the concept of controllability has been used. Different kinds of controllability definitions are given by Lindberg (1982). They include controllability according to time limit, or according to fuel limit, etc.. The efforts have been directed toward giving general consideration to the actuator location design. However, the problem becomes very complex with general cases.

In this study, the focus concentrates on a specific problem of finding the locations and sizes of the piezoelectric actuators for control systems applying the Independent Modal Space Control method. As discussed earlier, with the application of IMSC, the control design is decoupled from the implementation. However, converting the modal control forces to physical commands is not as straightforward as it seems to be. The amount of energy used during the control action must be considered in the design of actuator locations. The point force actuator placement problem has been studied by Baruh (1981) and Lindberg (1982). As pointed out by Lindberg(1982), the consequences of improperly chosen actuator locations can be disastrous. It is a simple matter to generate examples which demonstrate that the forces or moments required of a given actuator can grow without bound as the actuator location approaches a position for which the system is uncontrollable. However, thorough studies of piezoelectric actuator designs are few in the present literature. This study will address the search for the systematic method of designing piezoelectric actuator systems which perform most efficiently and effectively.

Hence, there are two primary objectives in optimizing the actuator design: firstly, to find feasible designs which require minimum control efforts with minimum spillover into the uncontrolled modes and secondly, to find the least-control-effort-requirement actuator designs for the systems of using fewer actuators than modes controlled.

Even though the controller design and the implementation are independent of each other in IMSC, this study will show that the optimal actuator design is still case sensitive. In other words, an optimal design for a system under certain vibration conditions may not be an optimum when the conditions change, i.e., initial conditions. Therefore, an optimal design for universal situations may be hard to find. There are two options: either confine the solutions to a narrow band of cases, or reach a compromise which is the optimal design according to the statistical mean of all the possible cases. While methods adopted in this dissertation would be suitable for the first option, the second option is emphasized. The second option yields solutions for more general cases, and is more difficult to solve.

1.3 Actuators

Actuator characterization is not the main concern of this study. Actuator modeling, however, constitutes the foundation of the control system. Thus, it is necessary to choose a well formulated actuator model to conduct the study.

Many studies have been made on point-force type actuators. The actuators used in this study are called induced strain type actuators. Induced strain type actuators are able to generate strains due to stimulus other than mechanical stress. The strains can be regulated by adjusting the intensiveness of the stimulus signal. Induced strains occur in many materials. Thermal expansion can be considered as such an induced strain. However, due to the small induced strain range and difficulties to be controlled, usual materials are not of much use as actuators in this regard. Shape memory alloy (Rogers, 1988) has been used as an induced strain actuator. Shape

memory alloy(SMA) possesses not only the properties of induced strain but also the ability to change its mechanical properties over a very large range. SMA fibers have been embedded in composite structures to form an integrated entity, capable of structural modification (Rogers, Liang, and Jia, 1989), structural acoust control (Rogers, Liang, and Fuller, 1989), and damage control. The structure can adapt to various environments to render the optimal performance by adjustment of the actuator's temperature. However, shape memory alloy actuators have a large time constant, which is a disadvantage when used in high frequency response situations.

Another family of materials able to generate induced strains are piezoelectric and electrostatic materials. These materials are mechanically deformable continua that are electrically polarizable. Piezoelectric materials can generate negative or positive induced strains when a voltage is applied along or against the polarization. Piezoelectric materials have relatively small time constants and can be actuated in the kHz region.

The characteristics of piezoelectric materials have been studied by Todda and Johnson(1979), Cross(1980), and many others. Systems using this kind of actuator have been studied by Bailey and Hubbard, (1985), Anderson and Crawley, (1989), Wang and Rogers(1991), and many others in the past five years. Forward(1981) has used piezoelectric actuators to control the bending modes in a cylindrical mast-experiment. In his very recent work, Anderson(1989) summarized various models describing the interactions in the substructure between the structure and bonded actuators. Finite element method has been used to check with the theoretical models. Crawley and de Louis(1989) and Im (1989) have both proposed mechanical models for piezoelectric actuators bonded to beam-like structures. The actuator model used in this study is

based on the results of Crawley and de Louis(1989).

1.4 Optimization

The optimization method used in this study is a numerical search technique. This technique starts from an initial design and proceed in small steps, which intends to improve on the values of the objective function and on the degree of compliance with the constraints. The search is terminated when no more progress can be made in improving the objective function without violating some of the constraints.

Trying to find the optimal actuator locations and sizes results in a global optimization problem of multivariables with a nonlinear objective function and linear inequality constraints. Global optimal solutions for nonlinear systems that contain several local minima are relatively difficult to find. Searching for a global optimal point is still a matter of active research in the optimization realm. Systematic approaches for global optimization are rare for most general cases. Therefore, the choice of which is the global optimum among a set of local optimums is made in this study according to engineering understanding and some mathematical rules.

The optimization in this study can be divided into two parts. One part is to find the optimal weighting matrix under preset actuator locations and sizes. The second optimization procedure is to use the weighted pseudoinverse method to find the optimal actuator designs. The actuator designs are then fed back into the first optimization procedure. This iteration will be repeated until a convergency criteria is reached.

1.5 Scopes of Study

This investigation has been grouped into the following two sections:

- Study the approaches to determining the optimal actuator designs with or without the spillover consideration, under the

Condition: an equal number of actuators are used to control an equal number of modes of modes; and

Assumption: all modes are equally likely and uncorrelated.

- Study the approaches to determining the optimal actuator designs with or without the spillover consideration, under the

Condition: fewer actuators are used than the modes to be controlled; and

Assumption: all modes are equally likely and uncorrelated.

In this second section, the weighted pseudoinverse method will be introduced.

Chapter 2

INDEPENDENT MODAL SPACE CONTROL

The Independent Modal Space Control method was devised to generate a control law for large dimensional systems(Meirovich,1981b). This control method can be utilized in several different categories of structural vibration control. The are of interest for this study is linear regulator systems.

Consider a distributed-parameter system whose behavior can be described by the following equation of motion

$$Lu(P,t) + m(P) \frac{\partial^2 u(P,t)}{\partial t^2} = f(P,t) \quad (2.1)$$

subjected to the boundary conditions

$$B_i u(P,t) = 0 \quad (i = 1, 2, \dots, n). \quad (2.2)$$

Here L is a linear, self-adjoint differential operator of order $2n$, $u(P,t)$ is the displacement, as a function of the position P and time t , $m(P)$ is the distributed mass,

and $f(P,t)$ is a distributed control force. The B_i 's are also linear-differential operators. The solution of the associated eigenvalues for such a system is an infinite set of eigenvalues $\lambda_k = \omega_k^2$ and corresponding eigenfunctions $\phi_k(P)$ ($k = 1, 2, \dots$). The eigenfunctions are orthogonal and can be normalized so as to satisfy

$$\int_D m(P) \phi_k(P) \phi_l(P) dD = \delta_{kl} \quad (2.3)$$

$$\int_D \phi_k(P) L \phi_l(P) dD = \omega_k^2 \delta_{kl} \quad (2.4)$$

where δ_{kl} is the Kronecker delta and the subscription D is the physical domain the system occupies. By making use of the modal expansion theorem (Meirovich, 1967), the displacement of the structure can be expressed as

$$u(P, t) = \sum_{k=1}^{\infty} \phi_k(P) u_k(t) \quad (2.5)$$

where u_k is the normal modal displacements. Introducing the above equation into the equation of motion, multiplying both sides of the result by $\phi_k(P)$, and integrating over region D , we obtain the open-loop modal ordinary differential equations of motion

$$\ddot{u}_k(t) + \omega_k^2 u_k(t) = f_k(t), \quad k = 1, 2, \dots \quad (2.6)$$

where

$$f_k(t) = \int_D \phi_k(P) f(P, t) dD, \quad k = 1, 2, \dots \quad (2.7)$$

are generalized modal control forces, and

$$u_k(t) = \int_D \phi_k(P) u(P, t) dD, \quad k = 1, 2, \dots \quad (2.8)$$

are the modal displacements. An auxiliary variable $v_k(t)$ may be introduced and defined as

$$v_k(t) = \dot{u}_k(t)/\omega_k \quad k = 1, 2, \dots \quad (2.9)$$

By introducing the two-dimensional modal state vector $w_k(t)$ and the associated control vector $W_k(t)$ in the form

$$\begin{aligned} w_k(t) &= \begin{Bmatrix} u_k(t) \\ v_k(t) \end{Bmatrix} \\ W_k(t) &= \begin{Bmatrix} 0 \\ f_k(t)/\omega_k \end{Bmatrix} \\ k &= 1, 2, \dots \end{aligned} \quad (2.10)$$

and introducing the 2x2 coefficient matrix

$$A_k = \begin{bmatrix} 0 & \omega_k \\ -\omega_k & 0 \end{bmatrix} \quad k = 1, 2, \dots, \quad (2.11)$$

the modal vibration equations can be written in the modal state form

$$\dot{w}_k(t) = A_k w_k(t) + W_k(t) \quad k = 1, 2, \dots \quad (2.12)$$

In Independent Modal Space Control, it is assumed that W_k depends on w_k alone,

i.e.,

$$W_k = W_k(w_k) \quad k = 1, 2, \dots \quad (2.13)$$

Independent Modal Space Control permits both linear and nonlinear control. Linear feedback is the case considered here,

$$W_k(t) = F_k w_k(t) \quad k = 1, 2, \dots \quad (2.14)$$

where

$$F_k = \begin{bmatrix} f_{k11} & f_{k12} \\ f_{k21} & f_{k22} \end{bmatrix} \quad k = 1, 2, \dots \quad (2.15)$$

is the 2x2 modal gain matrix. Substituting Eqs.(2.14) into Eq.(2.10), the following equation can be obtained,

$$\begin{Bmatrix} 0 \\ f_k/\omega_k \end{Bmatrix} = \begin{Bmatrix} f_{k11}u_k(t) + f_{k12}v_k(t) \\ f_{k21}u_k(t) + f_{k22}v_k(t) \end{Bmatrix} \quad k = 1, 2, \dots \quad (2.16)$$

which can be satisfied only if $f_{k11} = f_{k12} = 0$ ($k=1,2,\dots$), and from which it follows that the modal gain matrices have the form

$$F_k = \begin{bmatrix} 0 & 0 \\ f_{k21} & f_{k22} \end{bmatrix} \quad k = 1, 2, \dots \quad (2.17)$$

Therefore, Eq.(2.7) has the form

$$f_k(t) = \omega_k[f_{k21}u_k(t) + f_{k22}v_k(t)] = f_{k21}\omega_k u_k(t) + f_{k22}\dot{u}_k(t) \quad k = 1, 2, \dots \quad (2.18)$$

so that the modal control force f_k is proportional to both the modal displacement u_k and the modal velocity v_k . For optimal control, these gains can be determined by minimizing a quadratic cost function of the form

$$J = \sum_{k=1}^{\infty} J_k \quad (2.19)$$

where

$$J_k = \int_0^{t_f} (w_k^T Q_k w_k + W_k^T R_k W_k) dt \quad (2.20)$$

is the modal cost function, and t_f is the final time. Q_k and R_k are weighting matrices. Because W_k depends on w_k alone, the modal cost functions are independent. The J , therefore, can be minimized by minimizing each modal cost function J_k independently. Minimization of J_k leads to

$$W_k = -R_k^{-1} K_k(t) w_k(t) \quad (2.21)$$

where the elements of the 2x2 symmetric matrix $K_k(t)$ are the solutions of the matrix Riccati equation (Kirk, 1970)

$$\dot{K}_k = -k_k A_k - A_k^T K_k - Q_k + K_k R_k^{-1} K_k \quad (2.22)$$

Here $Q_k = \omega_k^2 I$ is chosen. Since the feedback solution, Eq.(2.21), must yield a generalized force vector of the form specified in Eq.(2.10), a further restriction on R_k is imposed. Expanding the second term in the modal cost function gives $w_k^T R_k w_k = (f_k(t)/\omega_r)^2 R_{k22}$, from which we can see that only the R_{k22} term from R_k influences

the cost function. The form of $W_k(t)$ in Eq.(2.10) can be obtained by required the first row of R_k^{-1} of Eq.(2.21) to be zero. Therefore, by symmetry the remaining off diagonal elements are zero. That is

$$R_k = \begin{bmatrix} \infty & 0 \\ 0 & R_k \end{bmatrix}. \quad (2.23)$$

The steady state solution is our interest. For convenience in later use, the gains factors are redifned as

$$\begin{aligned} g_k &= f_{k21} = -\omega_k^2 + \omega_k [\omega_k^2 + (1/r)]^{1/2} \\ h_k &= f_{k22} = \{-2\omega_k^2 + (1/r) + 2\omega_k [\omega_k^2 + (1/r)]^{1/2}\}^{1/2} \\ k &= 1, 2, \dots \end{aligned} \quad (2.24)$$

The above results can be interpreted as the optimum to keep the state vector as close to the origin of the state space as possible with minimum control effort, and without increasing the total energy of the open loop system. In this case, the final state is fixed, and the final time follows according to the minimal principal.

Substituting Eq.(2.24) into Eq.(2.18), and then the result into Eq.(2.6), we obtain the closed-loop modal equations

$$\ddot{u}_k(t) + h_k \dot{u}_k(t) + (\omega_k^2 + g_k)u_k(t) = 0, \quad k = 1, 2, \dots \quad (2.25)$$

Figure 2.1 shows the open-loop and closed-loop eigenvalues. It can be clearly seen that the control strategy is to influence the system characteristics. The control forces relocate the eigenvalues of the system. The control has little influence on the imagi-

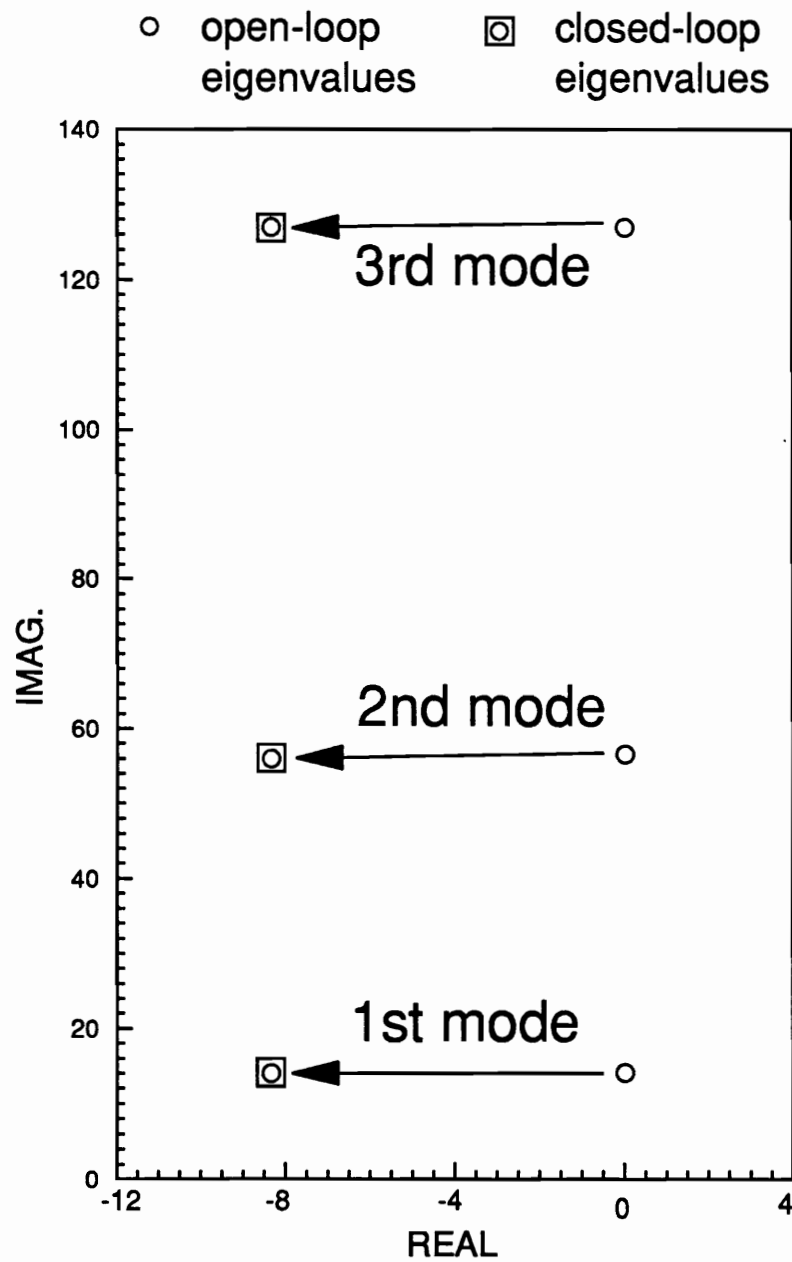


Figure 2.1: Open-loop and closed-loop eigenvalues

nary part of the eigenvalues, and gives nearly equal shift of the eigenvalues over the real axis. This shift means that the controlling time for each of these modes will be nearly the same. Due to the damping effect of the control, the closed-loop natural frequencies will be changed. The change ratios in this aspect vary from mode to mode, because the original open-loop eigenvalues are quite different.

Chapter 3

SUBSTRUCTURE MODELLING OF PIEZOELECTRIC ACTUATOR SYSTEMS

An introduction to piezoelectric materials, which are used as the actuator material of the present study, are given in the first section. In the second section, a mechanical model of piezoelectric actuators when used in beam-like structures is derived according to Crawley and Javier(1987). The incorporation of the actuators into the control system follows in the third section.

3.1 Piezoelectric Materials

Piezoelectricity is the ability of certain crystalline materials to develop an electric charge proportional to a mechanical stress. The prefix of piezoelectric, *piezo*, is a Greek word meaning “to press”. External stress of one kind or another on crystals of these classes will cause an electrical polarization. The converse is also true in the same materials. An applied electric voltage will generate a geometric strain (deformation) proportional to the voltage applied. A thorough and absorbing review of the early piezoelectric crystals can be found in the works by W. G. Cady(1946), Henry (1969), or Mason (1971).

Certain crystal structures result in the appearance of dipoles. Dipoles are positive-negative pairs: equal and opposite electric charges or magnetic poles separated by small distances. For the piezoelectric interaction to exist, certain axes of the medium must possess intrinsically polarity. Although this polarity is inherent in the symmetry of some crystal classes, it is absent in principle in other crystal classes and in isotropic bodies. Until 1944, Ceramic materials, being either oxides or mixtures of oxides, were not considered as possessing piezoelectricity (Jaffe, 1971). A process, called "poling", was found to generate the polarity to an originally isotropic polycrystalline ceramic. This poling is more or less permanently accomplished, by a temporary application of a strong electric field. The poling process is analogous to the magnetizing of a permanent magnet. Piezoelectric ceramics will be our main concern for this study. However piezoelectric polymers and rubber composites do exist, piezoelectric ceramics can transfer more strain energy for a given field due to their relatively high modulus (Anderson, 1989).

To maintain consistency with other literature on the piezoelectrics, the nomenclature used in this section will be according to the IEEE standard and will differ from the counterpart in mechanics. However, the differences will be explained, and use of this nomenclature will be confined to this section. Beyond this section, the results will be converted into general mechanical engineering terminology.

For the special case of a piezoceramic, the constitutive equations take the following

form (Jaffe, 1971 and Crawley, 1989)

$$\begin{Bmatrix} D_1 \\ D_2 \\ D_3 \\ S_1 \\ S_2 \\ S_3 \\ S_4 \\ S_5 \\ S_6 \end{Bmatrix} = \begin{bmatrix} \epsilon_1^T & 0 & 0 & 0 & 0 & 0 & 0 & d_{15} & 0 \\ 0 & \epsilon_2^T & 0 & 0 & 0 & 0 & d_{15} & 0 & 0 \\ 0 & 0 & \epsilon_2^T & d_{31} & d_{31} & d_{33} & 0 & 0 & 0 \\ 0 & 0 & d_{31} & s_{11}^E & s_{12}^E & s_{13}^E & 0 & 0 & 0 \\ 0 & 0 & d_{31} & s_{12}^E & s_{11}^E & s_{13}^E & 0 & 0 & 0 \\ 0 & 0 & d_{33} & s_{13}^E & s_{13}^E & s_{33}^E & 0 & 0 & 0 \\ 0 & d_{15} & 0 & 0 & 0 & 0 & s_{55}^E & 0 & 0 \\ d_{15} & 0 & 0 & 0 & 0 & 0 & 0 & s_{55}^E & 0 \\ 0 & 0 & 0 & 0 & 0 & 0 & 0 & 0 & s_{66}^E \end{bmatrix} \begin{Bmatrix} E_1 \\ E_2 \\ E_3 \\ T_1 \\ T_2 \\ T_3 \\ T_4 \\ T_5 \\ T_6 \end{Bmatrix} \quad (3.1)$$

where T and S are mechanical stress and strain, respectively; E and D are electrical field and electrical displacement. The s's are the mechanical compliance matrix elements, ϵ 's are the dielectric matrix elements, and d's are the electromechanical coupling matrix elements. The superscript T and E mean, respectively, that the quantities are taken at constant (or zero) stress and constant (or zero) field (also known as "short circuit").

The emphasis is placed on the one-dimensional effects of piezoelectric materials, because the application will be for beam-like structures. For this reason, only the portion of the constitutive relation required for this application is discussed further.

Let us first assume that the direction in which we orient the beam is x_1 . For the piezoelectric strain in the x_1 direction, the constitutive relation becomes

$$S_1 = d_{31}E_3 + s_{11}^ET_1 + s_{12}^ET_2 + s_{13}^ET_3 \quad (3.2)$$

where E_3 is the electrical field applied perpendicular to the piezoelectric surfaces.

The quantity E_3 is renamed V , i.e., the voltage applied. The quantity d_{31} is the “piezoelectric strain coefficient”. The piezoelectric strain coefficient, d_{31} , characterizes strain perpendicular to the poling direction due to the electric field (E_3 , or V) aligned with the poling direction. T_1 is the stress induced by mechanical forces. T_2 and T_3 are the stresses in the other two directions. s_{11}^E is the inverse of the piezoelectric stiffness and s_{12} and s_{13} are the coupling terms between the stress in other directions and the strain in x_1 direction. Figure 3.1 shows the coordinate system of a piezoelectric actuator. Here we assume that there is no stress in any direction except the x_1 direction. That is, let $T_2 = T_3 = 0$. Thus, the piezoelectric constitutive relation reduces to

$$S_1 = d_{31}E_3 + s_{11}^E T_1 . \quad (3.3)$$

Now, writing the above equation in mechanics terminology, letting ϵ_p be the piezoelectric strain in x_1 direction, V the voltage applied at x_3 direction, E_p the Young’s modulus of the piezoelectric, and σ_p the piezoelectric stress at x_1 direction, we have

$$\epsilon_p = d_{31}V + \frac{1}{E_p}\sigma_p \quad or \quad \epsilon_p = \Lambda + \frac{1}{E_p}\sigma_p . \quad (3.4)$$

The term $\Lambda = d_{31}V$ is the induced strain under stress free conditions. The properties d_{31} and E_p are not constants. They are dependent on the applied electric voltage. But the associated nonlinearity has been excluded from this study. Both d_{31} and E_p are treated as constants independent of the magnitude and frequencies of the applied mechanical stresses and electric field.

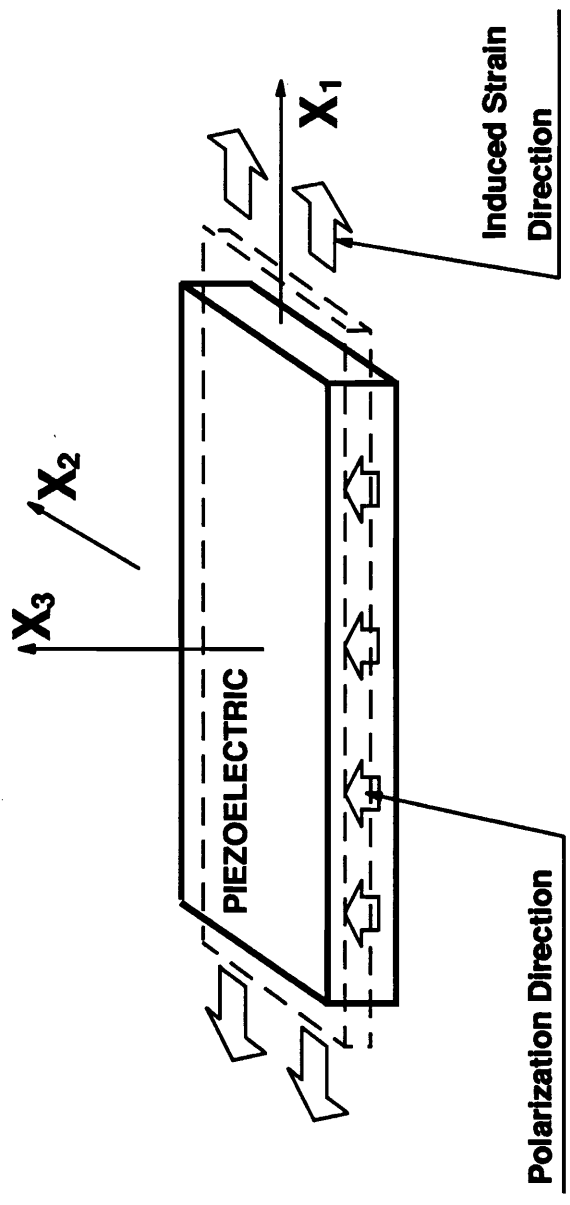


Figure 3.1: Coordinate System of Piezoelectric Elements

3.2 Mechanical Model

In this section, the mechanical model for the interaction between the actuator and the structure is derived from the work of Crawley and Javier(1987). Figure 3.2 shows the geometry of piezoelectric actuators bonded symmetrically by two finite-thickness bonding layers to two sides of an elastic structure. It is assumed that the voltages will be applied in opposite directions on the top and bottom piezoelectric actuators to initiate bending deformation in the structure. In this case, one of the actuators will expand and the other contract. They will cause a zero extension effect and an enhanced bending effect in the structure.

Figure 3.3 gives the assumed strain profile through the cross-sections of the actuators and the substructures. It should be noted that a uniform stress distribution throughout the actuator thickness has been assumed. The effects of this assumption are described in detail by Anderson and Crawley(1989).

First, let us take an infinitesimal length element of the structure, dx , as shown in Figure 3.2. The following two relationships can be derived for the displacement and strains in the actuators and on the surface of the beam, respectively,

$$\epsilon_p = \frac{du_p}{dx} , \quad (3.5)$$

$$\epsilon_s^s = \frac{du_s^s}{dx} . \quad (3.6)$$

The superscript s denotes that the quantity is on the surface of the beam structure.

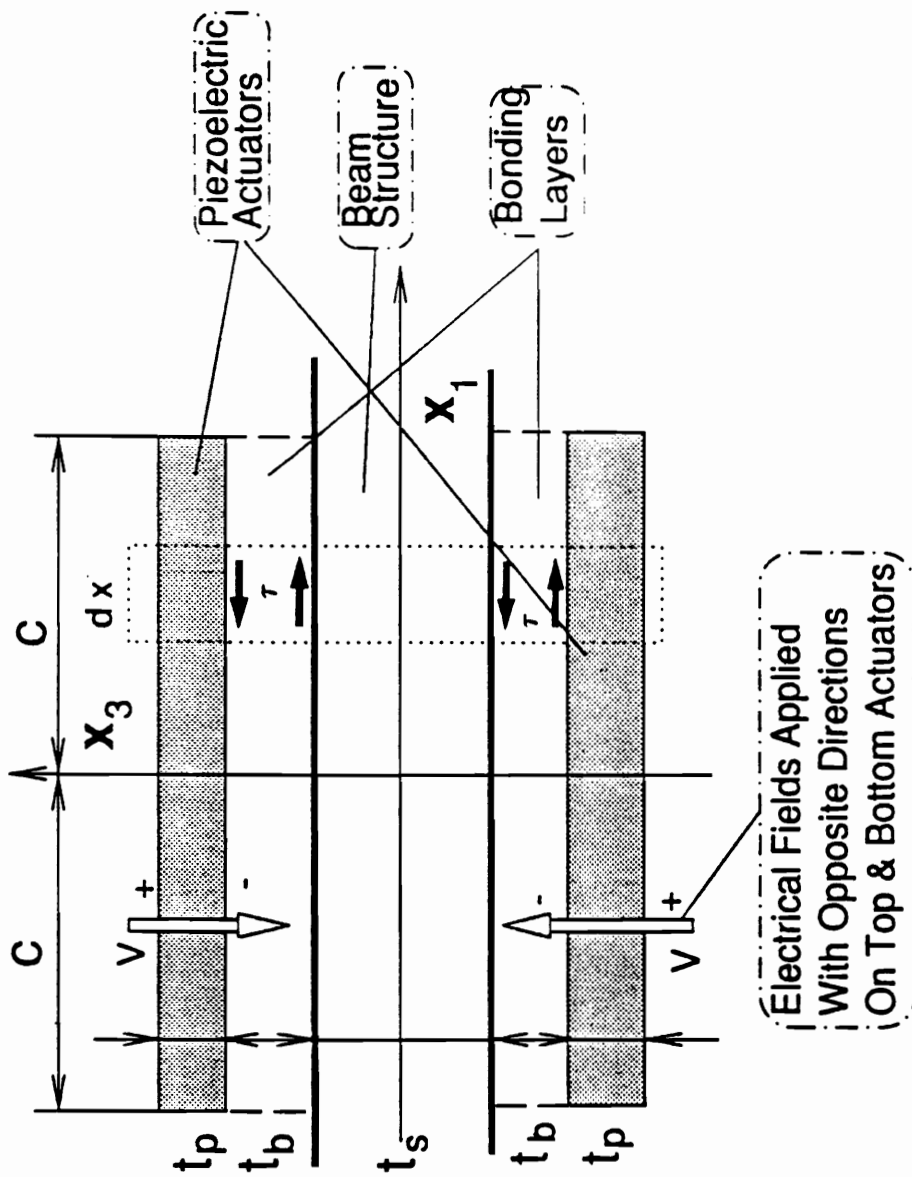


Figure 3.2: Geometry of Piezoelectric Actuators Bonded to an Elastic Substructure

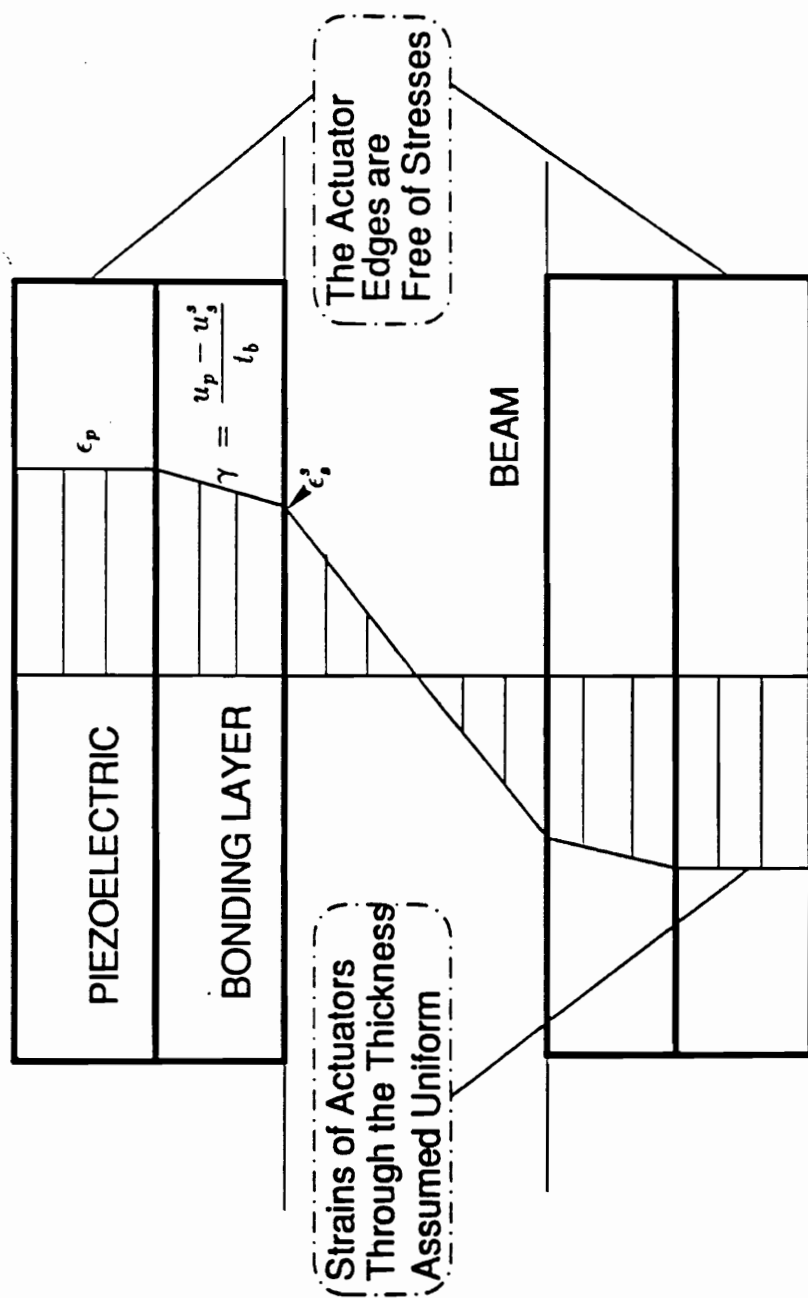


Figure 3.3: Strain Profile by Assuming Linear Bernoulli-Euler Strain Distribution

Subscripts p and s denote the piezoelectric actuator and structure, respectively. For example, u_s^s denotes the displacement on the surface of the beam. By assuming pure one-dimensional shear in the bonding layer, the shear strain in the bonding layer has the form

$$\gamma = \frac{u_p - u_s^s}{t_b} . \quad (3.7)$$

The equations of motion for an element of the actuator or that of the substructure are

$$\frac{d\sigma_p}{dx} - \frac{\tau}{t_p} = 0 \quad (3.8)$$

$$\frac{d\sigma_s}{dx} + \frac{\alpha\tau}{t_s} = 0 \quad (3.9)$$

where α is a constant depending on the assumed beam strain distribution. For a linear Bernoulli-Euler distribution, $\alpha = 6$.

The stress-strain relationship for the piezoelectric actuator was found in the last section to be

$$\sigma_p = E_p(\epsilon_p - \Lambda) . \quad (3.10)$$

For the beam and the bonding layer, the isotropic stress-strain relations are

$$\sigma_s^s = E_s \epsilon_s^s \quad (3.11)$$

$$\tau = G \gamma . \quad (3.12)$$

Substituting Eq.(3.7) into Eq.(3.12), we have

$$\tau = G \frac{u_p - u_s^s}{t_b} . \quad (3.13)$$

Then, combining the above equation into Eq. (3.8) and (3.9) yields

$$\frac{d\sigma_p}{dx} - \frac{G}{t_b t_p} (u_p - u_s^s) = 0 \quad (3.14)$$

$$\frac{d\sigma_s^s}{dx} + \frac{\alpha G}{t_b t_s} (u_p - u_s^s) = 0 . \quad (3.15)$$

Substituting Eq.(3.10) into Eq. (3.14) and Eq.(3.11) into Eq. (3.15), we obtain the equations of motion in terms of displacements and strains:

$$E_p \frac{d\epsilon_p}{dx} - \frac{G}{t_b t_p} (u_p - u_s^s) = 0 \quad (3.16)$$

$$E_s \frac{d\epsilon_s^s}{dx} + \frac{\alpha G}{t_b t_s} (u_p - u_s^s) = 0 . \quad (3.17)$$

Differentiating the above equation, then substituting Eq.(3.5) and Eq. (3.6) into the results, we obtain the equations of motion in terms of strains only,

$$E_p \frac{d^2 \epsilon_p}{dx^2} - \frac{G}{t_b t_p} (\epsilon_p - \epsilon_s^s) = 0 \quad (3.18)$$

$$E_s \frac{d^2 \epsilon_s^s}{dx^2} + \frac{\alpha G}{t_b t_s} (\epsilon_p - \epsilon_s^s) = 0 . \quad (3.19)$$

By manipulating Eqs. (3.18) and (3.19), the following relation can be found:

$$\frac{\alpha E_p}{t_s} \frac{d^2 \epsilon_p}{dx^2} = - \frac{E_s}{t_p} \frac{d^2 \epsilon_s^s}{dx^2} \quad (3.20)$$

Equation (3.20) gives the coupling between the two strains, ϵ_p and ϵ_s^s . Next, we want to decouple the two equations of motion. Again, the Eq.(3.18) and Eq.(3.19) are differentiated twice, and then substituting Eq.(3.20) yields

$$\frac{d^4 \epsilon_p}{dx^4} - \frac{G}{t_b t_p E_p} \left(1 + \frac{\alpha E_p t_p}{E_s t_s} \right) \frac{d^2 \epsilon_p}{dx^2} = 0 \quad (3.21)$$

$$\frac{d^4 \epsilon_s^s}{dx^4} - \frac{\alpha G}{t_b t_p E_s} \left(1 + \frac{E_s t_s}{E_p t_p \alpha} \right) \frac{d^2 \epsilon_s^s}{dx^2} = 0 . \quad (3.22)$$

According to the coordinate system given in Figure 3.2, we can nondimensionalize the x axis by letting $\bar{x} = x/c$. The two end-coordinates of the piezoelectric are 1 and -1, respectively. Equations (3.21) and (3.22) can be transformed into the nondimensional

coordinate form,

$$\frac{d^4 \epsilon_p}{d\bar{x}^4} - \frac{Gc^2}{t_b t_p E_p} \left(1 + \frac{\alpha E_p t_p}{E_s t_s} \right) \frac{d^2 \epsilon_p}{d\bar{x}^2} = 0 \quad (3.23)$$

$$\frac{d^4 \epsilon_s^s}{d\bar{x}^4} - \frac{\alpha c^2 G}{t_b t_p E_s} \left(1 + \frac{E_s t_s}{E_p t_p \alpha} \right) \frac{d^2 \epsilon_s^s}{d\bar{x}^2} = 0 . \quad (3.24)$$

Next naming

$$\Gamma^2 = \frac{Gc^2}{t_b t_p E_p} \left(1 + \frac{\alpha E_p t_p}{E_s t_s} \right) \quad (3.25)$$

and

$$\psi = \frac{E_s t_s}{E_p t_p} \quad (3.26)$$

we have the equations of motion in the decoupled form:

$$\frac{d^4 \epsilon_p}{d\bar{x}^4} - \Gamma^2 \frac{d^2 \epsilon_p}{d\bar{x}^2} = 0 \quad (3.27)$$

$$\frac{d^4 \epsilon_s^s}{d\bar{x}^4} - \Gamma^2 \frac{d^2 \epsilon_s^s}{d\bar{x}^2} = 0 , \quad (3.28)$$

and the Boundary conditions are

$$\begin{aligned} \bar{x} = +1 : \quad \epsilon_p &= \Lambda \quad \epsilon_s^s = \epsilon_s^{s+} \\ \bar{x} = -1 : \quad \epsilon_p &= -\Lambda \quad \epsilon_s^s = \epsilon_s^{s-} . \end{aligned} \quad (3.29)$$

Because the actuators have free edges, the strains of the actuators are equal to the free induced strain on the boundary. The terms ϵ_s^{s-} and ϵ_s^{s+} are the strains present without the piezoelectric actuators. They give a nonlinear boundary condition when used in the dynamic boundary situation.

The general solutions of Eq. (3.27) and (3.28) are

$$\epsilon_p = A_1^p + A_2^p \bar{x} + A_3^p \sinh \Gamma \bar{x} + A_4^p \cosh \Gamma \bar{x} \quad (3.30)$$

$$\epsilon_s^s = A_1^s + A_2^s \bar{x} + A_3^s \sinh \Gamma \bar{x} + A_4^s \cosh \Gamma \bar{x} . \quad (3.31)$$

Making use of the relationship given in Eq.(3.20), the second partial of beam surface strain with respect to x can be written as

$$\frac{d^2 \epsilon_p}{dx^2} = -\frac{\psi}{\alpha} \frac{d^2 \epsilon_s^s}{dx^2} . \quad (3.32)$$

By substituting Eq. (3.30) and (3.31) into Eq.(3.32), the number of arbitrary constants can be reduced to

$$\begin{aligned} A_3^p &= -\psi/\alpha A_3^s = -\psi/\alpha A_3 \\ A_4^p &= -\psi/\alpha A_4^s = -\psi/\alpha A_4 \\ A_1^p &= A_1^s = A_1 \\ A_2^p &= A_2^s = A_2 . \end{aligned} \quad (3.33)$$

Therefore, the general solution becomes

$$\epsilon_p = A_1 + A_2 \bar{x} - A_3 \frac{\psi}{\alpha} \sinh \Gamma \bar{x} - A_4 \frac{\psi}{\alpha} \cosh \Gamma \bar{x} \quad (3.34)$$

$$\epsilon_s^s = A_1 + A_2 \bar{x} + A_3 \sinh \Gamma \bar{x} + A_4 \cosh \Gamma \bar{x} . \quad (3.35)$$

Substituting the boundary conditions into Eqs.(3.34) and (3.35), the arbitrary constants can be determined

$$A_1 = \frac{\psi}{\psi + \alpha} \left(\frac{\epsilon_s^{s+} + \epsilon_s^{s-}}{2} \right) \quad (3.36)$$

$$A_2 = \frac{\psi}{\psi + \alpha} \left(\frac{\epsilon_s^{s+} - \epsilon_s^{s-}}{2} - \frac{\alpha}{\psi} \Lambda \right) \quad (3.37)$$

$$A_3 = \frac{\alpha}{(\psi + \alpha) \sinh \Gamma} \left(\frac{\epsilon_s^{s+} - \epsilon_s^{s-}}{2} - \Lambda \right) \quad (3.38)$$

$$A_4 = \frac{\alpha}{(\psi + \alpha) \cosh \Gamma} \left(\frac{\epsilon_s^{s+} + \epsilon_s^{s-}}{2} \right) . \quad (3.39)$$

Substituting the strains into Equations (3.5) and (3.6), then integrating the results, the displacements of the actuator and beam surface are calculated. The displacements

are used to find the shear stress as given in Eq.(3.12),

$$\tau = -\frac{Gc}{t_b\Gamma} \left[\left(\frac{\epsilon_s^{s+} - \epsilon_s^{s-}}{2} - \Gamma \right) \frac{\cosh \Gamma x}{\sinh \Gamma} + \frac{\epsilon_s^{s+} + \epsilon_s^{s-}}{2} \frac{\sinh \Gamma x}{\cosh \Gamma} \right] \quad (3.40)$$

which is the shear stress distribution in the bonding layer. Figure 3.4 shows the profile of the shear stress throughout the interface between the actuator and the beam under different values of Γ . It should be noted that when the bonding layer becomes thin and the value of Γ becomes larger, the distribution becomes concentrated on the two edges of the actuator. That means that the actuator begins to act as a concentrated force on the beam surface at the actuator edges.

In this study, the bonding between the actuator and the substructure is very thin and stiff. That is to say that $\Gamma \rightarrow \infty$. By performing the following calculation, the forces exerted by the actuator at the two edges and the strains of actuators at the beam surface can be determined

$$\epsilon_p = \lim_{\Gamma \rightarrow \infty} \epsilon_p(\Gamma, \bar{x}) \quad (\text{see Eq.3.34}) \quad (3.41)$$

$$\epsilon_s^s = \lim_{\Gamma \rightarrow \infty} \epsilon_s^s(\Gamma, \bar{x}) \quad (\text{see Eq.3.35}) . \quad (3.42)$$

In this special case, the two strains are equal,

$$\epsilon_p = \epsilon_s^s = \frac{\psi}{\psi + \alpha} \left[\frac{\epsilon_s^{s+} + \epsilon_s^{s-}}{2} + \frac{\epsilon_s^{s+} - \epsilon_s^{s-}}{2} \bar{x} \right] . \quad (3.43)$$

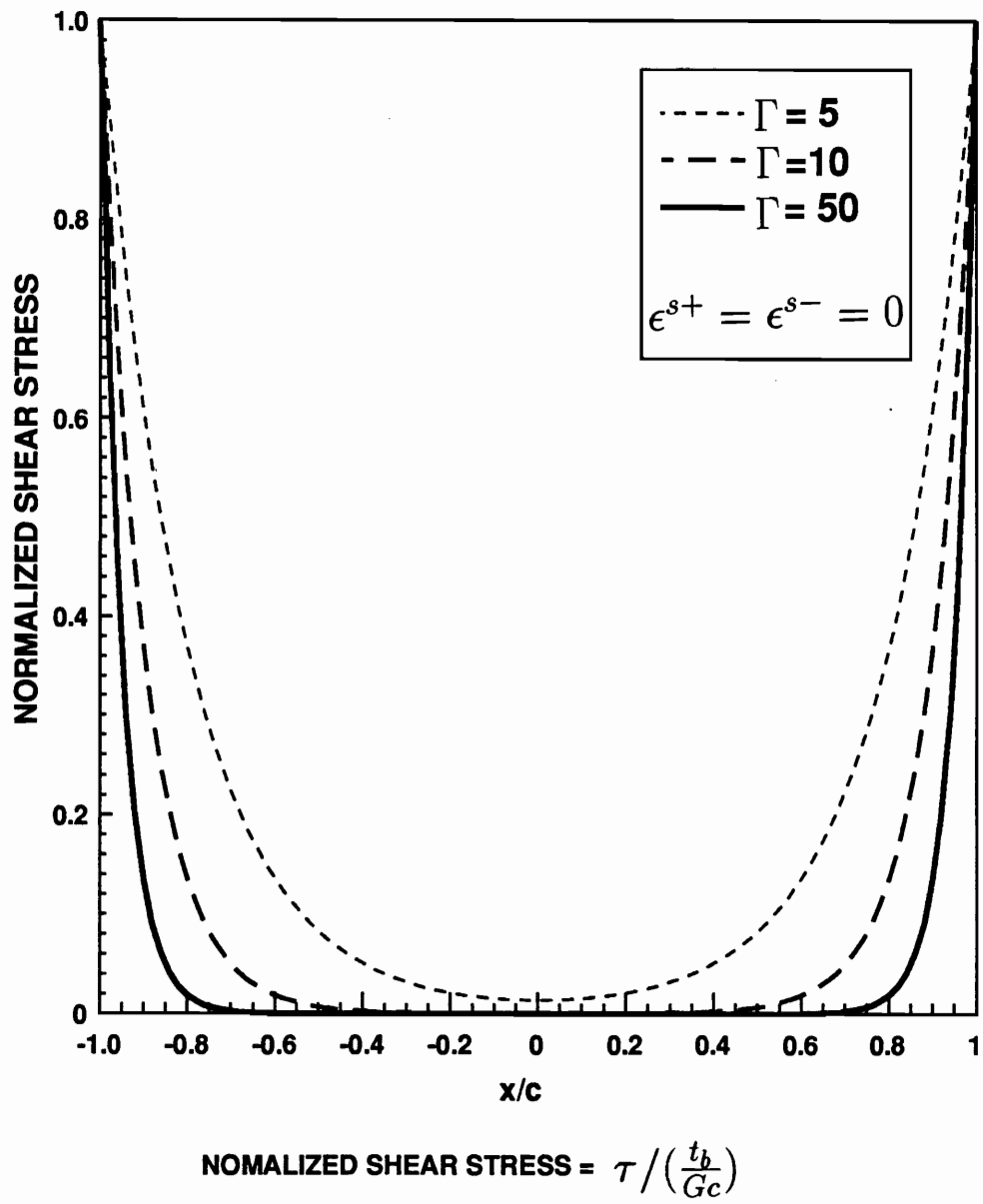


Figure 3.4: Shear stress distribution along the bonding layer

And

$$F = \lim_{\Gamma \rightarrow \infty} \int_0^c -\tau(\bar{x})dx . \quad (3.44)$$

By taking this limit, the entire shear force is effectively transferred to a concentrated force at the ends of the piezoelectric actuator. This force applied at $\bar{x} = \pm 1$, is

$$F = \frac{E_s t_s b}{\psi + \alpha} \left[\frac{\epsilon_s^{s+} + \epsilon_s^{s-}}{2} + \frac{\epsilon_s^{s+} - \epsilon_s^{s-}}{2} \bar{x} \right] - \frac{E_s t_s b}{\psi + \alpha} \Lambda . \quad (3.45)$$

Because the actuators have been arranged symmetrically and excited in opposite directions, the following moment is applied to the beam

$$M = Ft_s . \quad (3.46)$$

The voltage required to induce a desired moment applied on the beam is

$$V = \frac{1}{d_{31}} \frac{\psi + \alpha}{E_s t_s^2 b} - \frac{1}{d_{31}} \left[\frac{\epsilon_s^{s+} + \epsilon_s^{s-}}{2} + \frac{\epsilon_s^{s+} - \epsilon_s^{s-}}{2} \bar{x} \right] . \quad (3.47)$$

In Eq.(3.47), the second term is merely the representation of the additional passive stiffness added by bonding a reinforcement to the surface. It will be neglected, because it is not significant when the beam deformation is small.

3.3 Determination of Modal Control Forces

In the last section, It was shown that one-dimensional piezoelectric actuators can be modelled as a pair of moments acting on the beam at the two ends of the actuator under the assumption the bondings are very thin. The objective of this section

is to use this model to represent the control forces in Independent Modal Space Control systems. To include the moments into the equation of the beam vibrations, the moments are approximated in terms of two pairs of equal but opposite forces, thereby creating a couple. The forces in the same pair will have a distance dx between them (see Figure 3.5, b.). Figure 3.6 shows a beam system with n piezoelectric actuator pairs bonded to it. In this system, there are n pairs of moments which can be excited to satisfy the control requirement. Therefore, the forcing term in the equation of motion, Eq.(3.1), with n actuators in the system, can be written as

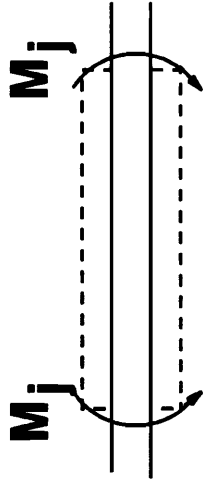
$$f(x, t) = \sum_{j=1}^n F_j(t) [\delta(a_j - c_j - \Delta x) - \delta(a_j - c_j) + \delta(a_j + c_j + \Delta x) - \delta(a_j + c_j)] . \quad (3.48)$$

The modal control forces are obtained by transforming Eq. (3.48) into modal space by following the same procedure used in Chapter 2. The modal control forces thus obtained are:

$$f_k(t) = \int_0^1 \sum_{j=1}^n \phi_k(x_j) F_j [\delta(a_j - c_j - \Delta x) - \delta(a_j - c_j) + \delta(a_j + c_j + \Delta x) - \delta(a_j + c_j)] dx \quad (3.49)$$

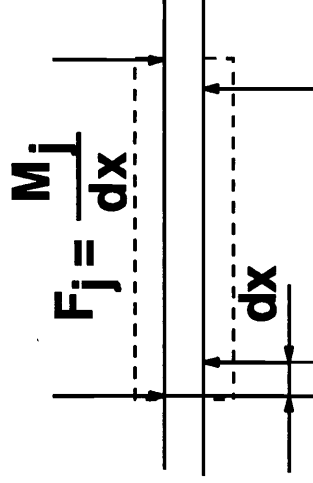
where δ is the Kroneker Delta. Integrating over the a length from 0 to 1, the modal forces are found

$$f_k(t) = \sum_{j=1}^n F_j [\phi_k(a_j + c_j + \Delta x) - \phi_k(a_j + c_j) - \phi_k(a_j - c_j) + \phi_k(a_j - c_j - \Delta x)] . \quad (3.50)$$



Perfectly Bonded Actuator Can
Be Treated as a Pair of Moments
Acting on the Actuator Edges

(a)



To Combine the Moments Into
Equations of Motion, a Moment
Is Approximated by a Pair of Forces

(b)

Figure 3.5: Mechanical model of piezoelectric Actuators

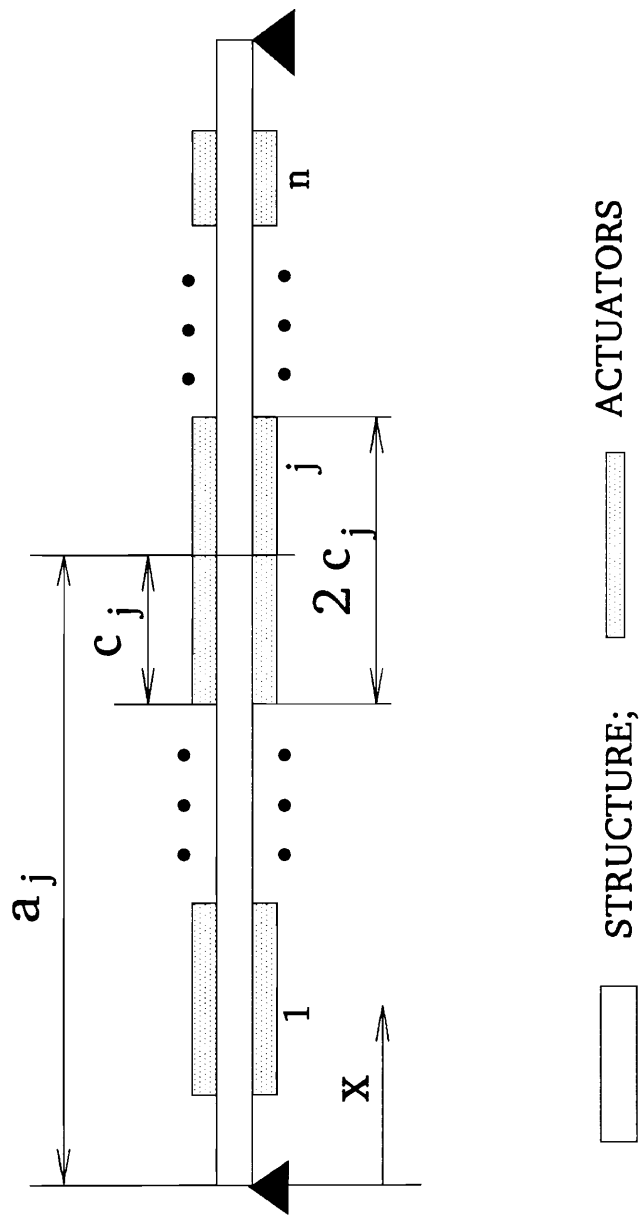


Figure 3.6: Beam Structure With Piezoelectric Actuators

Noting that the moment $M_j = F_j \Delta x$,

$$f_k(t) = \sum_{j=1}^n M_j [\phi_k(a_j + c_j + \Delta x) - \phi_k(a_j + c_j)] / \Delta x - \\ M_j [\phi_k(a_j - c_j) - \phi_k(a_j - c_j - \Delta x)] / \Delta x . \quad (3.51)$$

By taking the limit as $\Delta x \rightarrow 0$, we obtain

$$f_k(t) = \sum_{j=1}^n M_j [\phi'_k(a_j + c_j) - \phi'_k(a_j - c_j)] . \quad (3.52)$$

Therefore, the relationship between the optimal modal control forces and the actual control moments exerted by the piezoelectric actuators is:

$$\begin{pmatrix} f_1 \\ f_2 \\ \vdots \\ f_m \end{pmatrix} = \begin{bmatrix} B_{11} & B_{12} & \cdot & \cdot & \cdot & B_{1n} \\ B_{21} & B_{22} & \cdot & \cdot & \cdot & B_{2n} \\ \cdot & \cdot & \cdot & \cdot & \cdot & \cdot \\ B_{m1} & B_{m2} & \cdot & \cdot & \cdot & B_{mn} \end{bmatrix} \begin{pmatrix} M_1 \\ M_2 \\ \cdot \\ \cdot \\ M_n \end{pmatrix} \quad (3.53)$$

Here m is the number of the controlled modes and n is the number of actuators. The matrix B is called the modal participation matrix. The matrix B determines how much each mode will be affected by the actuators. By naming $\eta_j = a_j - c_j$ and $\zeta_j = a_j + c_j$, the matrix B has the form

$$B = [B_{ij}] = \phi'_i(\zeta_j) - \phi'_i(\eta_j) . \quad (3.54)$$

If $m \neq n$, i.e., if the number of actuators is not the same as that of the controlled modes, then the B matrix will not be square and the inverse of B cannot be found.

Chapter 4

OPTIMAL PIEZOELECTRIC ACTUATOR LOCATIONS AND DIMENSIONS

In this chapter, the problem of finding the optimal locations and dimensions of the actuators will be formulated and results presented, based on the fundamentals introduced in the proceeding chapters. This chapter deals with optimal piezoelectric actuator designs when the number of actuators is equal to the number of modes controlled.

The objective of this chapter is to formulate a methodology to search for the optimal design of the piezoelectric actuator systems which requires the least control effort, i.e., the polarization voltages to activate the actuators. Chapter 3 has shown that the polarization voltage is proportional to the required control moments. Therefore, the control moments can be used as the equivalent quantities to the polarization voltages in the optimization objective function. Because the moment terms appear directly in the equations of motion, the formulation using control moments will be simpler than using control voltages.

4.1 Introduction

Independent Modal Space Control decouples the distributed structural vibrations into a series of one degree of freedom modal vibrations. Each of the control laws are designed in the modal space. The modal control forces obtained by IMSC in modal space will be shown to be a deterministic function of time for each specific initial condition.

By utilizing IMSC, the controlled vibrations of each mode can be described by

$$\ddot{u}_k(t) + h_k \dot{u}_k(t) + (\omega_k^2 + g_k)u_k(t) = 0, \quad k = 1, 2, \dots \quad (4.1)$$

Name $\omega_k^c = \sqrt{g_k + \omega_k^2}$ and $\xi_k = \frac{h_k}{2\sqrt{g_k + \omega_k^2}}$, where superscript c denotes that the quantity is modified by adding the control forces. Equation (4.1) can then be written as

$$\ddot{u}_k(t) + 2\xi_k\omega_k^c\dot{u}_k(t) + (\omega_k^c)^2 u_k(t) = 0, \quad k = 1, 2, \dots \quad (4.2)$$

The solution of the above equation with an initial displacement u_{k0} and initial velocity \dot{u}_{k0} is

$$u_k(t) = e^{-\xi_k\omega_k^c t} [u_{k0} \cos(\omega_k^{c'} t) + \frac{\dot{u}_{k0} + \xi_k\omega_k^c u_{k0}}{\omega_k^{c'}} \sin(\omega_k^{c'} t)] \quad (4.3)$$

where $\omega_k^{c'} = \omega_k^c \sqrt{1 - \xi^2}$. The optimal modal control force, as described in Chapter

2, is

$$f_k(t) = g_k \omega_k u_k(t) + h_k \dot{u}_k(t). \quad (4.4)$$

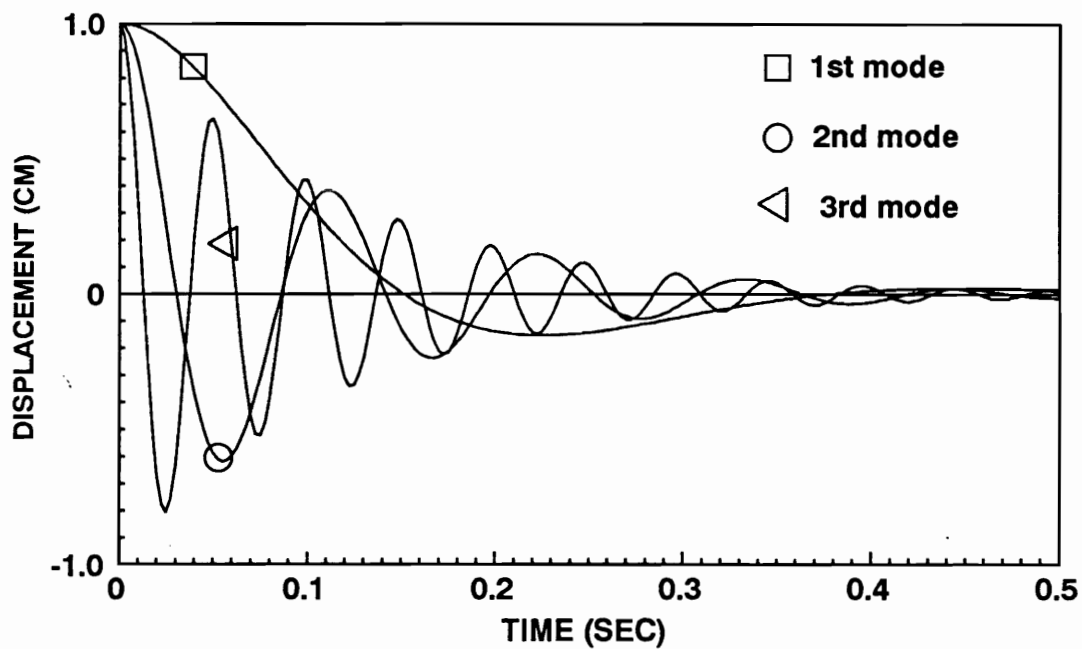
Figure 4.1 (a) shows vibrations of the first three modes. Figure 4.1 (b) shows the optimal modal control forces corresponding to the modal vibrations generated by initial displacements. These two figures demonstrate that the abstract modal control forces for each modal vibration of specific initial conditions are deterministic-function of time for each specific initial condition. Therefore, IMSC produces a vector of modal control forces, elements of which are state functions of time.

In chapter 3, the moments exerted by the piezoelectric actuators and the modal control forces were found to be related to each other by the following relationship:

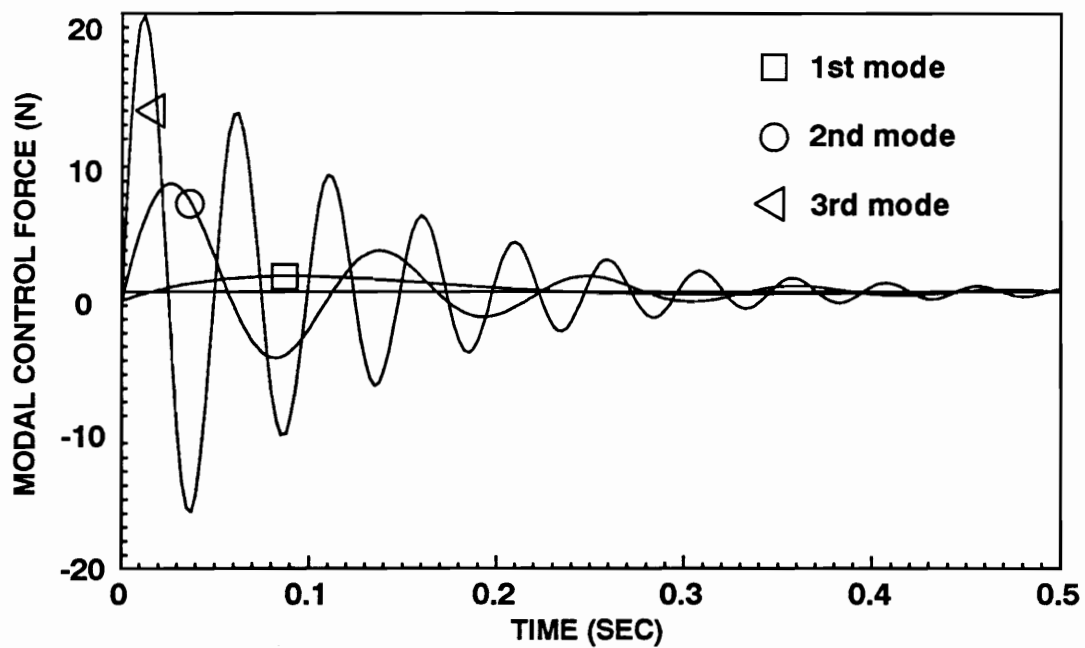
$$\begin{Bmatrix} f_1 \\ f_2 \\ \cdot \\ \cdot \\ \cdot \\ f_m \end{Bmatrix} = \begin{bmatrix} B_{11} & B_{12} & \cdot & \cdot & \cdot & B_{1n} \\ B_{21} & B_{22} & \cdot & \cdot & \cdot & B_{2n} \\ \cdot & \cdot & \cdot & \cdot & \cdot & \cdot \\ B_{m1} & B_{m2} & \cdot & \cdot & \cdot & B_{mn} \end{bmatrix} \begin{Bmatrix} M_1 \\ M_2 \\ \cdot \\ \cdot \\ \cdot \\ M_n \end{Bmatrix} \quad (4.5)$$

Here Matrix [B] is the so-called modal participation matrix, which is determined by the actuator location and dimensions.

Because vector $\{M\}$ is the actual moment exerted by the actuators, the magnitude of its components will be the main concern. Two arguments can be made at this point. The first argument is that the modal participation matrix directly affects how large the actual control moments must be to produce the abstract modal control forces $\{f\}$.



(a)



(b)

Figure 4.1: Controlled modal vibrations and optimal modal control forces

The second argument is that the modal participation matrix has different effects on different distributions of the modal vibrations.

The second argument can be visualized by referring to in Figure 4.2. In figure 4.2, the first two modal control forces are assumed to fall in the circle, shown at the left of the figure. Each point inside the dark circle will correspond to a possible modal control force vector(here, only for the first two modes). Then by choosing different modal participation matrices B , the modal control forces are transformed to different actual actuator moments, each of which falls into one of the three oval domains in the M_1 and M_2 coordinate systems, corresponding to the matrix B . A specific point marked by the circle is translated into three points in the actual control moment coordinates by different modal participation matrix B . In two cases, referring to the top and bottom oval domains, the modal control forces are enlarged; in the middle case, the modal control forces are reduced. It is shown clearly that the modal participation matrix affects to a great extent the translation of the modal control forces into the real control moments.

The modal participation matrix will have a very complex effect on the translation from modal control forces into actual control moments. The transformation effects are dependent on the type of combinations of modal forces. As pointed out earlier, the top case in Figure 4.2 shows enlarged actual control moments for the point marked by the circle; however, the point marked by the square is reduced. A conclusion can be reached that the transformation function of the modal participation matrix varies with respect to the different modal control force vectors.

Because the modal control force vector depends on the initial conditions, which are

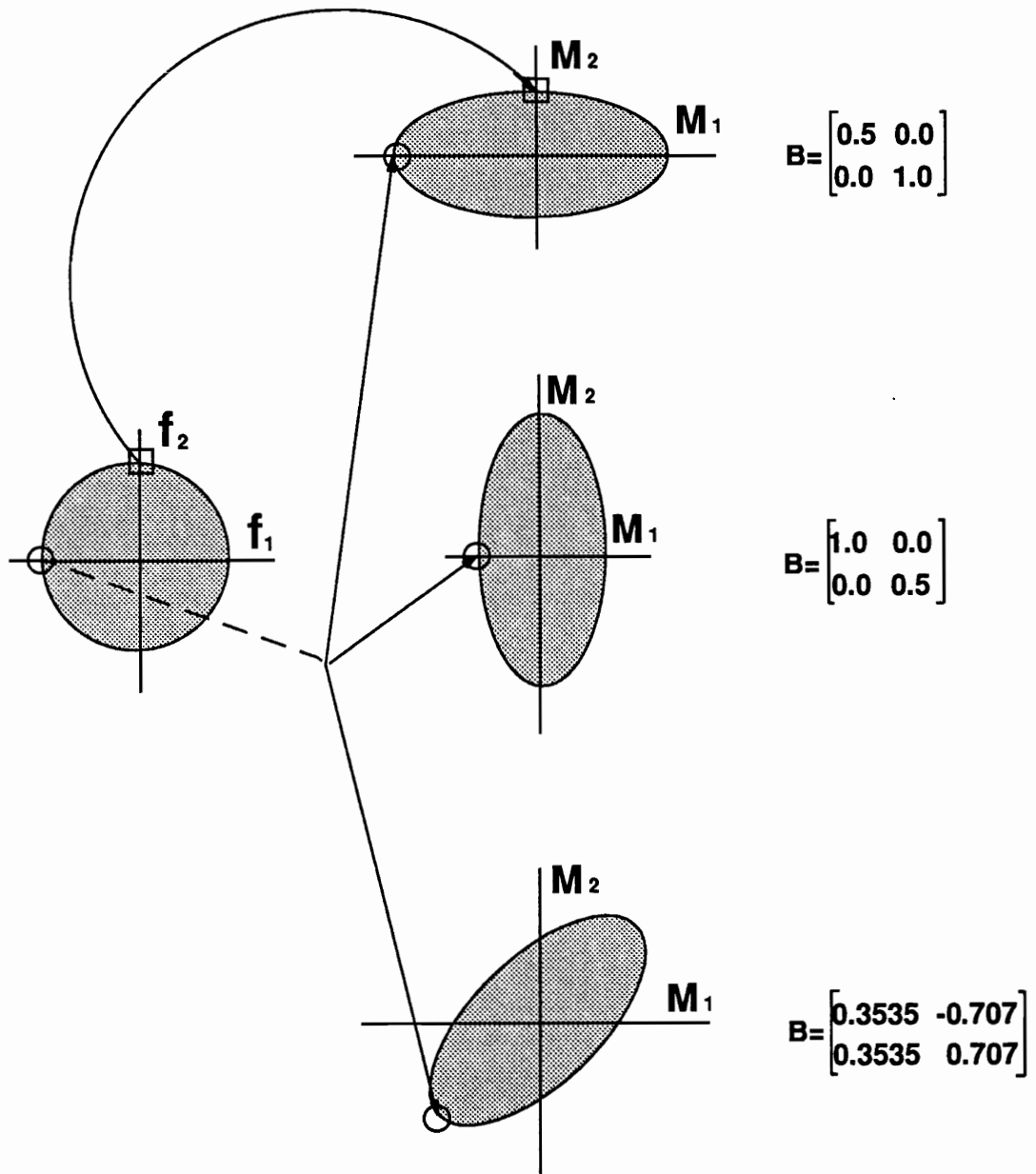


Figure 4.2: Transformation of modal control forces into actual control moments

not deterministic, and time, the modal control forces are treated as random variables, which randomly distributed in the modal forces domain according certain probability intensity function. As functions of the modal control forces, the actual control moments are also random variables.

The modal participation matrix plays as a parameter in the function relating these two sets random variables: the modal control forces and actual control moments. The final objective of this study is to find the optimal actuator locations and dimensions. The optimal actuator design will yield a modal participation matrix which requires minimal mean actual control moment to implement the design control.

4.2 Minimization of Control Effort

4.2.1 Objective Function

The last section demonstrated that the actuator locations and sizes affect the magnitude of the actual control efforts required to realize the modal control forces designed by Independent Modal Space Control. In this section, the derivation will be conducted to formulate the objective function for minimizing the control effort by properly locating and sizing the actuator. The search of the actuator locations and dimensions should be in a manner such that the design constraints of the piezoelectric actuators are satisfied. Defined in chapter 3, the vector $\{M\}$ is a collection of the moments generated by the piezoelectric actuators. The smaller the elements of $\{M\}$ are, the lower control efforts are. Although terms in $\{M\}$ can be either positive or negative, it is the magnitudes of their elements that are of greatest concern. Therefore, it is natural to use the norm of the vector, $\{M\}^T\{M\}$, as the quantity to minimize.

As mentioned before, the IMSC approach requires that the number of the controlled modes be equal to the number of actuators ($n_{act}=n_{modc}$). This implies that the modal participation matrix will be a square matrix. An inverse of the matrix will exist, if the system is controllable. This requirement of equal number of actuators as controlled modes will be complied with in this chapter. Using Eq. (3.53), the actual control moment vector can be found

$$\{M\} = B^{-1}\{f\}. \quad (4.6)$$

Therefore, the norm of the control moment vector is

$$\{M\}^T \{M\} = \{f\}^T B^{-T} B^{-1} \{f\}. \quad (4.7)$$

The matrix B^{-1} can be decompose into the product of two unitary orthogonal matrices and a diagonal matrix:

$$B^{-1} = V[\lambda_i]V^T \quad (4.8)$$

where $[\lambda_i]$ is a diagonal matrix, and λ_i is the i th eigenvalue of matrix B^{-1} . V is an orthogonal matrix consisting of the eigenvectors of B^{-1} . Substituting Eq.(4.8) into Eq. (4.7), the norm of the control moment vector becomes

$$\{M\}^T \{M\} = \{f\}^T V[\lambda_i]V^T V[\lambda_i]V^T \{f\}. \quad (4.9)$$

Because of the orthogonality of matrix V , $V^T V = I$,

$$\{M\}^T \{M\} = \{f\}^T V [\Lambda^2] V^T \{f\} \quad (4.10)$$

As discussed earlier, $\{f\}$ is assumed to be random. Therefore, the mean value of the control efforts is used

$$E[\{M\}^T \{M\}] = E[\{f\}^T V \Lambda^2 V^T \{f\}]. \quad (4.11)$$

Next, we define another vector $\{F\}$,

$$\{F\} = V^T \{f\} \quad (4.12)$$

where the terms in vector $\{F\}$ are

$$F_i = \sum_{j=1}^{nact} V_{ji} f_j. \quad (4.13)$$

Therefore, by defining this new vector, Eq. (4.11) will take a simpler form of

$$E[\{M\}^T \{M\}] = \sum_{i=1}^{nact} \lambda_i^2 E[F_i^2] \quad (4.14)$$

Here λ_i is the i th eigenvalue of matrix B^{-1} . The problem now is to find the solution of $E[F_i^2]$.

In order to obtain the mean values in Eq. (4.14), the following assumptions are made concerning the modal control forces:

- each modal control force considered will be within the range from -b to b;

- the modal control forces considered are uncorrelated with each other;
- each modal control force is uniformly distributed in the range from -b to b.

Based on these assumptions, the density function for the probability of n modes considered is (see Fig. 4.3)

$$p(f_1, \dots, f_n) = \frac{1}{(2b)^n} \quad (4.15)$$

Therefore, the mean value of the control efforts is, (Mendenhall, 1986),

$$E[F_i^2] = \int_{f_1} \dots \int_{f_{nact-1}} \int_{f_{nact}} \left(\sum_{j=1}^{nact} V_{ji} f_j \right)^2 \frac{1}{(2b)^{nact}} df_1 df_2 \dots df_{nact} \quad (4.16)$$

Expanding the summation term inside the integration and performing the integration yields

$$E[F_i^2] = \frac{b^2}{3} \sum_{j=1}^{nact} V_{ji}^2 = \frac{b^2}{3} \quad (4.17)$$

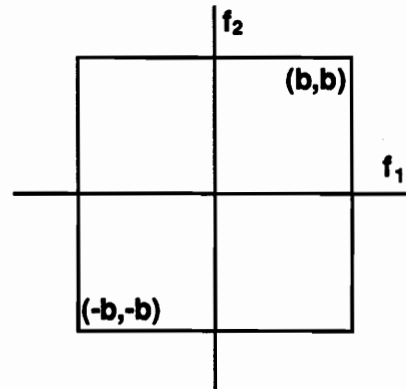
Substituting Eq.(4.17) into Eq. (4.14), the mean value of the control moments are found

$$E[\{M\}^T \{M\}] = \frac{b^2}{3} \sum_{i=1}^{nact} \lambda_i^2. \quad (4.18)$$

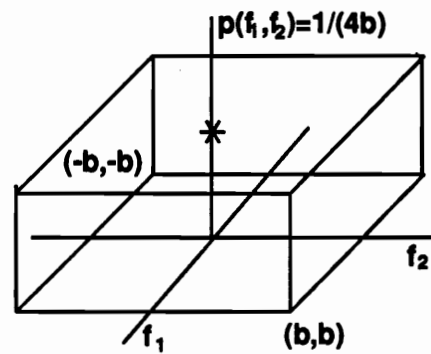
From Eq. (4.18), it can be determined that to minimize the control efforts, one must minimize the sum of the squared eigenvalues of B^{-1} .

$$Min.(E[\{M\}^T \{M\}]) = Min.\left(\frac{b^2}{3} \sum_{i=1}^{nact} \lambda_i^2\right). \quad (4.19)$$

(a) domain of three modal control forces



(b) probability distribution of modal control forces



(c) domain of three modal control forces

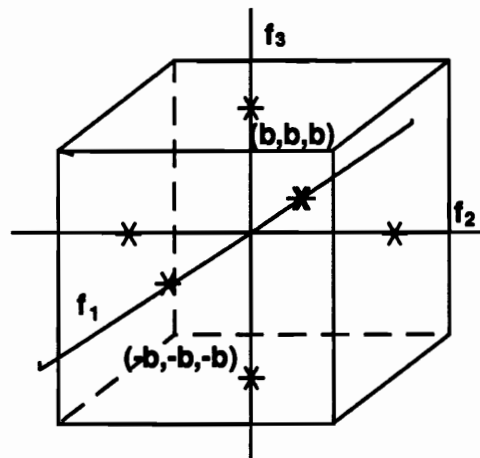


Figure 4.3: Demonstration of modal control force domains and probability distribution

Because a constant number will not influence the minimization process, the objective function becomes

$$Min.(E[\{M\}^T\{M\}]) = Min.(\sum_{i=1}^{nact} \lambda_i^2). \quad (4.20)$$

4.2.2 Constraints

The structure used as an example in this study is a beam simply-supported at two ends, which is shown by Figure 3.6. In this figure, the actuators and parameters describing a actuator are shown too. The design variables for each actuator are the location of its mid-point, a_i , and half its width, c_i , as shown in Figure 3.6. Each actuator consists of two patches symmetrically bonded on the top and bottom surface of the beam to eliminate the force of the actuators in lateral direction. The constraints on the the placement and size of m piezoelectric actuator on a uniform simply-supported beam are stated:

- The two actuators at both ends of the beam must be confined to the beam region. That is

$$G(x)_1 = a_1 - c_1 \geq 0; \quad (4.21)$$

and

$$G(x)_{nact+1} = L - (a_m + c_m) \geq 1; \quad (4.22)$$

where L is the beam length.

- Two adjacent actuators can not overlap. Thus, the constraints can be written as

$$G(x)_j = (a_j - c_j) - (c_{j-1} - c_{j-1}) \geq 0 \quad j = 2, 3, \dots, nact \quad (4.23)$$

4.2.3 Optimization Method

A summary of the derivation up to now and a comprehensive mathematical statement of the optimization problem are given as:

- Design variables:

$$\begin{array}{cccc} a_1 & a_2 & \dots & a_{nact} \\ c_1 & c_2 & \dots & c_{nact} \end{array}$$

- Objective function:

$$Min.(E[\{M\}^T\{M\}]) = Min.(\sum_{i=1}^{nact} \lambda_i^2); \quad (4.24)$$

- Constraints:

$$\begin{array}{ll} G(x)_1 & = a_1 - c_1 \geq 0; \\ G(x)_j & = (a_j - c_j) - (c_{j-1} - c_{j-1}) \geq 0 \quad j = 2, 3, \dots, nact; \\ G(x)_{nact+1} & = L - (a_m + c_m) \geq 1; \end{array}$$

- Side bounds on the design variables

$$\begin{array}{l} 0 \leq a_i \leq L; \\ 0 \leq c_i \leq L \end{array}$$

It is shown that this is an optimization problem of a nonlinear objective function with multiple design variables, with linear constraints, and side bounds on the design variables.

In the optimization process, Newton's method(Cooper, 1970) with approximate second derivatives is used in the direction finding of the unconstrained minimization. An extended interior penalty function formulation is used for the inequality constraints. A brief discription of the algorithm is given in the following section. More detailed theory and the numerical methods are found in reference of Thareja and Haftka (1985), Haftka (1985), and (Kavlie, 1971).

Extended Interior Penalty Function Method The idea of the penalty function method is to solve a constrained minimization problem by solving a sequence of unconstrained minimization problems. A modified objective function, therefore, must be defined which in some way incorporates the constraints.

The simplest way of doing this is to ensure that the new objective function becomes large when the constraints are violated or approached. By adding terms which have this behavior, multiplied by weighting factors which are successively reduced as the calculation proceeds. The sequence of unconstrained minima approaches the constrained minimum point of the design variables under certain conditions.

4.2.4 Structure Parameters

The simply-supported beam is used to demonstrate the effectiveness of the optimization procedures in this study. This beam has a length of 1m, Young's modulus

$E = 6.9 \times 10^{10} Pa$, and cross-sectional area moment of inertia $I = 1.125 \times 10^{-10} m^4$.

4.2.5 Actuator Locations and Dimensions

First the optimal designs are presented. The discussion of these designs follows at the end of this section. One notation should be explained here. An actuator i is denoted as (a_i, c_i) . Here the two numbers inside the parenthesis are the mid-point coordinate and the half length of the actuator.

Figure 4.4 shows the single actuator system designs when used to control the first, second, and the third mode. For controlling the first mode, the optimization optimization process gives only one design, $(0.5, 0.5)$, which means to cover the whole beam. For controlling the second mode, there are two optimal designs, $(0.25, 0.25)$, or $(0.75, 0.25)$. For controlling the third mode, three optimal designs, $(0.167, 0.167)$, $(0.5, 0.167)$, or $(0.833, 0.167)$. It should be noted that the optimal actuator length covers a whole lobe, in case of one actuator design. This is because the B matrix, now with only one element, has the maximum value when the actuator ends are at the two adjacent nodes of the controlled mode. More intuitively, the actuator has the most authority over the controlled mode when it can exert a moment pair of opposite direction at the nodes of the mode shape. The distance between the two moments should be as great as possible, as long as they can still enhance each other. If a actuator length covers beyond the lobe, the moments exerted at the two ends of the actuator will have cancelling effect on each other in controlling a specific mode.

Figure 4.5 is the optimal design for two actuators when used to control two modes. The cases shown control the first and second mode, the first and third mode, and the second and third mode. Figure 4.6 shows the optimal designs for three actuators

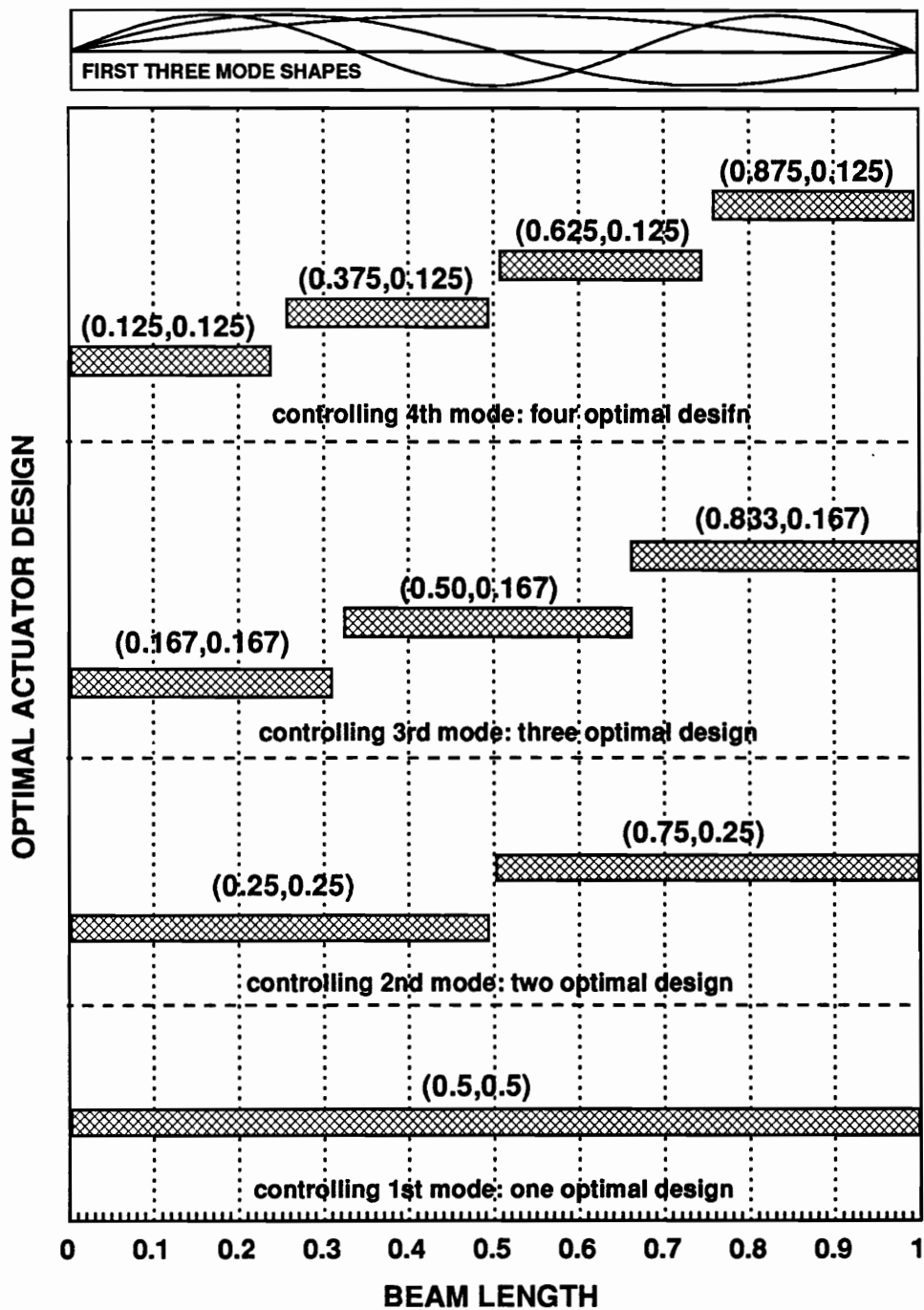
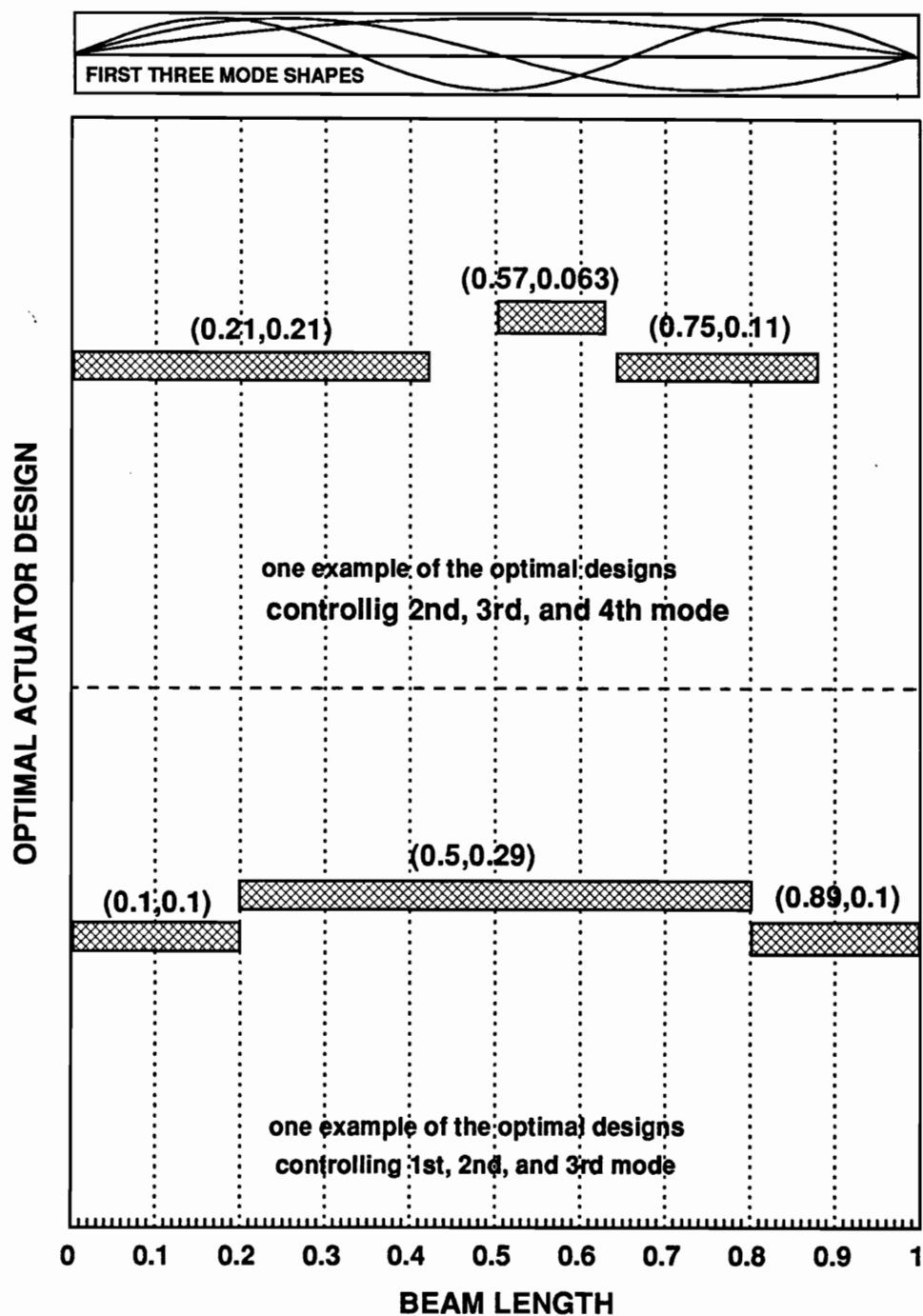


Figure 4.4: Optimal actuator designs:
one actuator controlling one mode



**Figure 4.6: Optimal actuator designs:
three actuators controlling three modes**

used to control two different sets of modes. The first three, and the second, third and forth modes. In these designs, it can be seen that the actuators cover most if not all of the beam. This agrees with the previous observation that the length of the actuators determine their authority. However, when some modes are skipped, as first and second modes showed in Fig. 4.5, and the first mode showed in Fig. 4.6, there are will be some areas of the beam which the actuators do not cover.

The optimal actuator design should yield higher control efficiency. Figure 4.7 demonstrates this effect. For certain modal control forces be realized, various actuator designs require the piezoelectric to apply different moments. It is clearly shown in Fig. 4.7 that the optimal design has a significantly smaller actuator moment than those of the non-optimal ones. It is interesting to observe that the moments become very large as the length of the actuator becomes shorter. The design of (0.5,0.1) needs a moment which is almost five times as large as the optimal design.

In two actuator cases, the number of involved parameters increases. Comparing the performance of the optimal and non-optimal designs is not so straightforward. A different approach is used to compare the performances of the optimal and non-optimal designs. Figure 4.8(a) shows the domain in which the modal control forces f_1 and f_2 fall. The actual control moment applied by the actuators are obtained by transforming the points in this modal force domain into another domain of coordinates consisting of actual control moments M_1 and M_2 . Because the modal participation matrix B is full rank, the translation is 1 on 1. This means that for every single point in the modal domain there is one and only one image point in the real control moment domain. The reverse is also true. The dark skewed rectangular area in Fig. 4.8(b) shows image for the square domain of the modal control forces in Fig. 4.8(a),

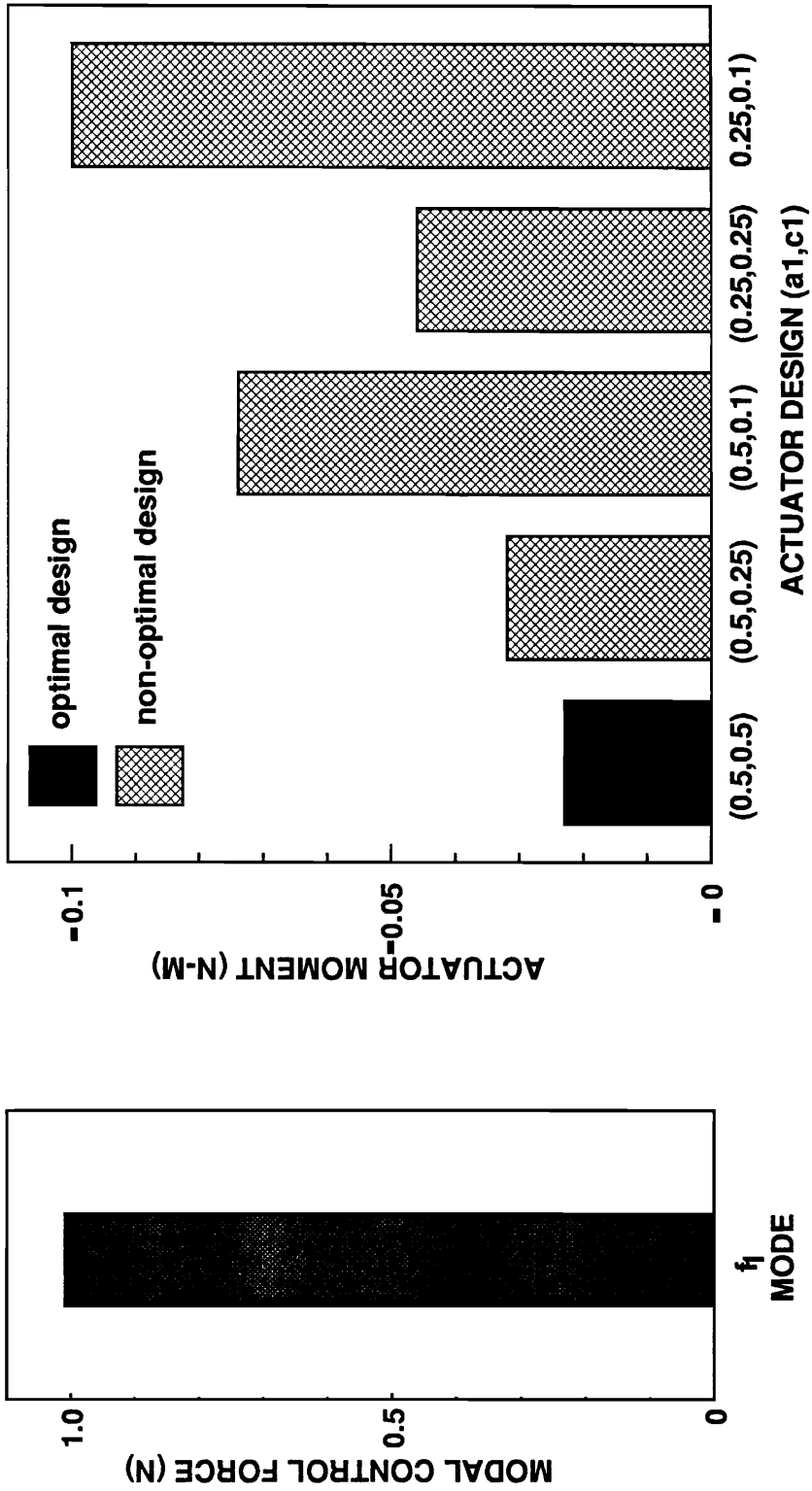
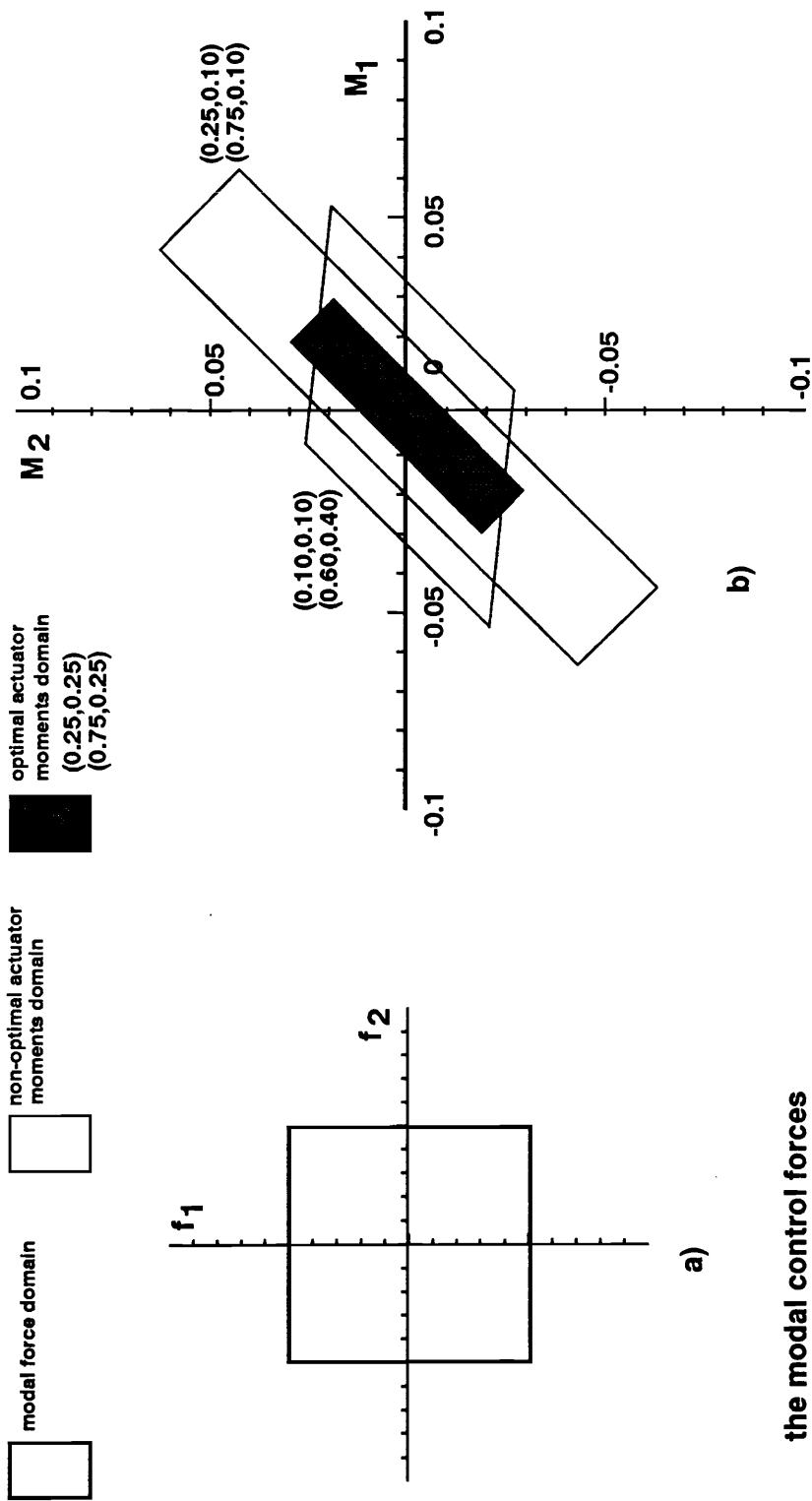


Figure 4.7: Modal forces transformed into actuator moments
when different actuator design are chosen



the modal control forces
are assumed to be within
a square domain

different actuator design transform modal
control forces into different actuator moment domain

Figure 4.8: Comparison between different actuator designs
using 2 actuators to control 1st & 2nd modes

using the optimal designs, $(0.25, 0.25)$ and $(0.75, 0.25)$. Also in Fig. 4.8(b), the two quadrilateral areas bordered by lines are the actual control moment domains when two non-optimal designs are used. Both moment domains of the non-optimal designs have larger areas than the optimal design. Therefore, the same modal control forces non-optimal design will more likely require a larger moment than the optimal design. One thing must be pointed out, not every actual control moment in the optimal design is smaller than the non-optimal counterpart. To demonstrate, in Fig. 4.8(b), the domain indicated by dark rectangular has two corners beyond one of the domain of the non-optimal design. As mentioned in the introduction, the optimal design sought is for a general situation in which all of the points in the modal domain are assumed equally likely to appear or to have uniform probability distribution in the specified modal control force domain. As long as the mean value of the moment of the optimal design under various conditions are superior to those of the non-optimal ones, the optimal design will satisfy the requirements.

Demonstrations of performances of three actuator designs will require a 3-dimensional figures which cannot be viewed clearly. Therefore, to present a comparison between control efforts required by various designs, the area of actual control moment domain is used as index for the corresponding to the actuator system design. Figure 4.9 shows the comparison between the applied moment's domain area from an optimal design and a non-optimal designs for a three actuator system. The bar shows the volume of the moments domain for different actuator designs. The optimal design has a smaller domain volume. Thus the optimal design will more likely generate smaller actuator moments than the non-optimal designs.

To give a better description of the effects of the optimal design, Figs. 4.10 and 4.11

modal force domain
for three modes
are a cubic $b=1$

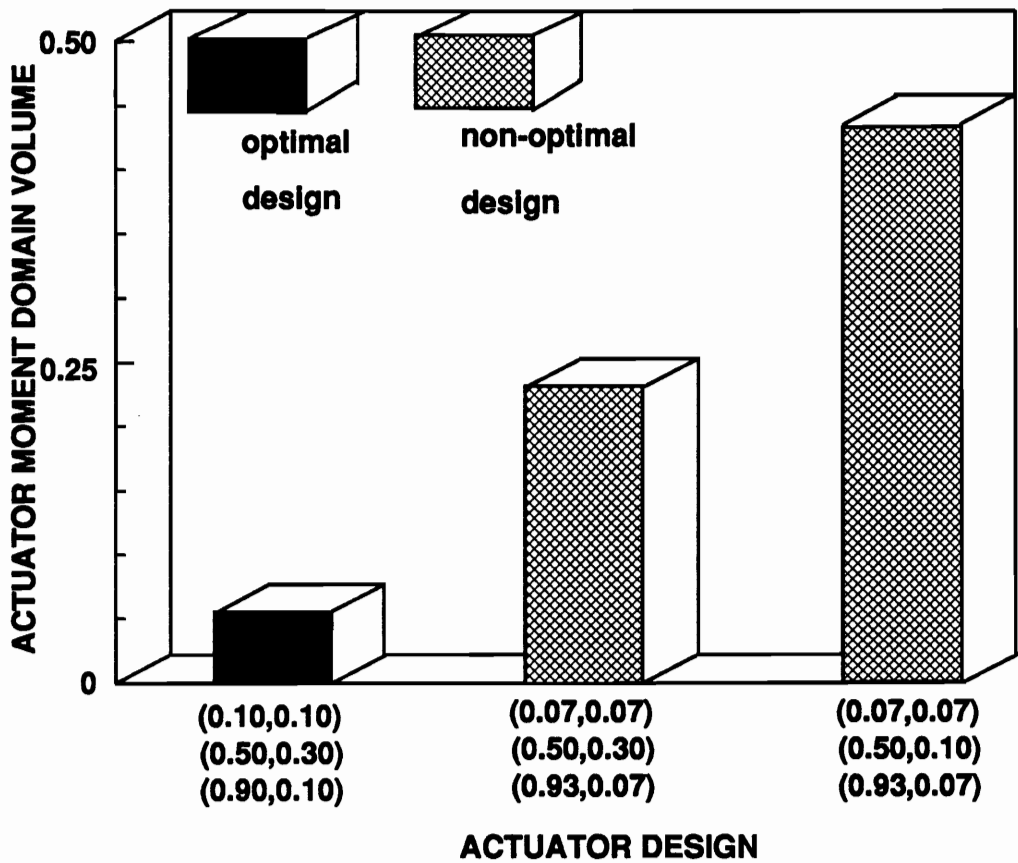
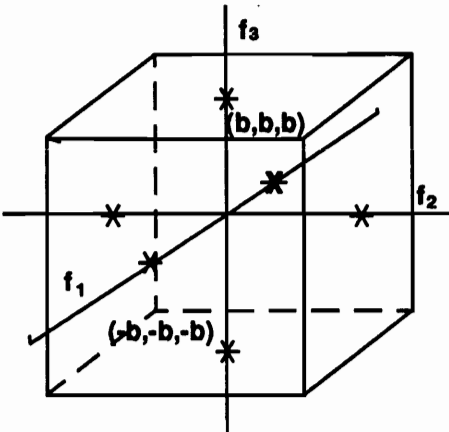


Figure 4.9: Comparison between volumes of domains of actuator moments for different three actuator designs

are drawn. These two figures are the time history of the moments applied by the actuators. Each mode has been given one centimeter initial displacement. For the one actuator and two actuator systems, Figs. 4.10 and 4.11,, respectively, indicate that the optimal designs yield smaller moments than the non-optimal ones.

Figures 4.12 and 4.13 introduce the subject which will be studied in the next section. In Fig. 4.12, only an initial displacement is given to the first mode. All other modes are set to have zero initial conditions. However, when controlling the first mode, the third mode is excited. The thick line in the figure represents the third mode. In figure 4.13, two actuators are used to control the the first two modes. Other modes should have no vibration. The first two modes are controlled, but the third mode is also excited. The following section investigates how the spillover can be reduced by adjusting the actuator locations and sizes.

4.3 Minimization of Control Effort With Spillover Consideration

As discussed in the last section, due to the discrete nature of the actuators, the control energy will not go exclusively into the controlled modes. The uncontrolled modes are also affected. This effect is known as control spillover. We want to determine the actuator locations and sizes such that the energy dumped into the residual modes is minimized. However, by taking into consideration the spillover, more constraints to finding the most efficient actuator designs for the control effort are added. The spillover consideration and the control efficiency are two conflicting design goals, and need to be balanced.

In the following discussions, it will be assumed that the first n modes are controlled.

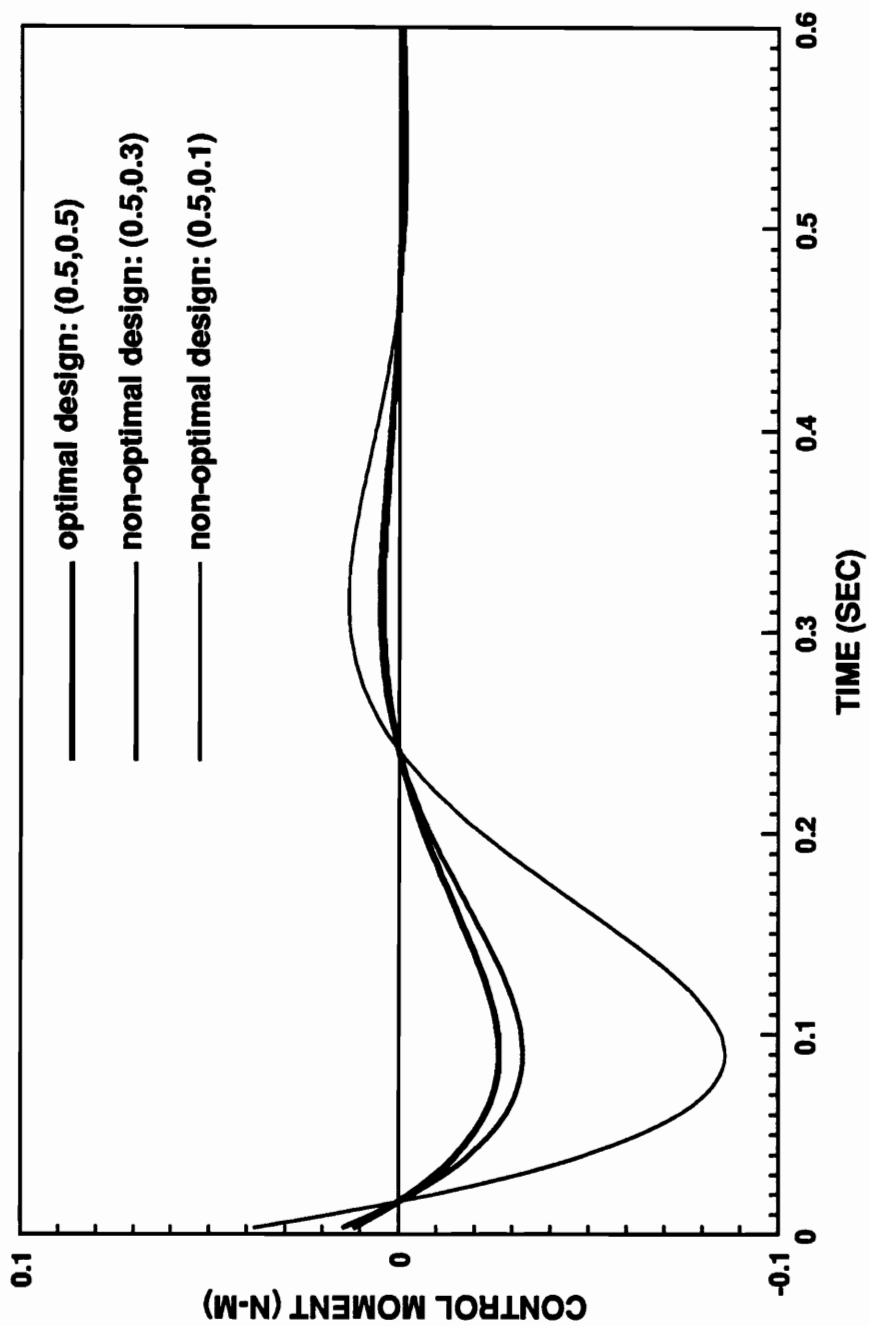
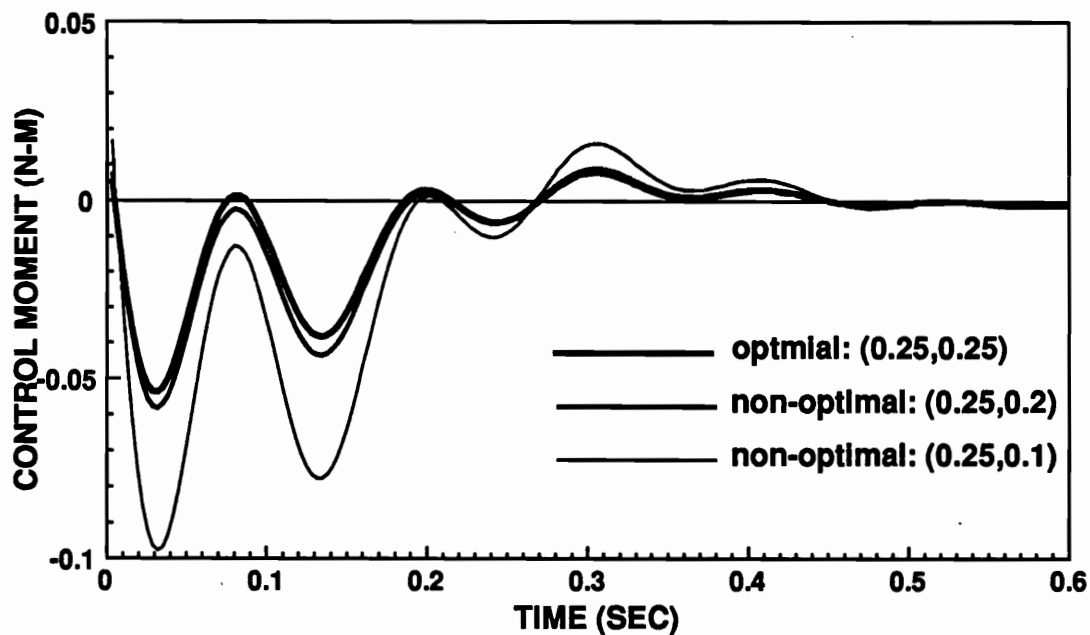
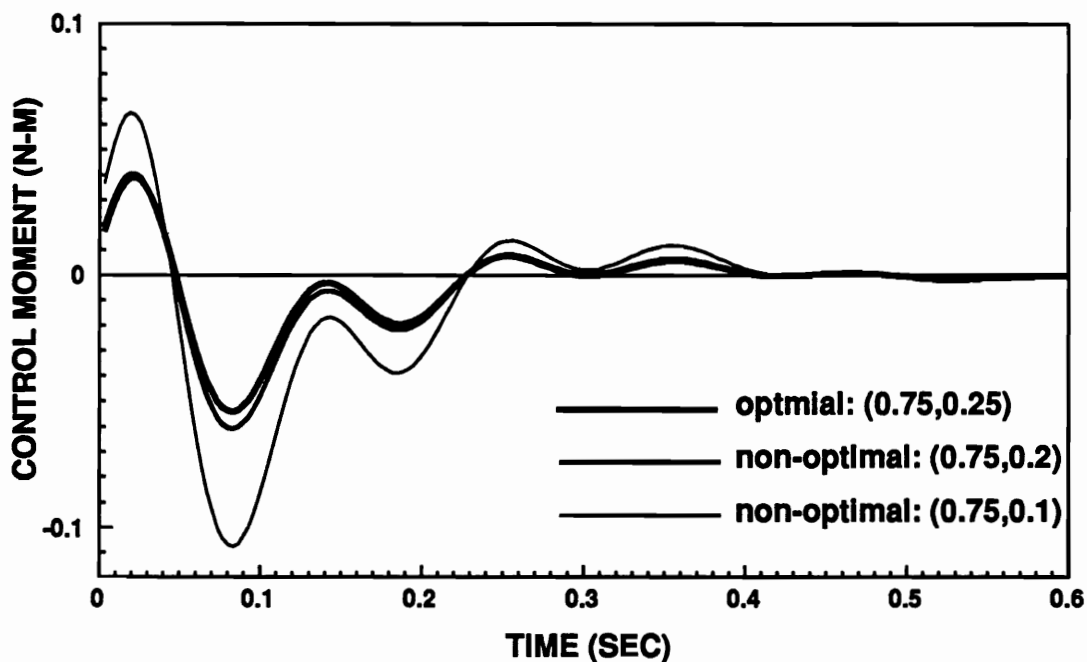


Figure 4.10: Time history of actuator moment when using one actuator to control the first mode



(a) MOMENT OF THE FIRST ACTUATOR



(a) MOMENT OF THE SECOND ACTUATOR

Figure 4.11: Time history of control moments for optimal and non-optimal designs (when two actuators control first two modes)

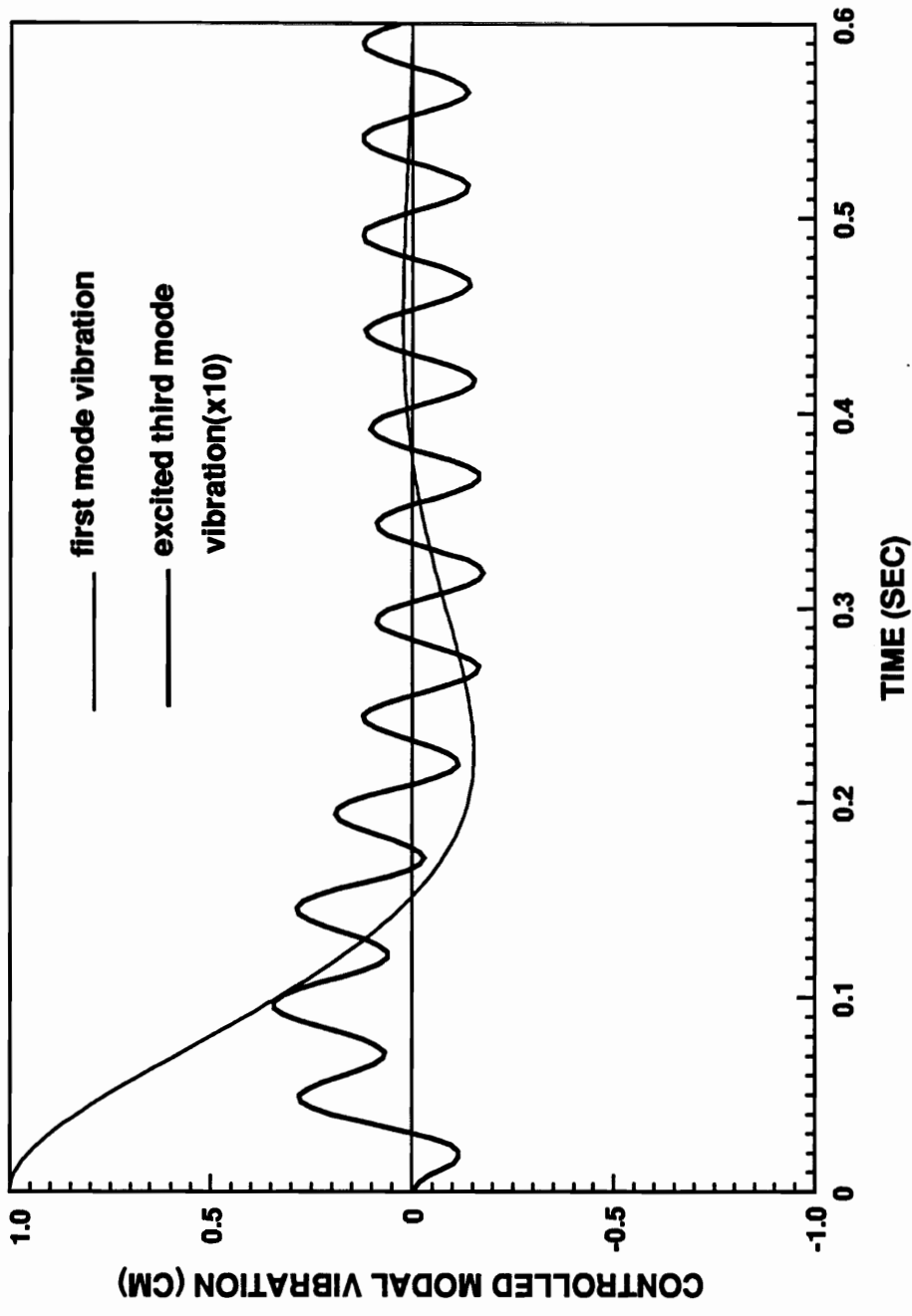


Figure 4.12: Spillover Into the third mode when using one actuator, (0.5,0.5), to control the first mode

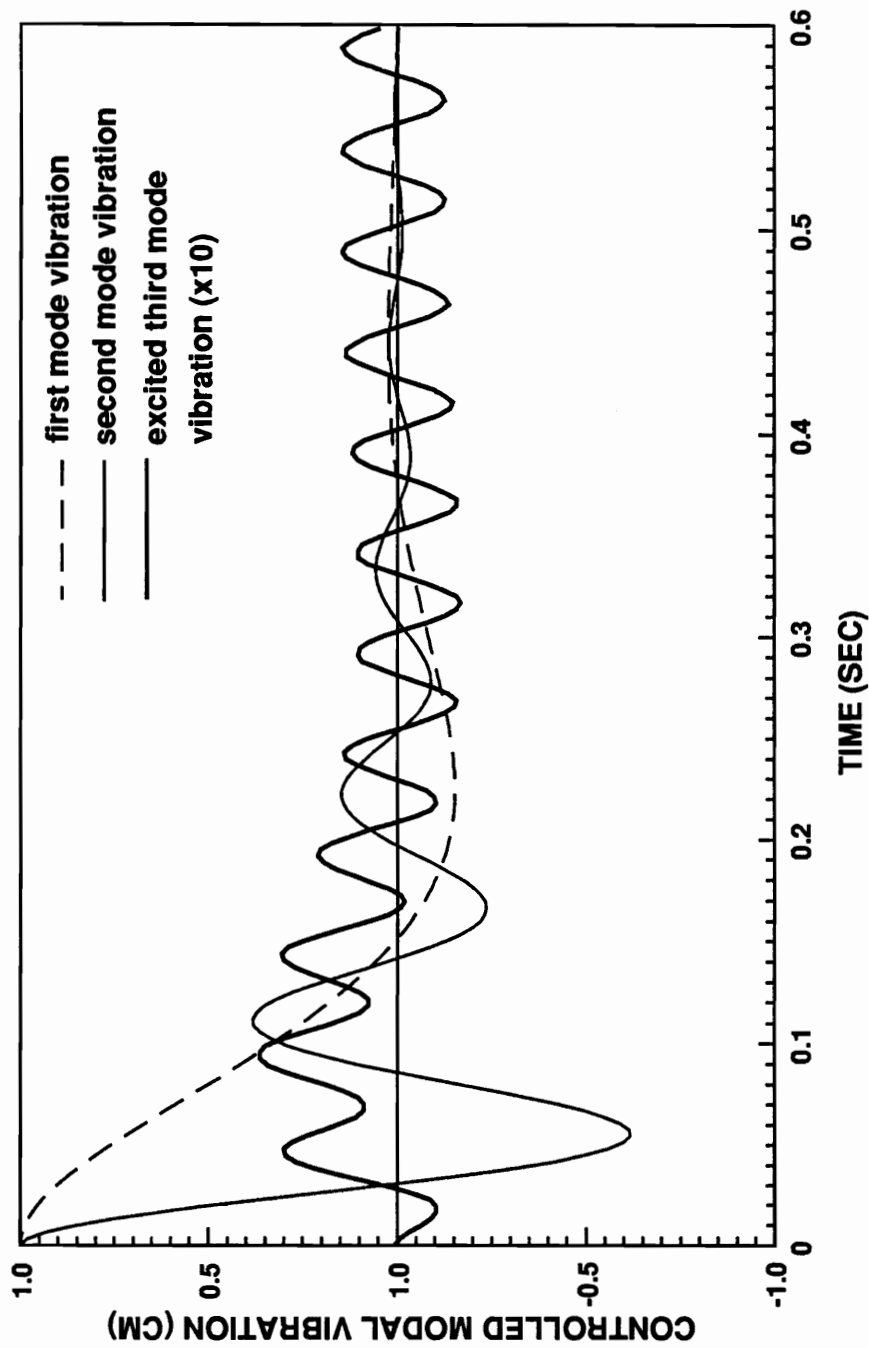


Figure 4.13: Spillover into the third mode when using two actuators to control first two modes
actuator design: (0.25,0.25) (0.75,0.25)

The energy spilled into other modes beyond the n controlled modes can be shown to be

$$\begin{Bmatrix} f_{n+1} \\ f_{n+2} \\ \vdots \\ \vdots \end{Bmatrix} = \begin{bmatrix} B_{(n+1)1} & B_{(n+1)2} & \cdot & \cdot & \cdot & B_{(n+1)n} \\ B_{(n+2)1} & B_{(n+2)2} & \cdot & \cdot & \cdot & B_{(n+2)n} \\ \cdot & \cdot & \cdot & \cdot & \cdot & \cdot \\ \cdot & \cdot & \cdot & \cdot & \cdot & \cdot \end{bmatrix} \begin{Bmatrix} M_1 \\ M_2 \\ \vdots \\ \vdots \\ M_n \end{Bmatrix}. \quad (4.25)$$

In short form, if the subscription s is used to denote the spillover,

$$\{f\}_s = B_s \{M\}. \quad (4.26)$$

The norm of the spilled control efforts into the uncontrolled modes is

$$\{f\}_s^T \{f\}_s = \{M\}^T B_s^T B_s \{f\}. \quad (4.27)$$

Substituting Eq. (4.6) into the above equation, norm of the spilled control efforts becomes

$$\{f\}_s^T \{f\}_s = \{f\}^T (B_s B^{-1})^T B_s B^{-1} \{f\}. \quad (4.28)$$

For convenience of derivation, the matrix G_s is defined

$$G_s = (B_s B^{-1})^T B_s B^{-1} \quad (4.29)$$

Following the same derivation as in the last section, minimization of the sum of the

eigenvalues of G_s ,

$$Min.\{f_s\}^T\{f_s\} = Min.[\sum_{i=1}^{modc} \lambda_i(G_s)], \quad (4.30)$$

should give an actuator design which spilled minimal control effort into the residual modes. However, the reduction of the energy pumped into the controlled modes may yield a design which requires an increased control effort $\{M\}^T\{M\}$. Thus, there may be a conflict between maximizing the efficiency of pumping energy into the controlled modes and reducing the energy spilled into the residual modes. The following composite objective function is used to reach a compromise

$$Min.[\{M\}^T\{M\} + \alpha\{f\}_s^T\{f\}_s] = Min.[\sum_{i=1}^{nact} \lambda_i + \alpha \sum_{i=1}^{nact} \lambda_i(B_s)]. \quad (4.31)$$

Here α is a weighting parameter which determines the relative weighting of the spillover reduction and the control over the controlled modes. In actual practice, the number of modes considered as residual modes will be one or a few modes beyond the controlled modes instead of infinite number.

The following are three example cases demonstrating the minimization of the residual mode vibrations. Figure 4.14 gives the actuator design for a one actuator case controlling only the first mode with residual second and third modes. The designs are shown in Fig. 4.14 for various spillover weighting factors. It is clearly shown that when the weighting factor approaches zero, the actuator design becomes the optimal designs without spillover consideration. Figure 4.15 shows the actuator design of two actuators controlling the first and second modes with residual third and forth modes. Figure 4.16 is the actuator design for the same case as in Fig. 4.15 except

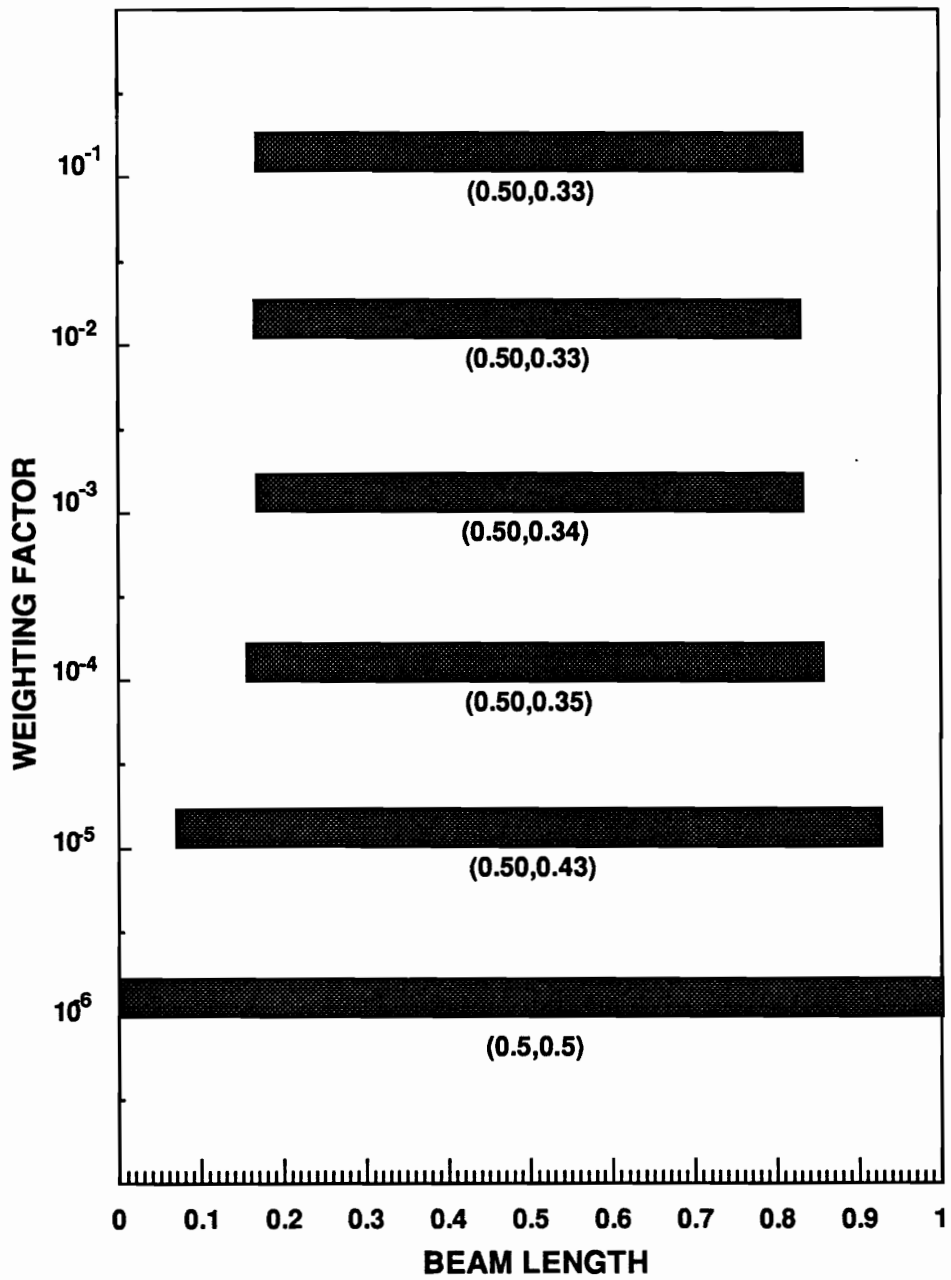


Figure 4.14: The actuator designs with different weighting factor when one actuator controlling first mode with second and third modes as residual

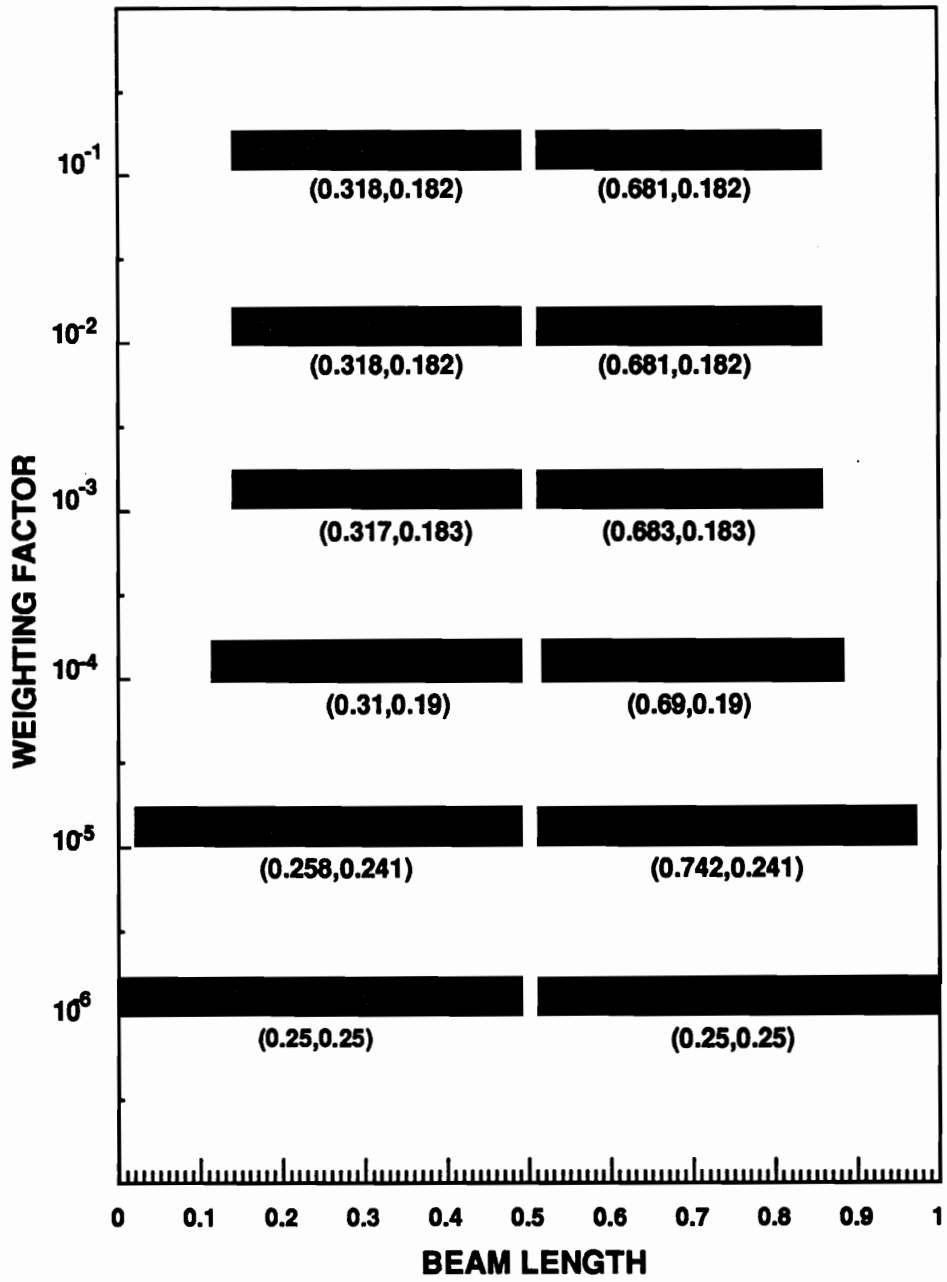


Figure 4.15: The actuator designs with different weighting factor when two actuator controlling first two modes with the third and forth modes as residual

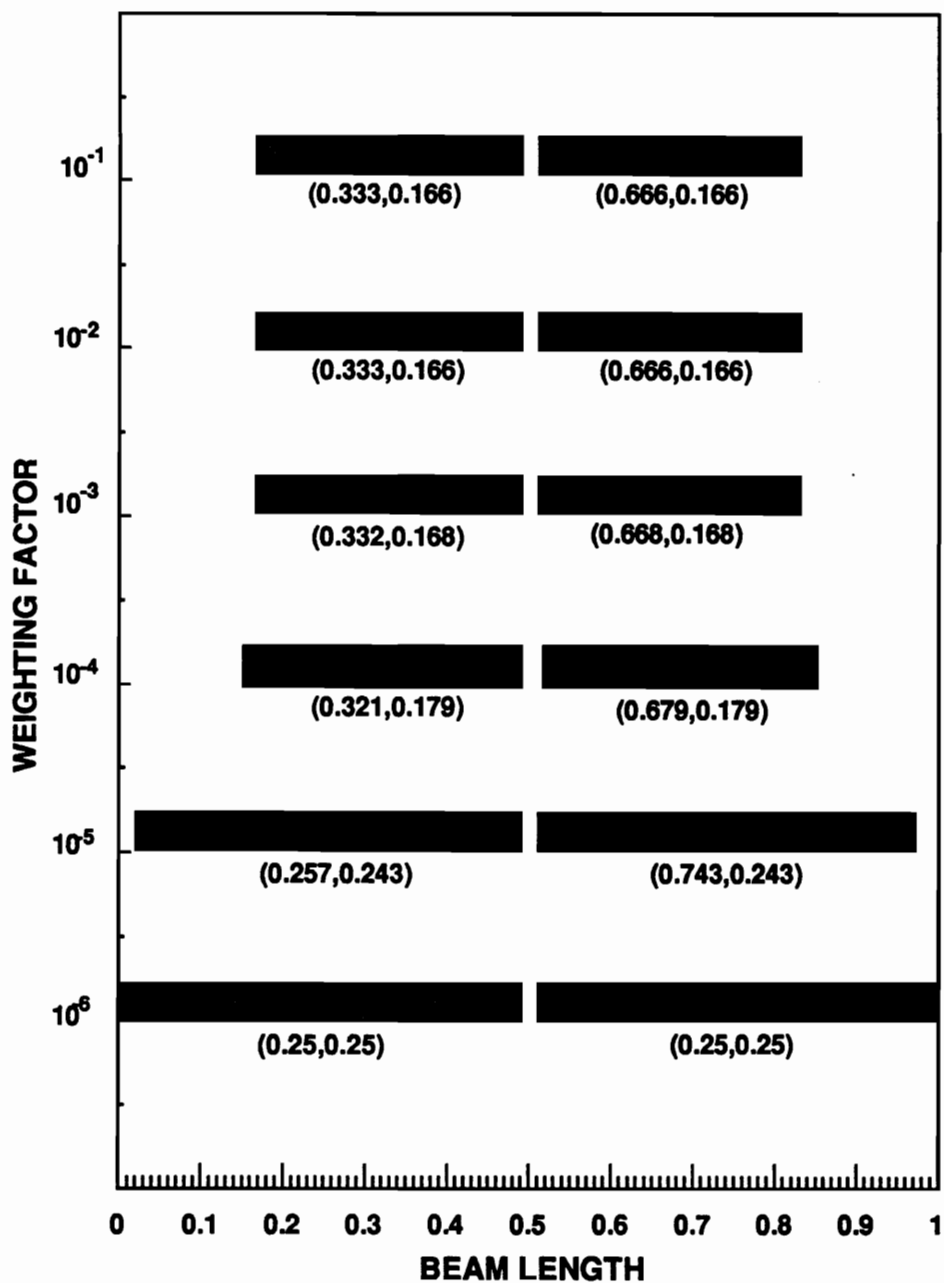


Figure 4.16: The actuator designs with different weighting factors when two actuator controlling first two modes with the third mode as residual

with only the third mode as residual.

The actuator length in the designs with spillover considerations is shorter than without spillover considerations. It has been discussed in last section that a shorter actuator has less control authority than a longer actuator. However, the shorter actuator is the result of compromising between reducing the spillover into the residual modes and increasing the control efficiency over the controlled modes. As pointed out earlier, the spillover reduction by actuator location design comes at the expense of increasing the control efforts. This will be shown more clearly in Figs. 4.18 and 4.20.

The performances of actuator designs with spillover considerations are demonstrated in Figs. 4.17 and 4.19. Figure 4.17 shows the third mode vibration due to the spillover when only the first mode has an initial displacement. The magnitude of the third mode vibration is reduced by a large factor in the actuator designs with the spillover considerations. When one actuator is used to control first mode, the actuator is always placed at the middle of the beam. At this position, the actuator is not able to excite the second mode. This is why only the third mode is shown here. The same trend of results are shown for the two actuators controlling the first two modes with a residual third mode in Fig. 4.19.

Figures 4.18 and 4.20 show the actual control moments with and without spillover considerations, for one actuator and two actuator systems, respectively. It can be observed that the control moments have large values when the spillovers are considered than when they are not considered. This is due to the shorter actuator lengths as a result of compromising the minimization of the control effort with the reduction of

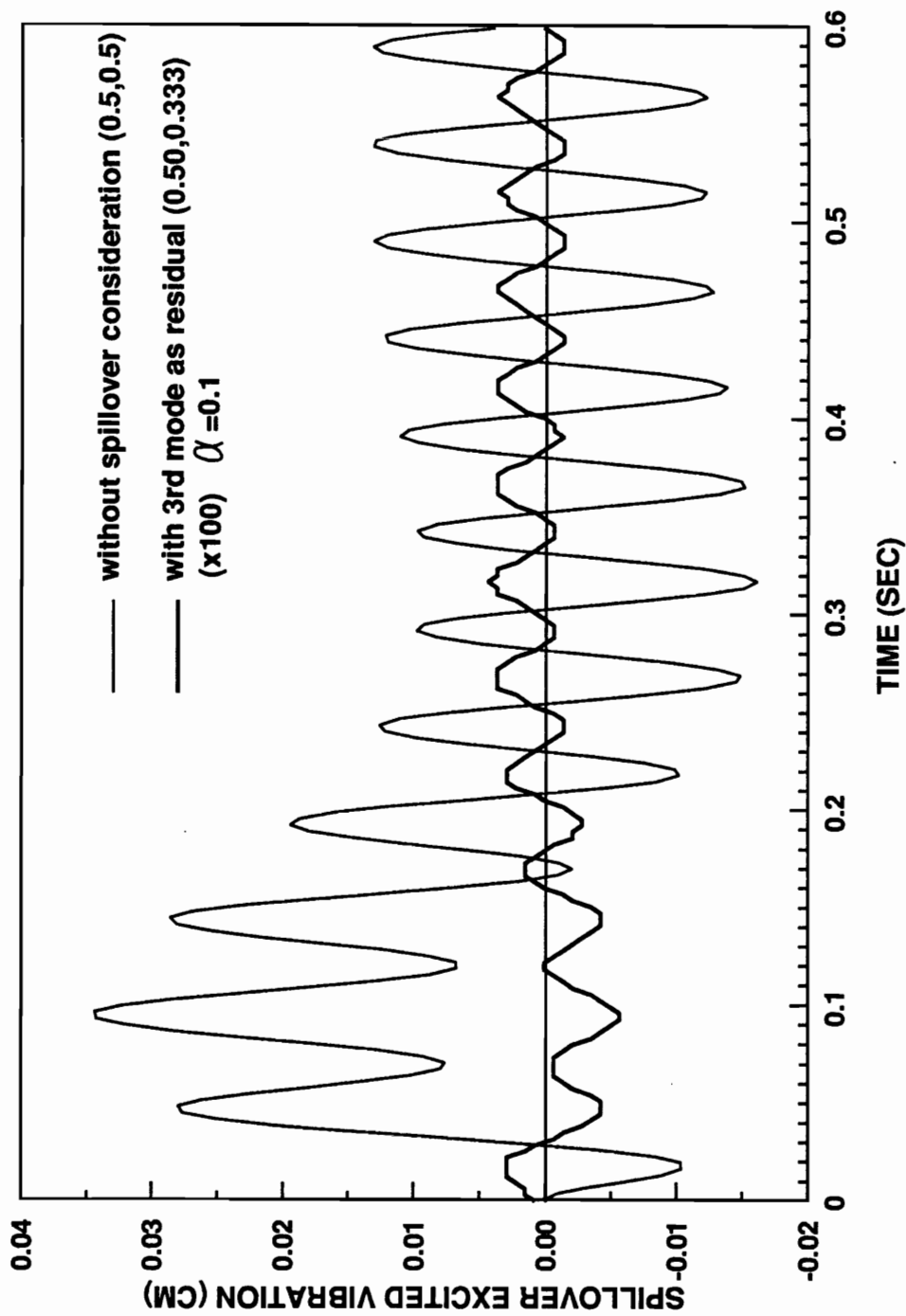


Figure 4.17: Residual mode vibrations before and after spillover consideration of one actuator design

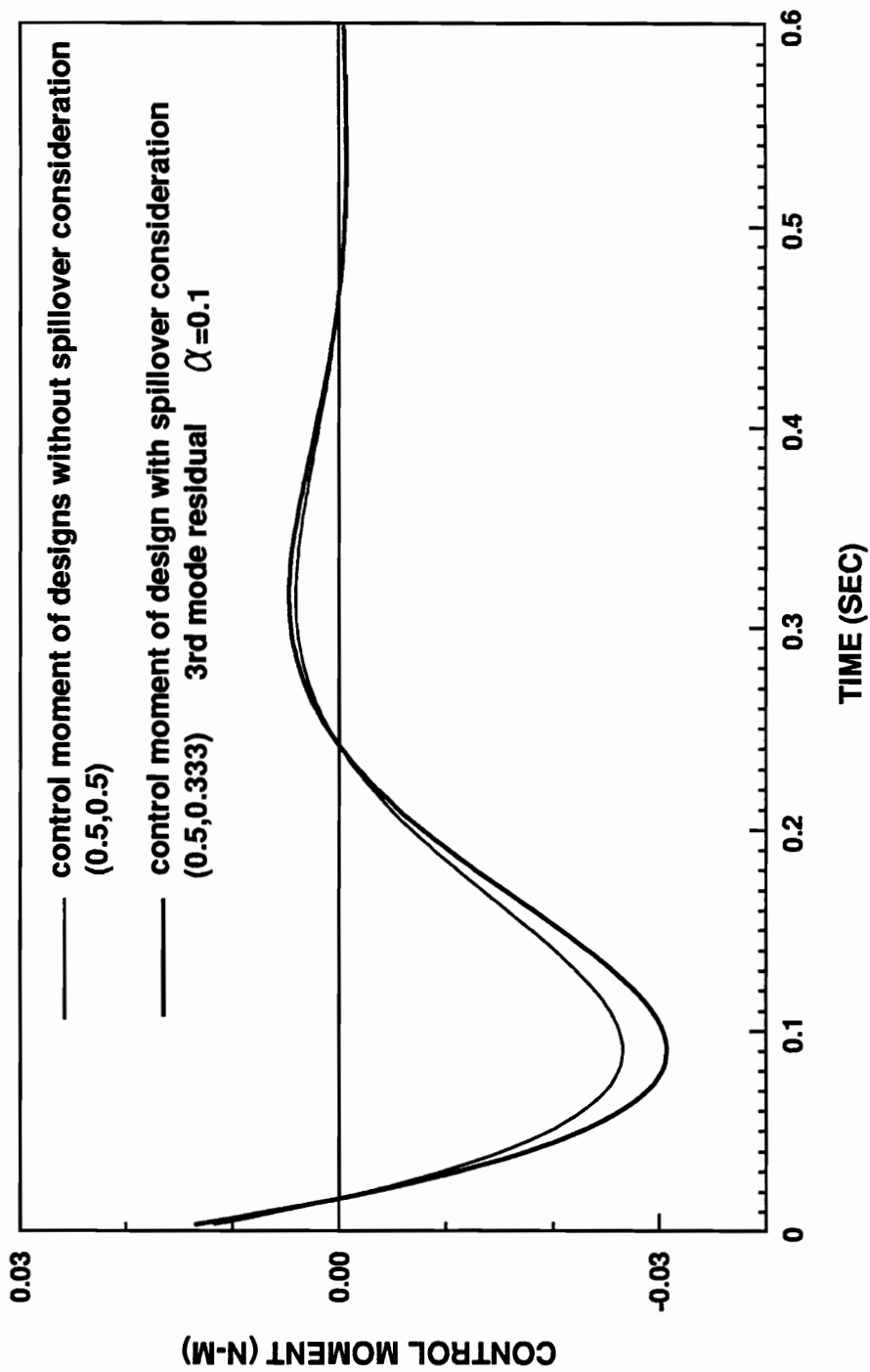


Figure 4.18: Comparison between control moments with and without spillover consideration of one actuator design

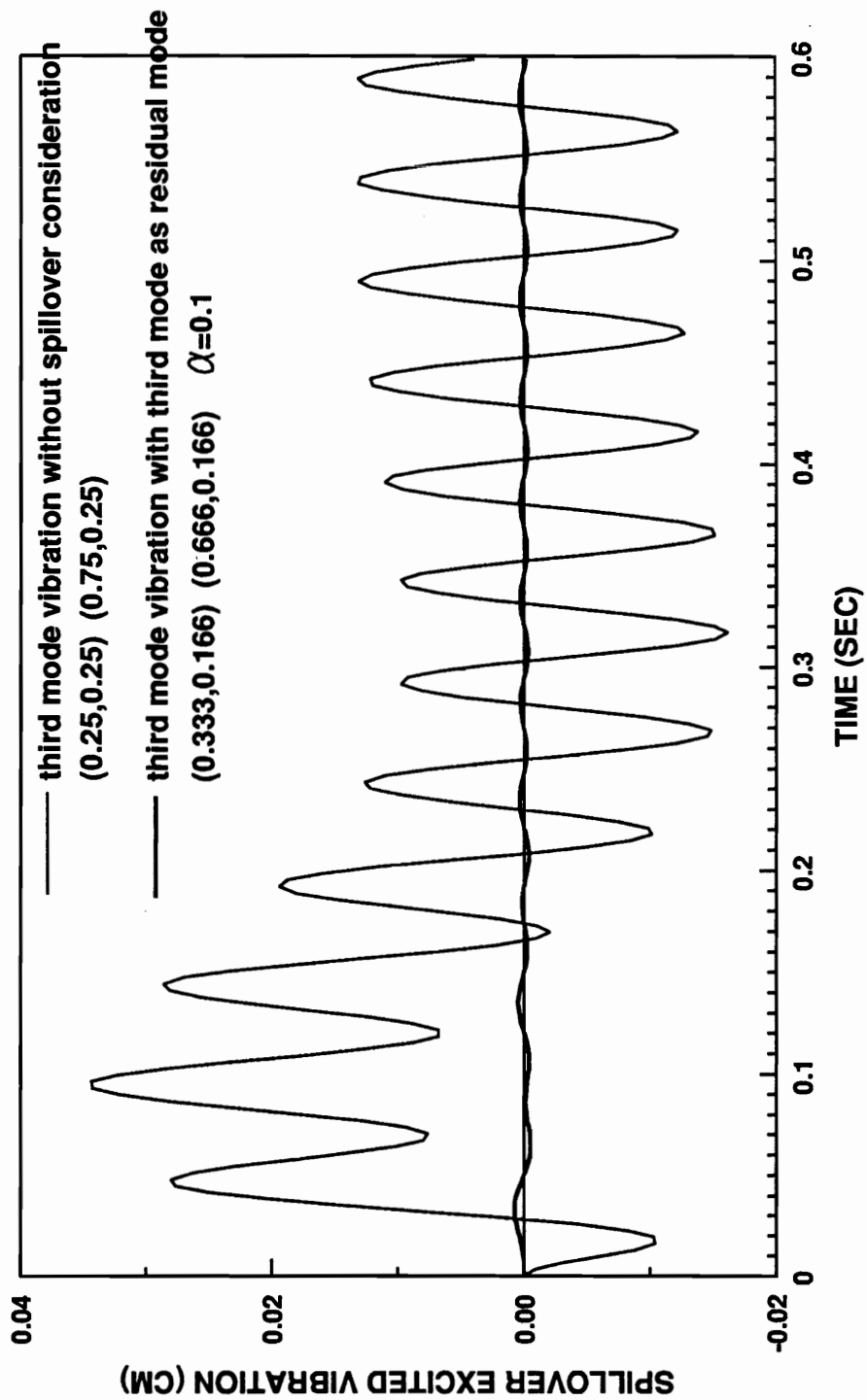
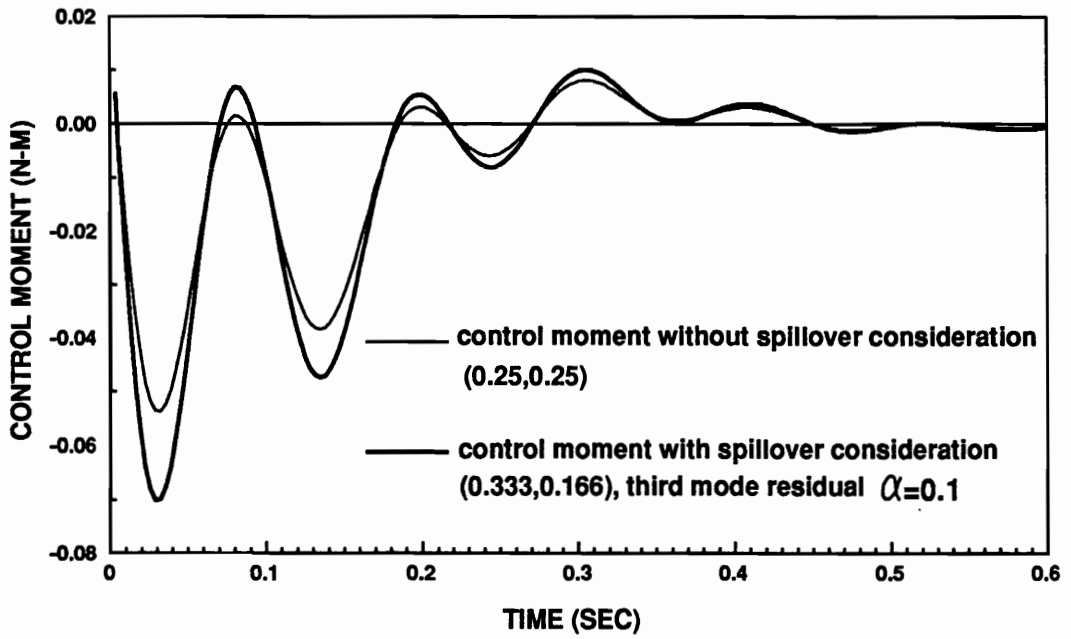
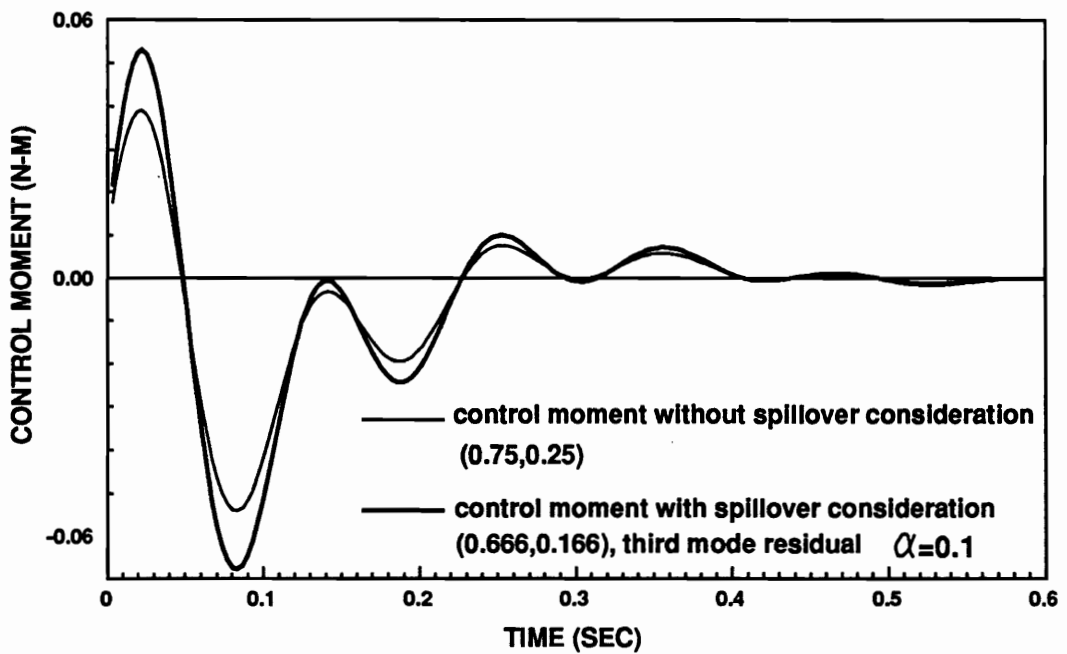


Figure 4.19: Residual mode vibrations with or without
spillover considerations for two actuator system



(a) First actuator moments



(b) Second actuator moments

Figure 4.20: Comparison of control moments between designs with and without spillover consideration for two actuators

spillover into the residual modes.

The methodologies derived in this chapter have been shown to be very effective by the simulated numerical results. The csae study of one, two, and three actuator designs have been given. The results show that the optimal actuator designs tend to have the largest length possible. However, the consideration of spillovers into the residual modes will make the actuators shorter, which reduces the actuator control authority over the controlled modes and spillover into the residual modes. The optimal designs give the best compromising combination of these two objectives according to the weighting factor specified to the spillover into the residual modes.

Chapter 5

FEWER ACTUATORS THAN CONTROLLED MODES

It has been discussed in the previous chapters that a limitation using IMSC is that the number of actuators required is equal to the number of controlled modes. The actuator number requirement can become a serious obstacle when a relatively large number of modes are required to be controlled such that the structural design can not accommodate the required number of actuators. In this chapter, this actuator number problem will be addressed. Approaches will be formulated and addressed to alleviate this stringent actuator requirement of IMSC.

The existence of the actuator requirement is a result of transforming the IMSC designed modal control forces into the actuator applied moments. From a mathematical point of view, this problem is due to a linear transformation from a smaller dimension space into a larger dimension space and is not a one-to-one transformation. It is the main concern of this chapter to study the transformation between the modal control forces and the actual actuator moments when the number of actuators is smaller than the number of the controlled modes. Therefore, the formulation and discussions in this chapter will assume that the number of actuators, n_{act} , is smaller than that of

the controlled modes *modc*.

5.1 Introduction

Three theorems of matrix theory and algebra, which will be referred to very frequently in this chapter, will be given and briefly described. A detailed introduction to the matrix algebra used in this chapter can be found in Foesythe (1967) and Halmos (1974).

Statement 1: If matrix U is unitary and real and $U^T U = I$, where I is *unit* matrix, U is called an orthogonal matrix. A transformation $Y=UX$ is then called an *orthogonal transformation*. Here both Y and X are vectors.

THEOREM 1: (Hohn, 1964, p255) In E_n , a linear transformation $Y=AX$ leaves the length of all vectors invariant if and only if it is a orthogonal transformation.

THEOREM 2: (Hohn, 1964, p255) em In E_n , the inner product $X^T Y$ is invariant under an orthogonal transformation.

Here E_n denotes a n -dimensional space.

THEOREM 3: Singular Value Decomposition (Lawson, Hanson, 1974, p18)

Let A be an $m \times n$ matrix of rank k . Then there is an $m \times m$ orthogonal matrix U , an $n \times n$ orthogonal matrix V , and an $m \times n$ diagonal matrix S such that

$$U^T A V = S, \quad A = U S V^T. \quad (5.1)$$

Here the diagonal entries of S can be arranged to be non-increasing; all of these entries are non-negative and exactly k of them are identically positive.

The diagonal entries of S are called the *singular values of A* , which are invariant for each matrix B .

The relationship between the modal control forces $\{f\}$ and the actual moments $\{M\}$ applied by the piezoelectric actuators was derived in Chapter 2 and is repeated here

$$\{f\}_{modc} = B_{modc \times nact} \{M\}_{nact} \quad (5.2)$$

where B is the modal participation matrix. Terms of B are functions of the actuator location and dimensions as well as the modes controlled. Since an assumption has been made in this chapter that $nact \leq modc$, the modal participation matrix is $modc$ by $nact$, a non-square matrix.

Applying the singular value decomposition theorem quoted at the beginning of this section to the modal participation matrix, the modal participation matrix can be decomposed into

$$B_{modc \times nact} = U_{modc \times modc} S_{modc \times nact} V_{nact \times nact}^T \quad (5.3)$$

where

$$S_{modc \times nact} = \begin{bmatrix} \sigma_1 & 0 & 0 & \dots & 0 & \dots & 0 \\ 0 & \sigma_2 & 0 & \dots & 0 & \dots & 0 \\ \dots & \dots & \dots & \dots & \dots & \dots & \dots \\ 0 & 0 & 0 & \dots & \sigma_k & \dots & 0 \\ 0 & 0 & 0 & \dots & 0 & \dots & 0 \\ \dots & \dots & \dots & \dots & \dots & \dots & \dots \\ 0 & 0 & 0 & \dots & 0 & \dots & 0 \end{bmatrix}, \quad (5.4)$$

The element σ_i are the singular values of the modal participation matrix B, and $\sigma_i > 0$ and $i \leq nact$. Substitution of Eq.(5.3) into Eq.(5.2) gives

$$\{f\}_{modc} = U_{modc \times modc} S_{modc \times nact} V_{nact \times nact}^T \{M\}_{nact}. \quad (5.5)$$

Multiply both sides by U^T and define

$$\{F\} = U^T \{f\} \quad \{\tilde{M}\} = V^T \{M\}, \quad (5.6)$$

then

$$\{F\} = U^T U S \{\tilde{M}\}. \quad (5.7)$$

From the fact that both U and V are unitary orthogonal, the above transformation will leave the lengths of the two vectors invariant. What happens, geometrically, is that the coordinate systems are rotated without changing the actual existence of $\{f\}$ or $\{M\}$. Through these transformations, the following form of the relationship

between modal control forces and actuator forces is derived:

$$\{F\} = S\{\tilde{M}\}. \quad (5.8)$$

The two orthogonal transformations introduced in Eq. (5.6) rotated the orientations of coordinates in the modal space and the actual moment space. Because the singular value matrix S is a diagonal matrix, Eq. (5.8) will show clearly the problem when fewer actuators are used to control more modes. It needs to be pointed out that the maximum value of the number of the singular values k in Eq. (5.4) is *act*, i.e., the number of the actuators. Substituting Eq.(5.4) into Eq.(5.8),

$$\begin{Bmatrix} F_1 \\ F_2 \\ \dots \\ F_{modc} \end{Bmatrix} = \begin{Bmatrix} \sigma_1 \tilde{M}_1 \\ \sigma_2 \tilde{M}_2 \\ \dots \\ \sigma_k \tilde{M}_k \\ 0 \\ \dots \\ 0 \end{Bmatrix} \quad (5.9)$$

Therefore, no $\{\tilde{M}\}$ can be found to satisfy the above equation if the number of actuators is less than the number of controlled modes. Because $\{M\} = V\{\tilde{M}\}$, no vector of piezoelectric actuator moments can make the two sides of the above equation exactly equal. In other terms, it can be said that, when a fewer number of actuators are used than the controlled modes, the actuators can not realize exactly the control forces in the modal space as designed by control theories.

Two remarks can be made at this point, first, the full advantages of *nact* actuators can be taken only when the modal participation matrix has a rank of *nact*, which will produce *nact* singular values. Secondly, since the relationship between the modal

control forces and moment applied by the actuators possesses the unequal nature as is shown by Eq. (5.9), the modal control forces cannot be exactly realized by acting the actuators. However, it is logical to assume that different methods of controlling the actuator moments will yield varying discrepancies from the designed modal forces when transformed into modal space. It can be further argued that there should be a set of actuator applied moments which give the minimal discrepancies between the designed modal forces and the realized ones than any other set. For the remainder of this chapter, the approaches to finding this optimal solution of the actuator control moments are investigated to lower the actuator number requirement.

5.2 Pseudoinverse Method

5.2.1 Introduction to Pseudoinverse Method

As shown in the last section, a fewer number of actuators than the number of controlled modes cannot realize exactly the modal control forces designed by IMSC. However, a specific set of the actuator control moments can be sought to yield the closest modal control forces to the designed modal control forces. This specific set of actuator moments is the compromise point. At this point, the control efforts from the actuators give certain control to all of the controlled modes even though none of the modes receives the control effort that is optimal.

With the above argument in mind, the norm of error vectors between the designed modal control forces and the realized modal control forces by piezoelectric actuators

are formulated:

$$\Phi = \{e\}^T \{e\} = \{\{f\} - B\{M\}\}^T \{\{f\} - B\{M\}\}. \quad (5.10)$$

By differentiating Φ with respect to $\{M\}$,

$$\frac{\partial \Phi}{\partial \{M\}} = -B^T \{\{f\} - B\{M\}\} - \{\{f\} - B\{M\}\}^T B, \quad (5.11)$$

and letting

$$\frac{\partial \Phi}{\partial \{M\}} = \{0\} \quad (5.12)$$

which yields

$$-B^T \{\{f\} - B\{M\}\} - \{\{f\} - B\{M\}\}^T B = \{0\} \quad (5.13)$$

or

$$-B^T \{\{f\} - B\{M\}\} = \{0\} \quad (5.14)$$

$$B^T B\{M\} = B^T \{f\}. \quad (5.15)$$

To take full advantage of the actuators, the rank of B is retained to be *nact* which

yields an inverse of $B^T B$. Therefore, control moments are

$$\{M\} = (B^T B)^{-1} B^T \{f\}. \quad (5.16)$$

The actuator moments thus obtained are the least squares solution of the equation system relating the modal control forces and the actuator applied moments. The expression derived above is a type of inversion of a singular system of linear equations and is called the *pseudoinverse*. We define B^+ to be the pseudoinverse of B,

$$B^+ = (B^T B)^{-1} B^T \quad (5.17)$$

This solution has been adopted by Lindberg(1982) to treat the fewer number of actuators than controlled modes case.

5.2.2 Essence of Pseudoinverse Method

Define

$$\{\tilde{f}\} = B\{M\} \quad (5.18)$$

which is the realized modal control forces by applying the actuator moments $\{M\}$. Substitute the pseudoinverse results (Eq. 5.17) into the above equation

$$\{\tilde{f}\} = BB^+ \{f\} = B(B^T B)^{-1} B^T \{f\} \quad (5.19)$$

where $\{ f \}$ is the designed modal control forces according to IMSC.

Application of the pseudoinverse theorem cited earlier gives

$$B = USV^T ; \quad B^T = VS^T U^T. \quad (5.20)$$

Substitution of the above equations into Eq.(5.19) yields

$$\{\tilde{f}\} = USV^T (VS^T U^T USV^T)^{-1} VS^T U^T \{f\}. \quad (5.21)$$

Considering the fact that for unitary orthogonal matrices U and V

$$UU^T = U^T U = I; \quad VV^T = V^T V = I, \quad (5.22)$$

and

$$\{\tilde{f}\} = USV^T (VS^T SV^T)^{-1} VS^T U^T \{f\}. \quad (5.23)$$

Making use of the definition of matrix S in Eq. (5.4) yields

$$S^T S = [diag(\sigma_i^2)]_{nact \times nact}; \quad (S^T S)^{-1} = [diag(1/\sigma_i^2)]_{nact \times nact} \quad (5.24)$$

$$\{\tilde{f}\} = USV^T (V[diag(\sigma_i^2)]V^T)^{-1} VS^T U^T \{f\}. \quad (5.25)$$

Because both V and $[diag(\sigma_i^2)]$ may be inverted and $V^{-1} = V^T$,

$$\{\tilde{f}\} = USV^T V[diag(1/\sigma_i^2)]V^T VS^TU^T\{f\} \quad (5.26)$$

$$\{\tilde{f}\} = US[diag(1/\sigma_i^2)]S^TU^T\{f\}. \quad (5.27)$$

Expanding $S[diag(1/\sigma_i^2)]S^T$, Eq.(5.27) becomes

$$\{\tilde{f}\} = U \begin{bmatrix} 1 & 0 & 0 & \dots & 0 & \dots & 0 \\ 0 & 1 & 0 & \dots & 0 & \dots & 0 \\ \dots & \dots & \dots & \dots & \dots & \dots & \dots \\ 0 & 0 & 0 & \dots & 1 & \dots & 0 \\ 0 & 0 & 0 & \dots & 0 & \dots & 0 \\ \dots & \dots & \dots & \dots & \dots & \dots & \dots \\ 0 & 0 & 0 & \dots & 0 & \dots & 0 \end{bmatrix} U^T\{f\}. \quad (5.28)$$

The above equation can be written as

$$\{\tilde{f}\} = \left\{ \sum_{j=1}^{nact} \sum_{k=1}^{modc} U_{ij} U_{jk} f_k \right\} \quad (5.29)$$

The Eq.(5.29) demonstrates that the realized modal control forces are linear combinations of the designed modal control forces. The realized modal control forces are determined by the actuator moments from the pseudoinverse method. This linear combination gives a minimal value of Φ as defined by Eq.(5.9).

Equation 5.28 shows a linear transformation which is a one-to-one when the rank of the transformation matrix is equal to the number of the controlled modes. However, when the transformation is not full rank, the dimension of the image vector space

will be smaller than that of the original space. This can be seen clearly in Figure 5.1. Figure 5.1 shows the design modal control force domain and the domain of the realized modal control forces by using the pseudoinverse method when one actuator is used to control the first two modes. The realized modal control forces fall within a subspace of one dimension.

5.2.3 Problems of the Pseudoinverse Solution

To demonstrate the problems of the pseudoinverse approach, a case study involving a one-actuator design: $(0.25, 0.25)$, to control the first two modes will be used. The actual control moment of the actuator is determined by using the pseudoinverse method. Figure 4.1 has shown the controlled vibrations of the first two modes when an equal number of actuators to the controlled modes is used. For comparison with Fig. 4.1, Fig. 5.2 shows the vibrations of the first two modes when using one actuator and the pseudoinverse method.

In Fig. 5.2, the vibration of the second mode is well controlled. The controlled vibration of the second mode is very close to controlled vibrations shown in Fig. 4.1 which is under the optimal control according to IMSC. However, the control over the first mode is not as satisfactory as the control over the second mode and is in fact very poor. This phenomena is not limited to this specific case. Figures 5.3 and 5.4 show cases of one actuator controlling the first three modes and two actuators controlling the first three modes, respectively. In Fig. 5.3, the control over the first mode is the poorest, and control over the second mode is poorer than the control over the third mode. In figure 5.4, the control over the second mode becomes better because one more actuator has been added, but the first mode is still poorly controlled.

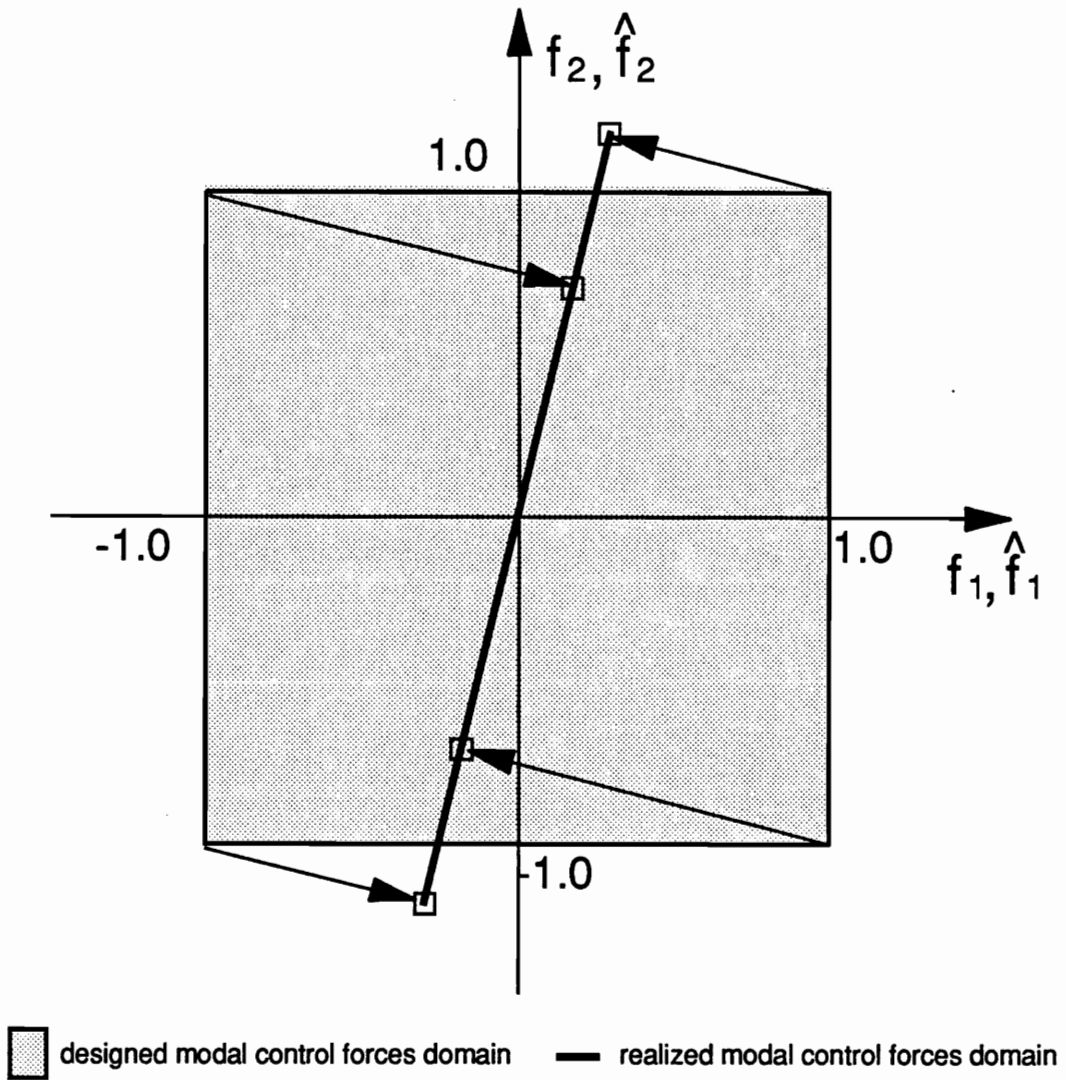


Figure 5.1: Designed modal control forces domain
 and the realized modal control forces domain
 by using pseudoinverse method
 one actuator, (0.177,0.177), controlling two modes

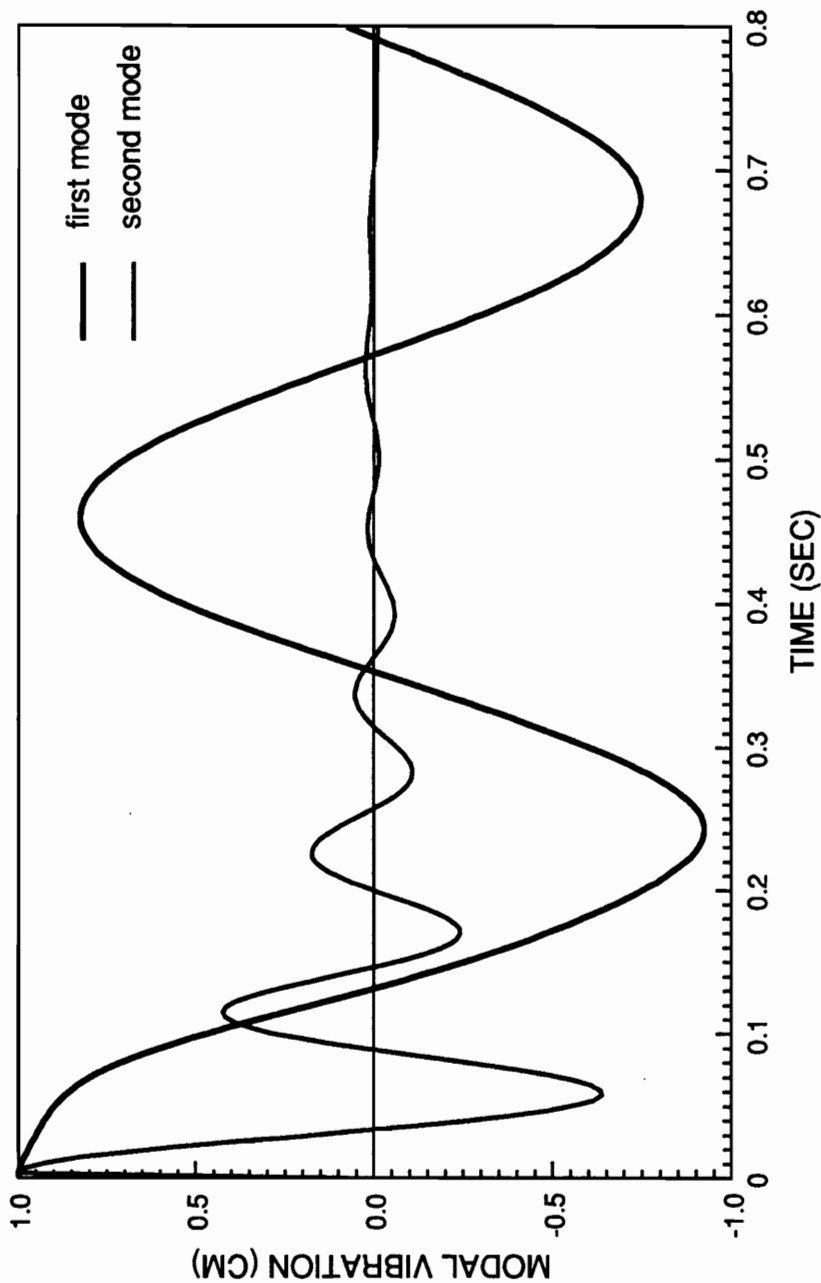


Figure 5.2: Vibrations of the first two modes when one actuator is used to control two modes, based on pseudoinverse method
Actuator design (0.25,0.25)

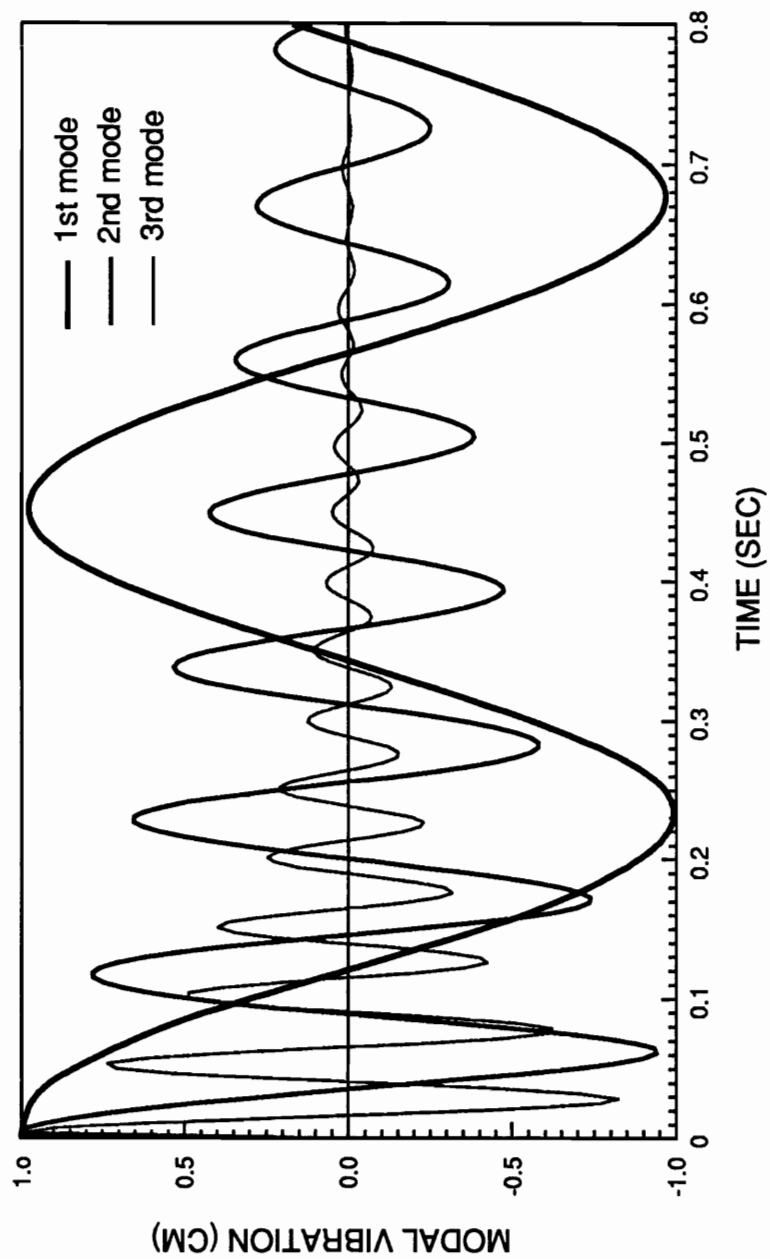


Figure 5.3: Vibrations of the first three modes when one actuator is used to control three modes, based on pseudoinverse method
Actuator design (0.177,0.177)

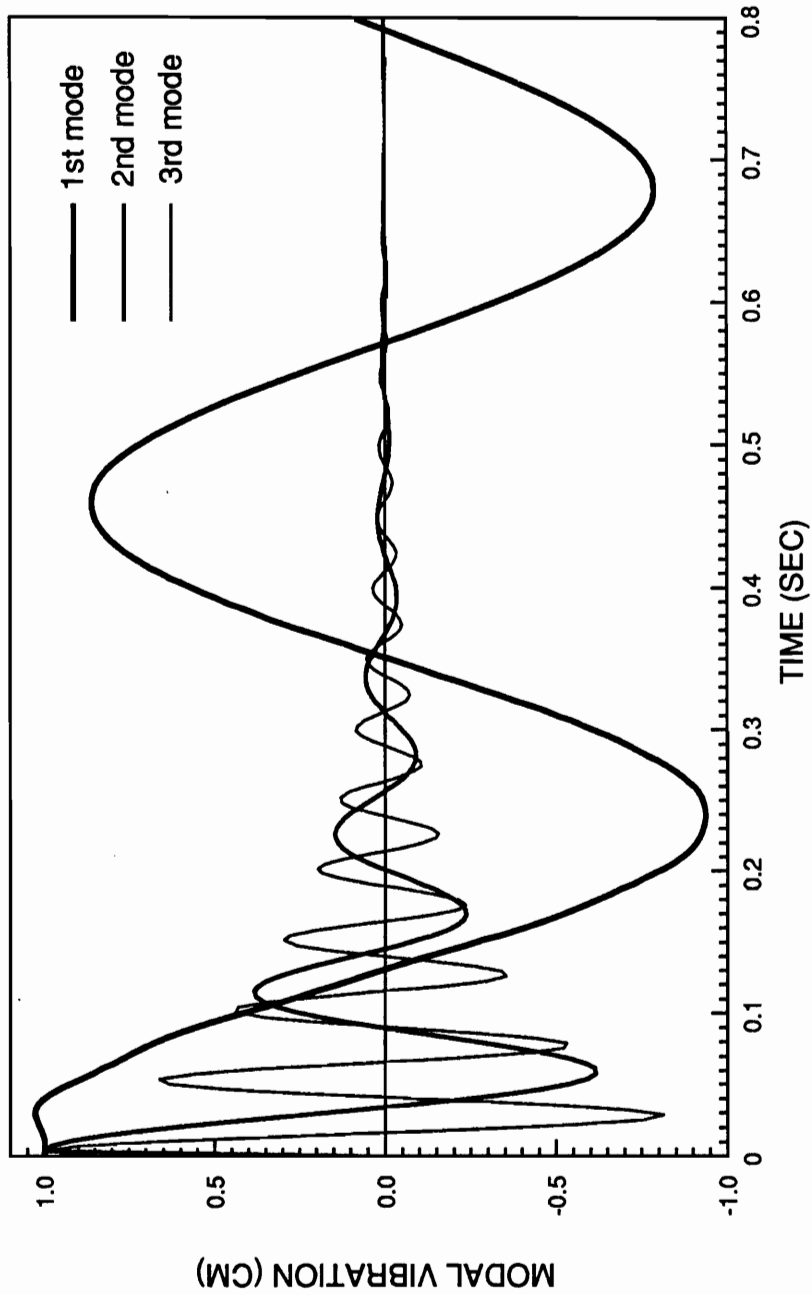


Figure 5.4: Vibrations of the first three modes when two actuators are used to control three modes, based on pseudoinverse method
 Actuator design (0.233,0.233), (0.767,0.233)

Further insight may be gained by looking at the closed-loop eigenvalues when the pseudoinverse method is used. It has been shown, in Chapter 2, that the Independent Modal Space Control determines the modal control forces which shift the closed-loop eigenvalues of the system. Because of the fact that fewer actuators can not implement these designed modal control forces, the shifts of the eigenvalues should not be the same as that of the optimal ones.

Write the Eq.(2.25) in vector form,

$$\{\ddot{u}\} + [h]\{\dot{u}\} + ([\omega] + [g])\{u\} = 0 \quad (5.30)$$

where

$$\{\ddot{u}\} = \{\ddot{u}_1, \dots, \ddot{u}_{modc}\}^T; \quad \{\dot{u}\} = \{\dot{u}_1, \dots, \dot{u}_{modc}\}^T; \quad \{u\} = \{u, \dots, u_{modc}\}^T \quad (5.31)$$

and

$$[h] = [diag(h_i)]; \quad [\omega] + [g] = [diag(\omega_i)] + [diag(g_i)]. \quad (5.32)$$

From the linear equation system, Eq.(5.30), the designed eigenvalues can be determined. In the case of fewer actuators than controlled modes, the modal control forces are given by:

$$\{\tilde{f}\} = BB^+ \{f\} = B(B^T B)^{-1} B^T \{f\}. \quad (5.33)$$

Substituting $\{f\} = -[h]\{u\} - [g]\{u\}$ into the above equation,

$$\{\tilde{f}\} = BB^+\{f\} = B(B^TB)^{-1}B^T(-[h]\{u\} - [g]\{u\}). \quad (5.34)$$

Using these approximate modal control forces, the close-loop modal vibration equations become

$$\{\ddot{u}\} + B(B^TB)^{-1}B^T[h]\{\dot{u}\} + (B(B^TB)^{-1}B^T[g] + [\omega])\{u\} = 0. \quad (5.35)$$

Where $K = B(B^TB)^{-1}B^T([g] + [\omega])$ and $C = B(B^TB)^{-1}B^T[h]$. It is shown in Appendix 1 that the eigenvalues of the above equations can be solved from

$$\begin{vmatrix} 0 & I \\ -K & -C - [diag(\lambda)] \end{vmatrix} = 0. \quad (5.36)$$

Figure 5.5 shows the comparison between the designed closed-loop eigenvalues and the closed-loop eigenvalues when using the pseudoinverse method. Figure 5.5 (a), (b), and (c) correspond to the actuator designs showed by Figs. 5.2, 5.3, and 5.4, respectively. Figure 5.2 shows the controlled modal vibrations when one actuator is used to control the first two modes; Fig. 5.3 shows the vibrations when one actuator is used to control the first three modes; Fig. 5.4 shows the vibrations when two actuators are used to control the first three modes. It can be seen that the realized eigenvalues will have a very large deviation from the designed close-loop eigenvalues when the modes are poorly controlled. For example, the first mode in all the cases has a large discrepancy from its designed counterpart.

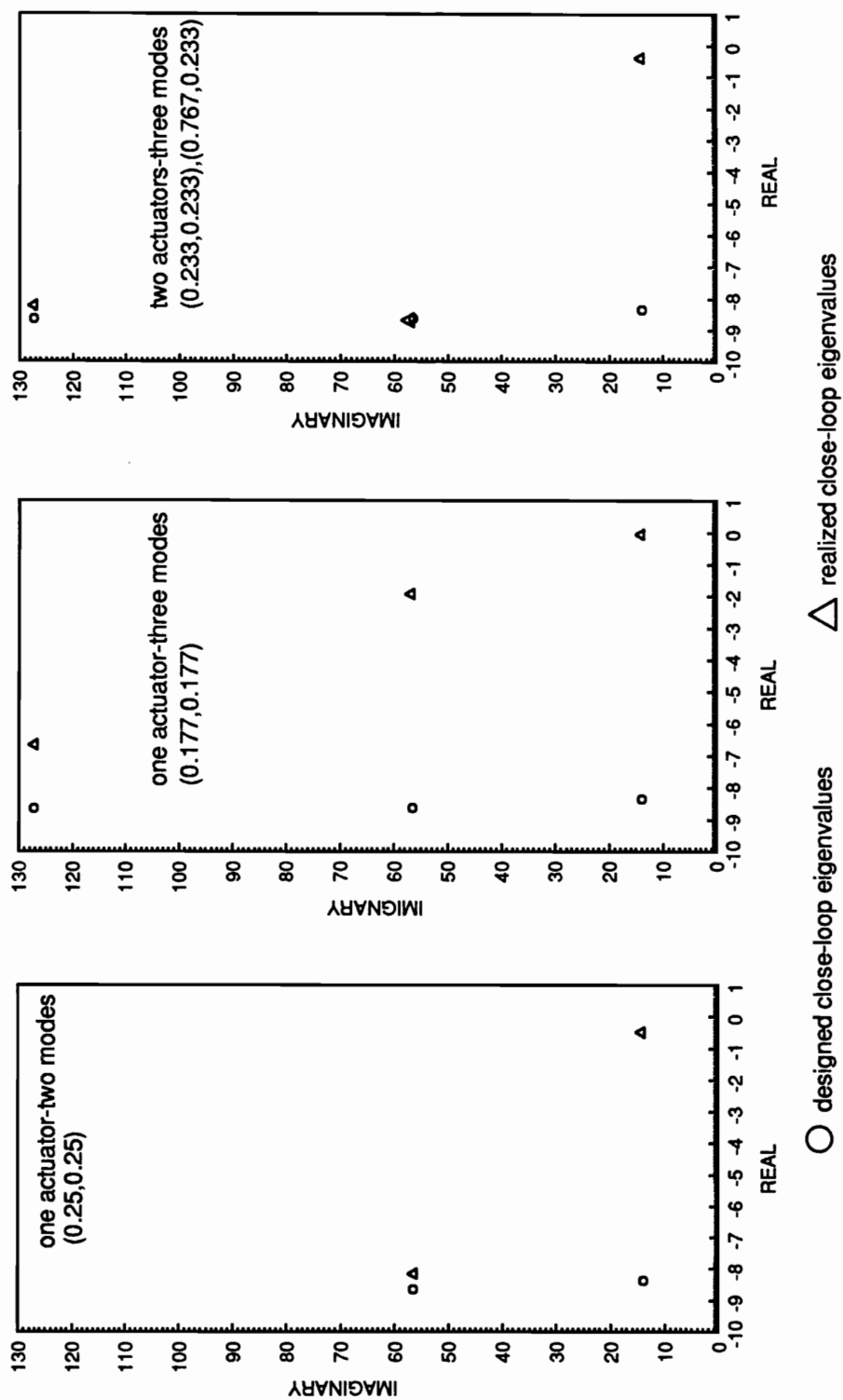


Figure 5.5: Comparison between the designed closed-loop eigenvalues and the realized closed-loop eigenvalues

5.2.4 Analysis of the Problem

The error measure used in deriving the pseudoinverse is defined as

$$\{e\} = \{\{f\} - B\{M\}\}. \quad (5.37)$$

The following scalar quantity is used as the index to be minimized to derive the pseudoinvers,

$$\{e\}^T \{e\} = \sum_{i=1}^{modc} e_i^2 \quad (5.38)$$

where $e_i = f_i - \sum_{j=1}^{nact} B_{ij} M_j$.

By letting the derivatives with respect to $\{M\}$ be equal to zero, the following linear equation systems result

$$\begin{aligned} B_{11}e_1 + B_{21}e_2 + \dots + B_{modc\ 1}e_{modc} &= 0 \\ B_{12}e_1 + B_{22}e_2 + \dots + B_{modc\ 1}e_{modc} &= 0 \\ B_{1\ nact}e_1 + B_{2\ nact}e_2 + \dots + B_{modc\ nact}e_{modc} &= 0. \end{aligned} \quad (5.39)$$

By solving the above equation, the pseudoinverse results are found for vector M . Inspecting the above equation, it can be seen that the i th error component has coefficients from the i th row of the modal participation matrix, which is calculated by Eq.(3.54), and dependent only on the i th eigenfunction. It can be shown that the values of the elements in the i th row of the modal participation matrix are always larger than those in row $i-1$. This means that the error components, which indicates the error for each corresponding mode, are treated unequally in the pseudoinverse method because of the inherent characteristics of the error formulation for this spe-

cific problem. By emphasizing certain modes in the error measure, more attention is given to those modes. This results in more control effort being given to the emphasized modes, and less effort to the other modes. Because of this characteristic, the lower modes are always poorly controlled, and the closed-loop eigenvalues of the lower modes always have larger deviations from the designed values.

5.3 Weighted Pseudoinverse Method

From the analysis in the last section, it has been shown that a problem with the pseudoinverse method is that the errors of the control over different modes are weighted differently because of special properties of the modal participation matrix. To counter this problem, a weighting matrix is proposed in constructing the error index used to find the actuator applied moments.

To avoid the problems discussed earlier with the pseudoinverse method, another error index can be constructed:

$$\Phi = \{e\}^T Q \{e\} = \{\{f\} - B\{M\}\}^T Q \{\{f\} - B\{M\}\}. \quad (5.40)$$

where Q is a diagonal weighting matrix introduced here to adjust the emphasis on each of the error components. For the convenience of later derivation, Q is represented by the product of another positive definite diagonal matrix R ,

$$Q = R R = [diag(q_i^2)] \quad (5.41)$$

where

$$R = \begin{bmatrix} q_1 & 0 & \dots & 0 \\ 0 & q_2 & \dots & 0 \\ \dots & \dots & \dots & \dots \\ 0 & 0 & \dots & q_{modc} \end{bmatrix} \quad (5.42)$$

and the elements of R are larger than 0, i.e., $q_i > 0$.

Differentiating Φ with respect to $\{M\}$ yields

$$\frac{\partial \Phi}{\partial \{M\}} = -B^T Q \{\{f\} - B\{M\}\} - \{\{f\} - B\{M\}\}^T Q B. \quad (5.43)$$

Letting

$$\frac{\partial \Phi}{\partial \{M\}} = \{0\} \quad (5.44)$$

yields the equation:

$$-B^T Q \{\{f\} - B\{M\}\} - \{\{f\} - B\{M\}\}^T Q B = \{0\} \quad (5.45)$$

which is equivalent to

$$-B^T Q \{\{f\} - B\{M\}\} = \{0\}. \quad (5.46)$$

Equation (5.46) can be further arranged into the form:

$$B^T Q B \{M\} = B^T Q \{f\}. \quad (5.47)$$

The rank of B is assumed to be *nact*. Thus B^TQB may be inverted. Therefore, the control moments can be found by

$$\{M\} = (B^TQB)^{-1}B^TQ\{f\} \quad (5.48)$$

which differs from the previous pseudoinverse solution given by Eq. (5.16). Equation (5.48) can be rewritten as

$$\{M\} = G\{f\} \quad (5.49)$$

where

$$G = (B^TQB)^{-1}B^TQ. \quad (5.50)$$

In the present study, G is named the *weighted pseudoinverse*.

5.3.1 Essence of Weighted Pseudoinverse Method

Substituting $Q=RR$ into the weighted pseudoinverse G,

$$G = (B^TRRB)^{-1}B^TRR. \quad (5.51)$$

Because R is diagonal, $R^T = R$, then

$$G = ((RB)^T(RB))^{-1}(RB)^T R. \quad (5.52)$$

By representing RB with another matrix P, i.e., $P=RB$, G can be written in the following form:

$$G = (P^T P)^{-1} P^T R = P^+ R \quad (5.53)$$

When the weighted pseudoinverse method is used, the relationship between the realized modal control forces and the designed modal control forces is

$$\{\tilde{f}\} = BG\{f\} = BP^+R\{f\} \quad (5.54)$$

where $\{f\}$ is the designed modal control forces according to IMSC. Premultiply a unit matrix, $I = R^{-1}R$, in the above equation,

$$\{\tilde{f}\} = R^{-1}R BP^+R\{f\}, \quad (5.55)$$

$$\{\tilde{f}\} = R^{-1}PP^+R\{f\}. \quad (5.56)$$

Decomposing P by using singular value decomposition

$$P = U'S'V'^T \quad (5.57)$$

where U' and V' are orthogonal matrices, and S' is the diagonal matrix consisting of the singular values. The number of nonzero singular values will still be *nact*, because the rank of P remains at *nact*. Utilizing the properties of the orthogonal matrices U'

and V' as in section 5.2.2, the following expression can be obtained

$$\{\tilde{f}\} = R^{-1}U' \begin{bmatrix} 1 & 0 & 0 & \dots & 0 & \dots & 0 \\ 0 & 1 & 0 & \dots & 0 & \dots & 0 \\ \dots & \dots & \dots & \dots & \dots & \dots & \dots \\ 0 & 0 & 0 & \dots & 1 & \dots & 0 \\ 0 & 0 & 0 & \dots & 0 & \dots & 0 \\ \dots & \dots & \dots & \dots & \dots & \dots & \dots \\ 0 & 0 & 0 & \dots & 0 & \dots & 0 \end{bmatrix} U'^T R \{f\} \quad (5.58)$$

The above equation can be written as

$$\{\tilde{f}\} = \left\{ \sum_{j=1}^{nact} \sum_{k=1}^{modc} \frac{R_k}{R_i} U'_{ij} U'_{jk} f_k \right\}. \quad (5.59)$$

It can be seen that the weighted pseudoinverse method also yields modal control forces as linear combination of the designed modal control forces. However, in the expression of the linear combinations of the weighted pseudoinverse method, a factor, $\frac{R_k}{R_i}$, is added. Intuitively, by adjusting these weighting factors, certain modal control forces can be given more or less attentions. The next step is to determine the weighting factors to arrive at the best results.

5.3.2 Determination of Q Matrix

In earlier discussions, it was shown that the pseudoinverse method has an unequal control effort distribution among the controlled modes. It also was shown that the unequal control effort distribution causes poor control over certain modes. The unequal control effort distribution is because larger deviations exist between the designed close-loop eigenvalues and the realized eigenvalues of these poorly controlled modes. Introduction of the weighted pseudoinverse method gives the capability of adjusting the control effort distributions among the controlled modes into the transformation

process of the modal control forces to actuator moments. The next step is to find the matrix Q which produces equal deviations between the optimal and non-optimal closed-loop eigenvalues of the controlled modes.

Let $\tilde{\lambda}_i$ be the realized closed-loop eigenvalues and λ_i be the designed close-loop eigenvalues. Since the eigenvalues are complex numbers, we use $Re(\lambda_i)$ to denote the real part, and $Im(\lambda_i)$ the imaginary part. The following index is used

$$\Phi_Q = \sum_{i=1}^{modc} \left[\left(\frac{Re(\lambda_i) - Re(\tilde{\lambda}_i)}{Re(\lambda_i)} \right)^2 + \left(\frac{Im(\lambda_i) - Im(\tilde{\lambda}_i)}{Re(\lambda_i)} \right)^2 \right]. \quad (5.60)$$

The objective function is then

$$Min.(\Phi_Q(Q)). \quad (5.61)$$

It should be pointed out that the determination of Q is dependent on the B matrix which is a function of the actuator locations and dimensions. Therefore, finding the optimal Q is based on the results from finding the optimal actuator designs. On the other hand, optimal actuator designs are not independent of Q . Thus an iteration process is needed to search for both the optimal q and optimal actuator designs. Figure 5.6 show the flow chart of the process.

5.4 Optimal Actuator Designs

With the application of the weighted pseudoinverse method, the transformation from designed modal control forces into the actuator moments has the form

$$\{M\} = G\{f\}. \quad (5.62)$$

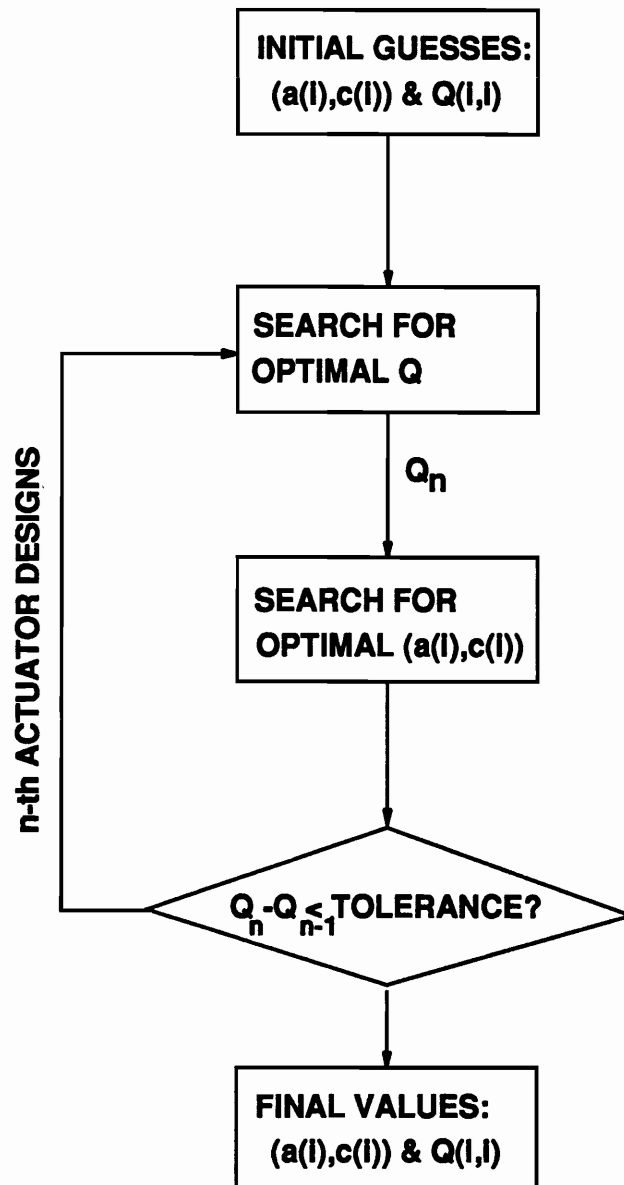


Figure 5.6: Program structure for finding the optimal Q and actuator designs

As in the case where an equal number of actuators to controlled modes are used, the norm of the actuator applied moments is constructed

$$\{M\}^T \{M\} = \{f\}^T G^T G \{f\}. \quad (5.63)$$

Utilizing singular value decomposition and properties of the unitary orthogonal matrix, the objective function for finding the optimal actuator designs based on the weighted pseudoinverse method can be derived:

$$Min.(E[\{M\}^T \{M\}]) = Min.(\sum_{i=1}^{nact} \lambda_i^2). \quad (5.64)$$

The quantities λ_i is the singular values of the matrix G . It should be noted that G is not a full rank matrix. Even though G is $modc \times modc$, the rank of G is less than or equal to $nact$.

5.5 Results and Analysis

5.5.1 Actuator Designs

Figure 5.7 shows the optimal designs for one actuator systems, using the weighted pseudoinverse method. The designs for controlling two, three, and four modes are shown when one additional work is considered the residual. It is apparent that the actuator length becomes shorter when more modes are controlled. This is because the controllable region for more modes are narrower than for fewer actuators. It can also be observed that the values of the entries in the weighting matrix, Q , decreases from $Q(1,1)$ to $Q(n,n)$, which increases the control over the lower modes.

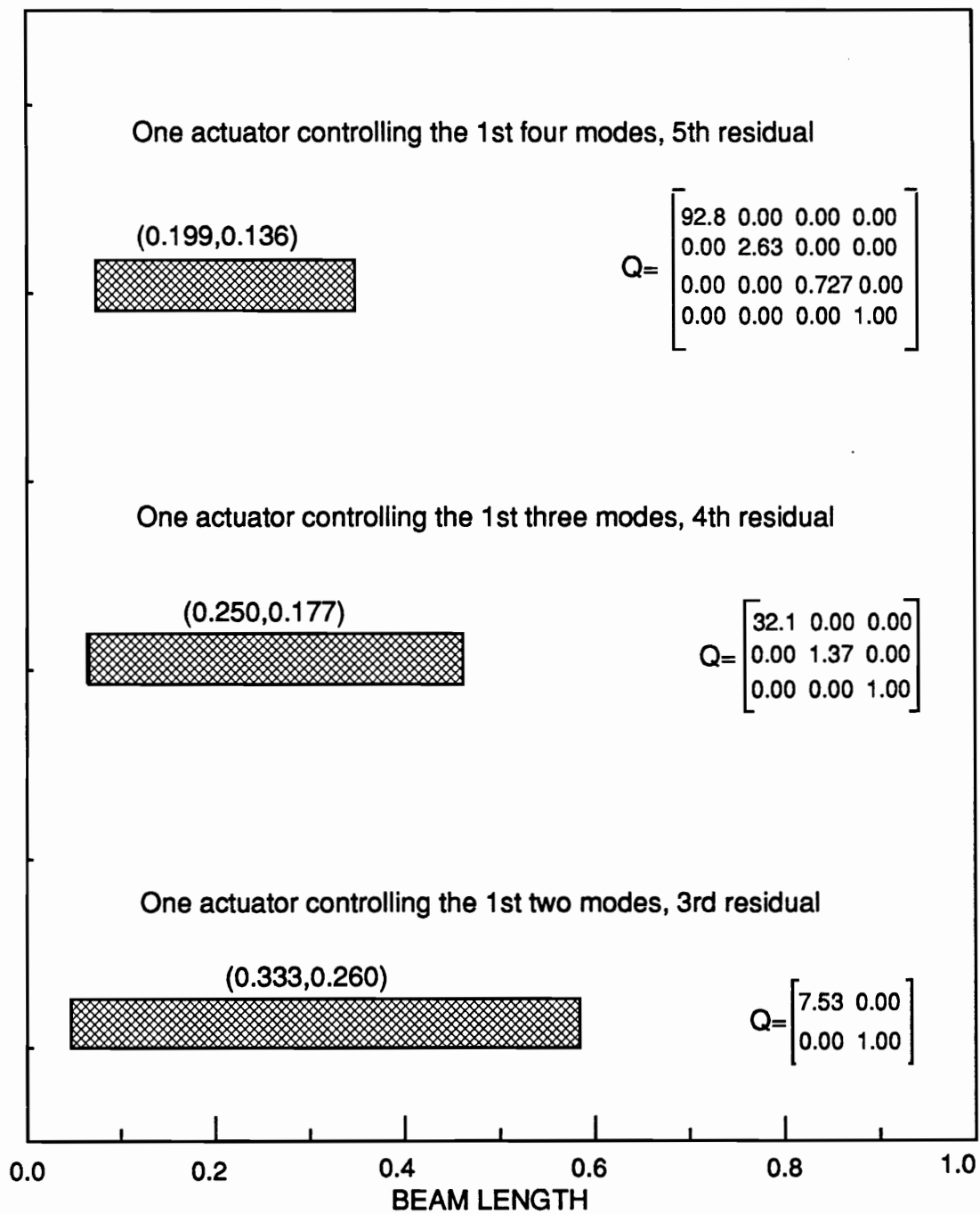


Figure 5.7: One actuator controlling more modes

Figure 5.8 shows the optimal actuator designs for two actuators using the weighted pseudoinverse method to control three, or four modes. In Fig. 5.8, one additional mode beyond the controlled modes is considered as residual. Again, it can be observed that the lengths of the actuators becomes shorter and shorter when the number of controlled modes becomes larger. The weighting matrix entries have descending values from $Q(1,1)$ to $Q(n,n)$.

Figure 5.9 (a) shows the controlled modal vibrations when one actuator is used to control the first two modes. For comparison, the controlled modal vibration are shown in figure 5.9 (b) when pseudoinverse method is used. From figure 5.9 (a) and (b), it can be seen that the extremely poorly controlled first when using pseudoinverse method are well under control by utilizing weighted pseudoinverse.

Figure 5.10 demonstrates the actuator moments. The darker line represents the results by utilizing the weighted pseudoinverse method. The lighter line represents the actuator moments when pseudoinverse method is used. It can be noticed that the control moments for weighted pseudoinverse are smaller than the control moments for pseudoinverse for a period of time in the beginning. Then the weighted gives larger control moments than pseudoinverse does. In weighted pseudoinverse method, the actuator applied moments are synthesized from the modal control forces of the control modes by equal percentage. Therefore, the modes are equally controlled in pseudoinverse method. But because each mode is given equal percentage of the control effort, the control force over each of them is only corresponding percent of the designed modal control force. In pseudoinverse method, the second mode is given more control effort than equal share. Thus the second mode is controlled quickly. Generally, the modal control forces for the second mode is larger than the control

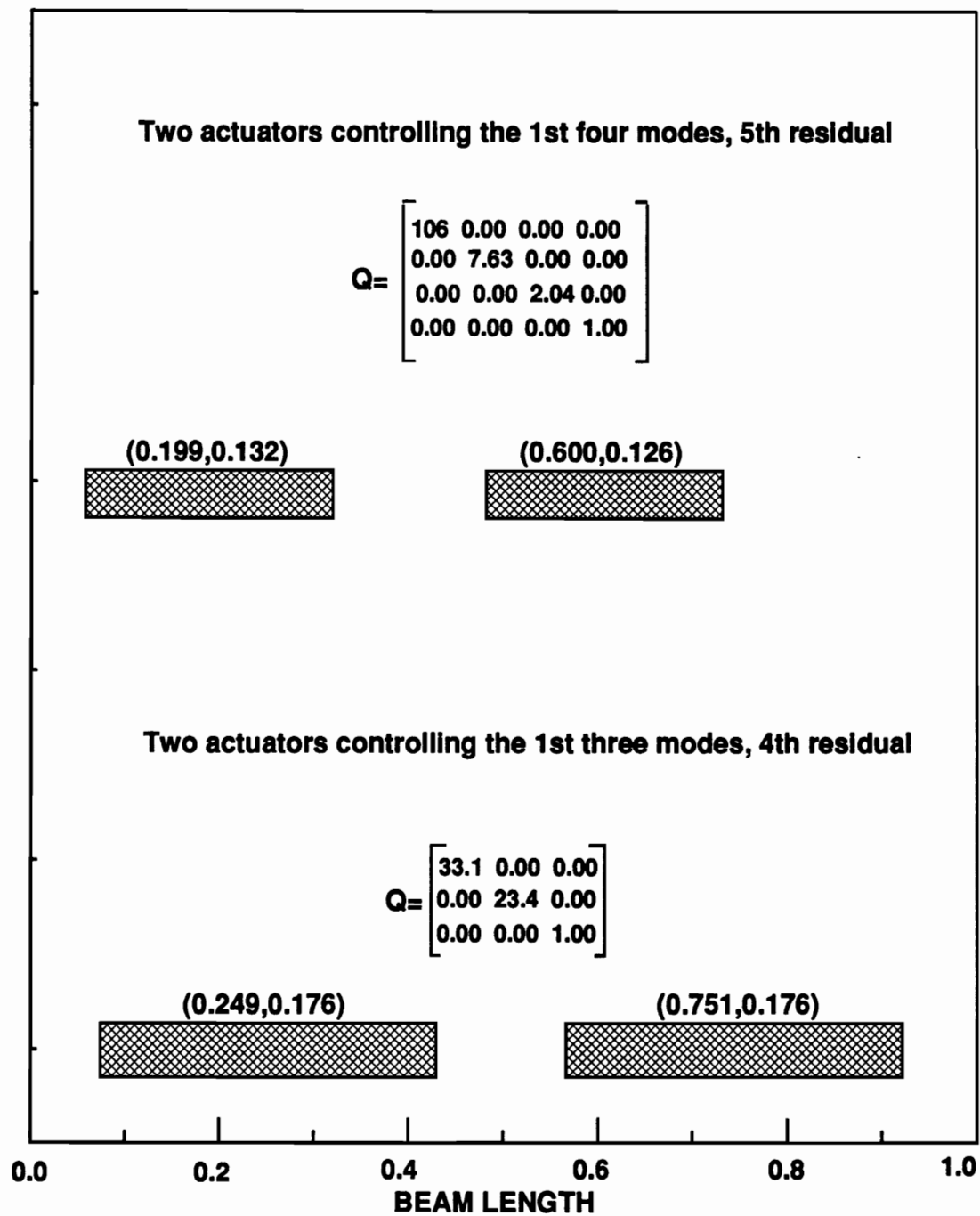
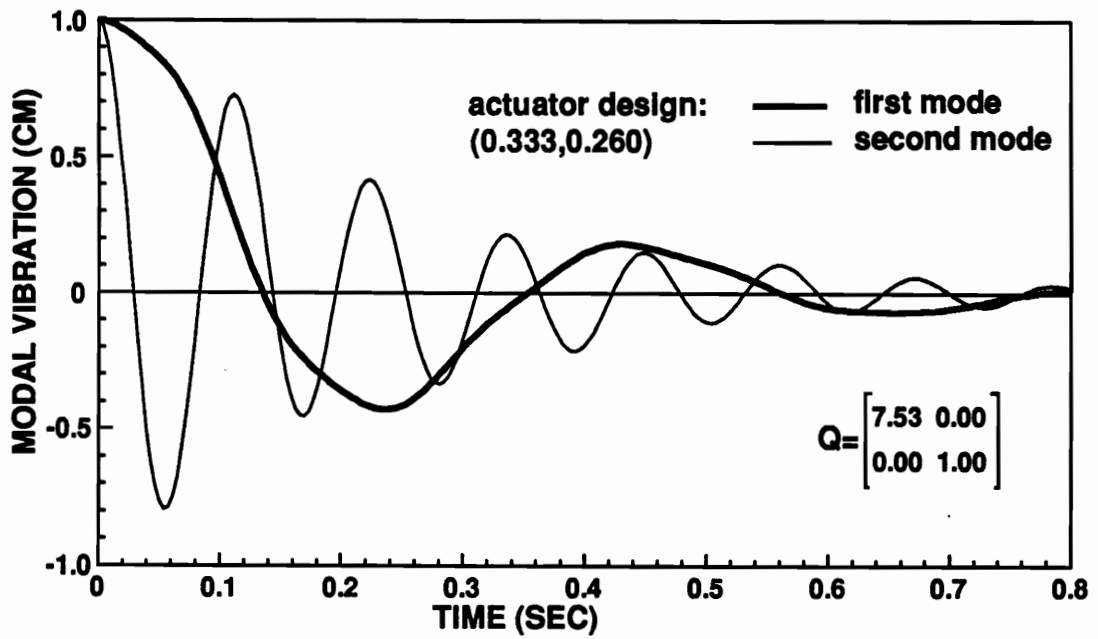
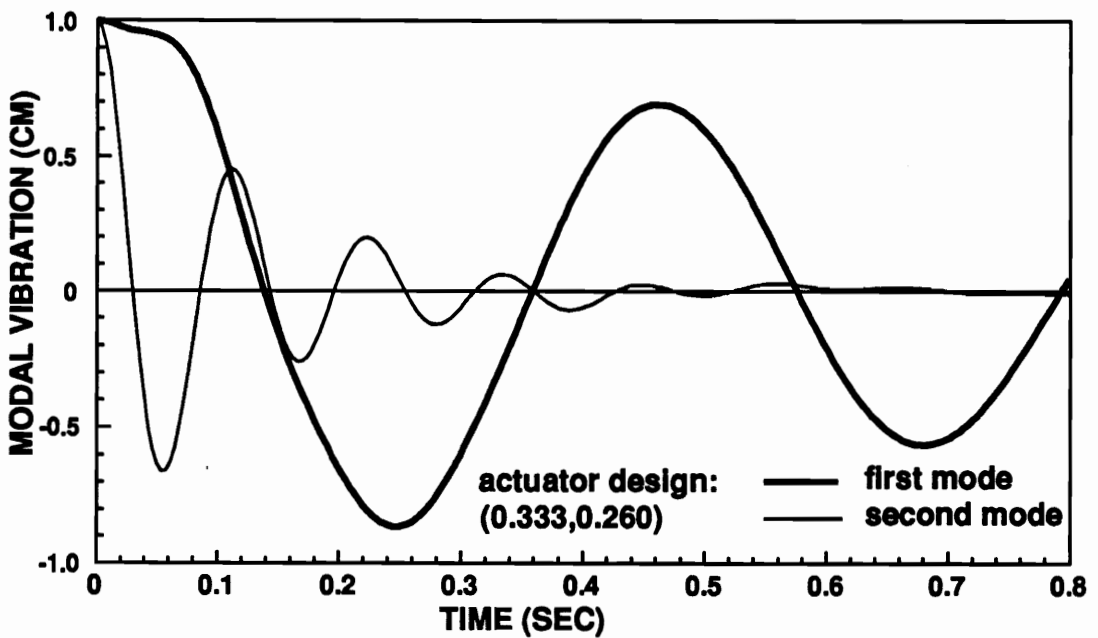


Figure 5.8: Two actuators controlling several modes



a) Weighted pseudoinverse method



b) Pseudoinverse method

Figure 5.9: Controlled modal vibrations of weighted pseudoinverse and pseudoinverse methods

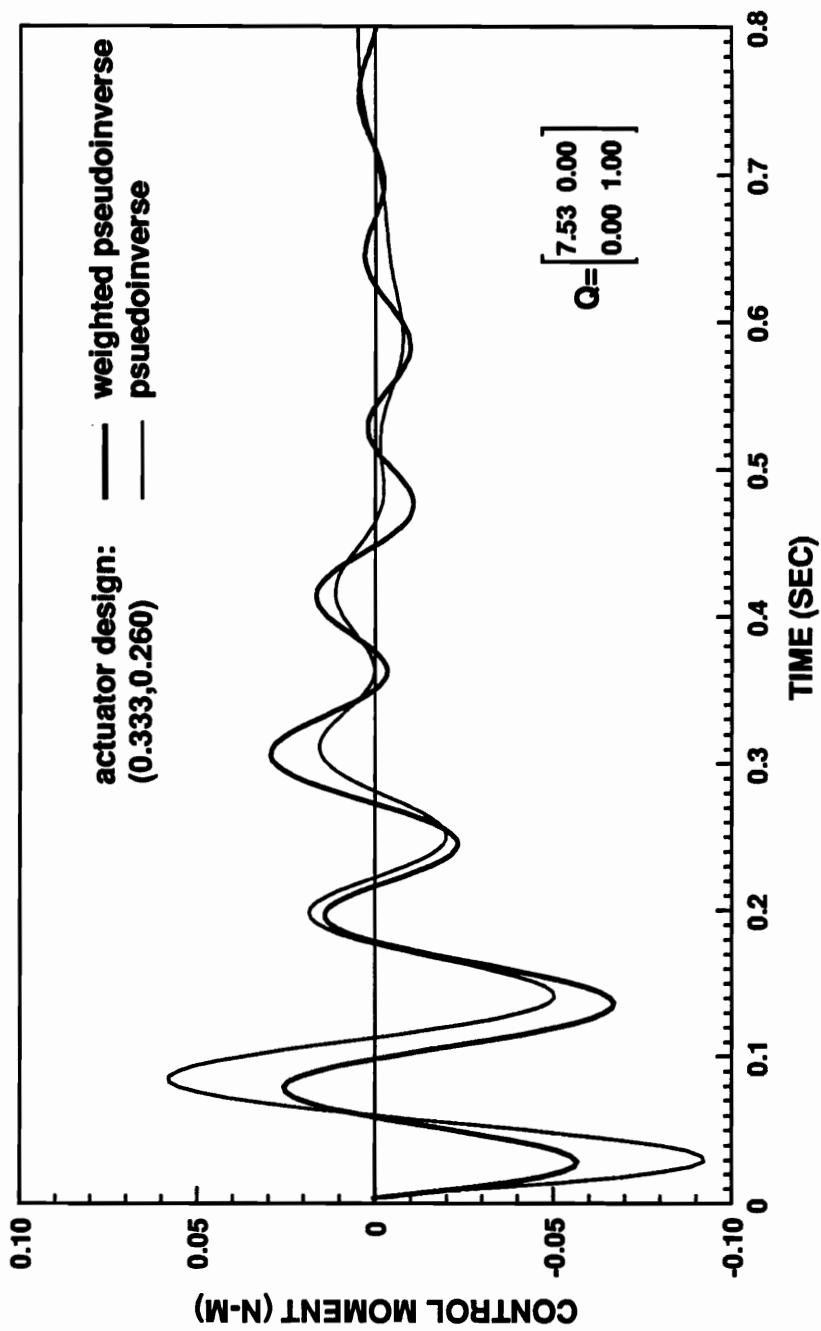


Figure 5.10: Comparison of actuator applied control moments by using weighted pseudoinverse and pseudoinverse methods

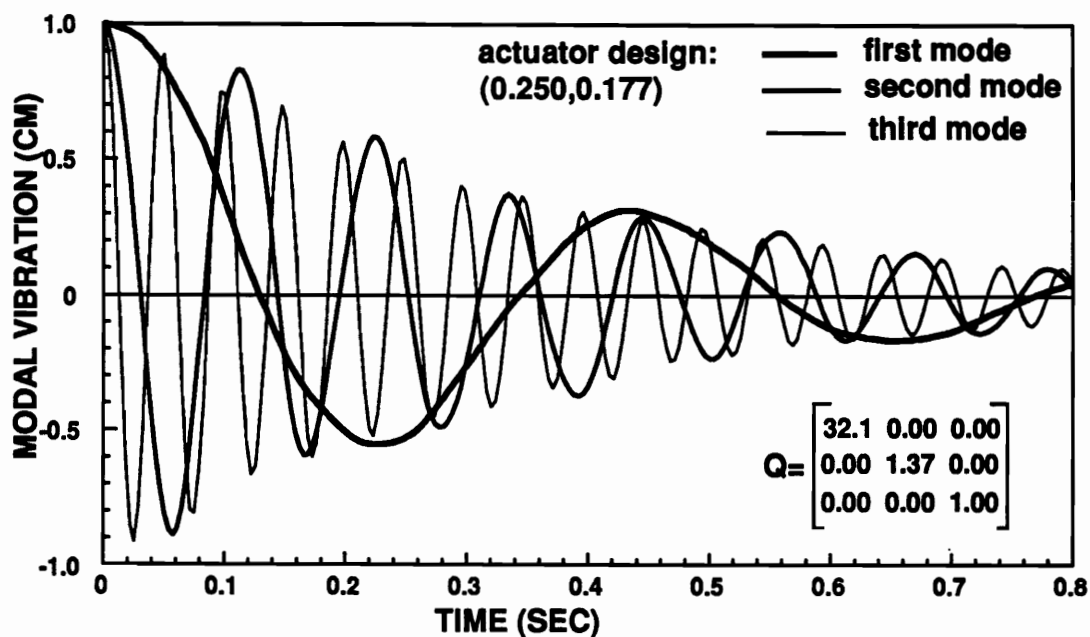
force of the first mode. Therefore, the control moments for pseudoinverse, when control effort is given to the second mode in the starting period of time, are larger than the control moments of the weighted pseudoinverse method. After the second mode is under control, only a small portion of the first modal control forces is reflected in the actuator control moment. However, in weighted pseudoinverse method, the control over both of modes are stretched over the process, which explains why the control moments of weighted pseudoinverse are larger than the control moments by using pseudoinverse method.

In figure 5.11, the modal vibrations of the first three modes, in one actuator systems, are shown. Figure 5.11 (a) shows the weighted pseudoinverse method. Figure 5.11 (b) shows the results from pseudoinverse. Figure 5.12 demonstrates the actuator moments by using the two different methods. Figure 5.11 shows the same trend of comparison between the actuator control moments by using weighted pseudoinverse and pseudoinverse.

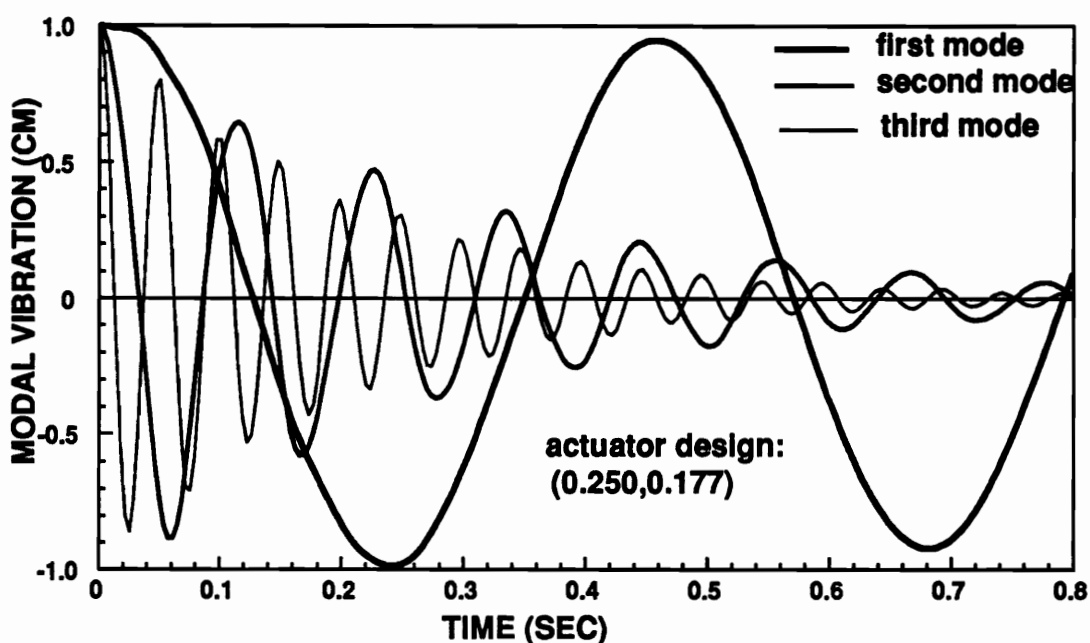
In two actuator systems, some results are shown in figure 5.13 and figure 5.14. The actuator control moments are smoothed out throughout the control process by weighted pseudoinverse method. The sharp peaks in pseudoinverse method are avoid in weighted pseudoinverse method.

5.5.2 Closed-Loop Eigenvalues

As shown in figure 5.5, some of the closed-loop eigenvalues by pseudoinverse deviates very much from the designed closed-loop eigenvalues. Figure 5.15 shows the closed-eigenvalues by using weighted pseudoinverse method. It can be observed that the distance between the designed and realized closed-loop eigenvalues are evenly



a) Weighted pseudoinverse method



b) Pseudoinverse method

Figure 5.11: Controlled modal vibrations when weighted pseudoinverse and pseudoinverse method are used under the same Initial conditions

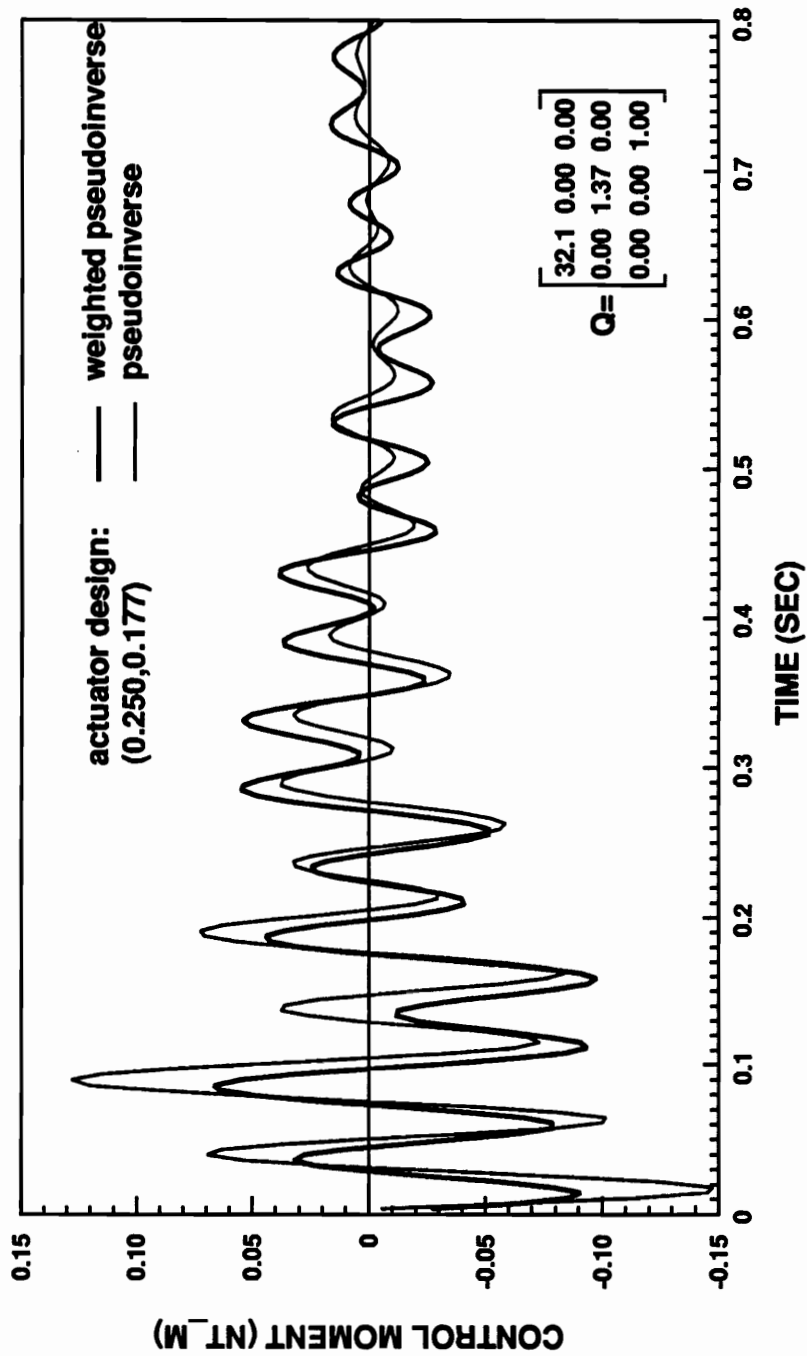
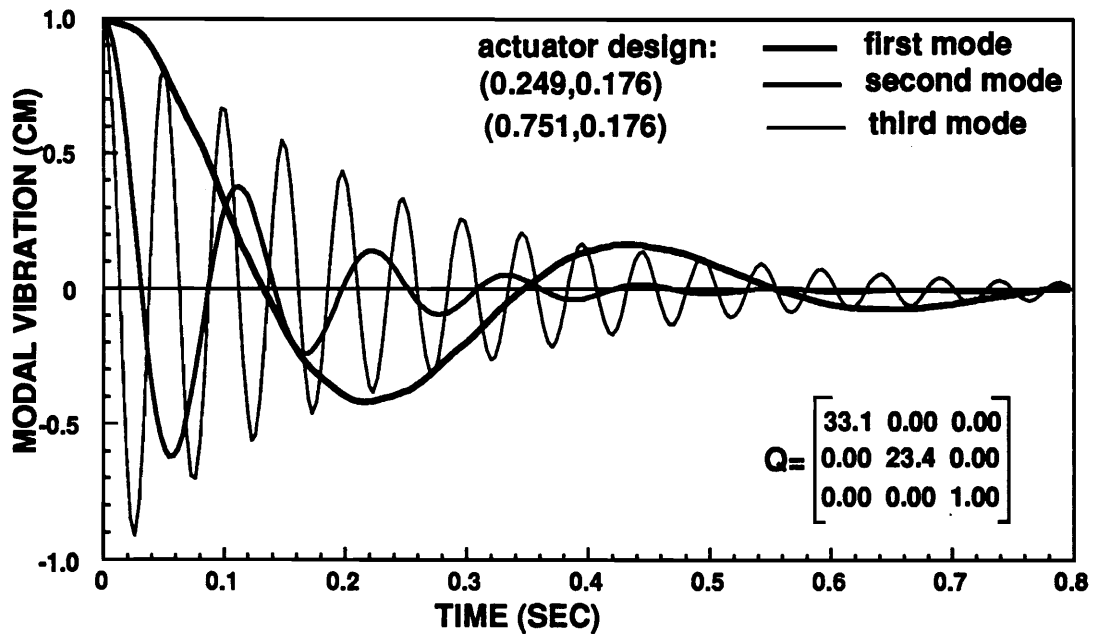
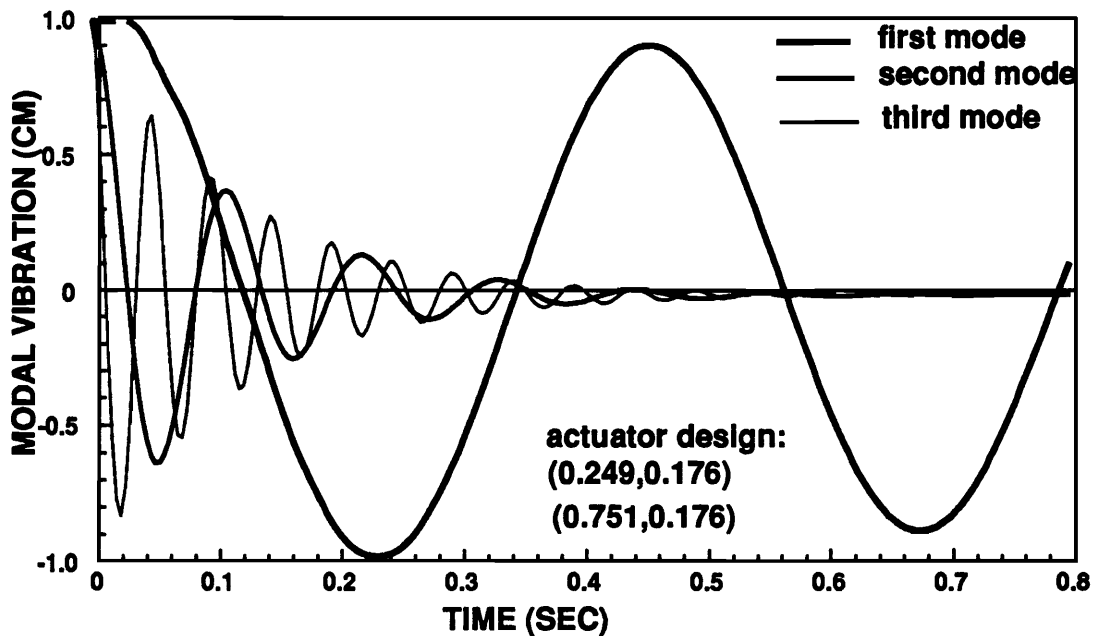


Figure 5.12: Comparon of actuator applied control moments by using
weighted pseudoinverse and pseudoinverse method

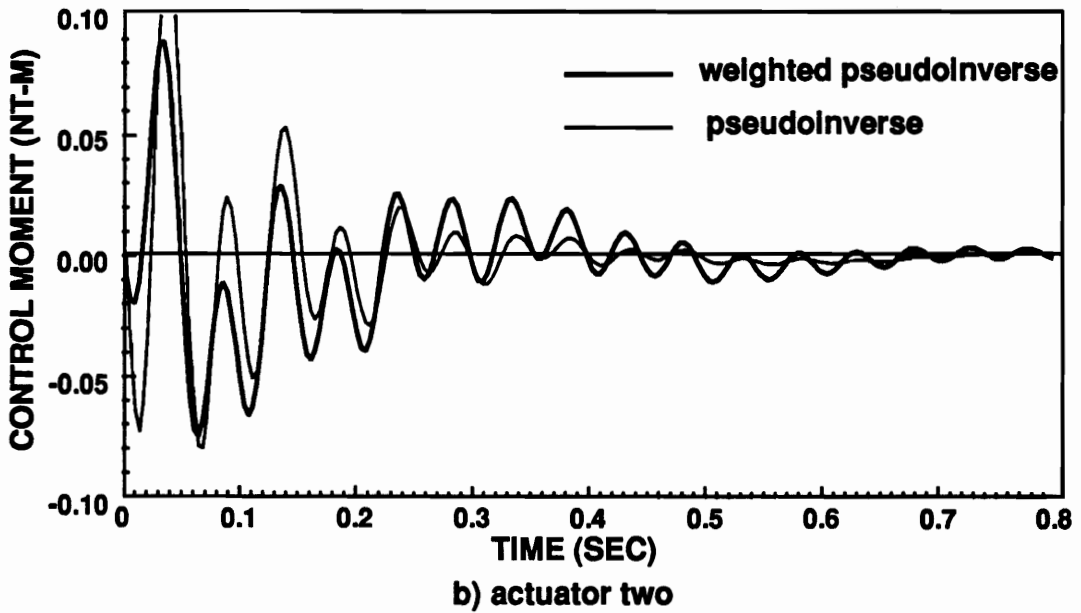
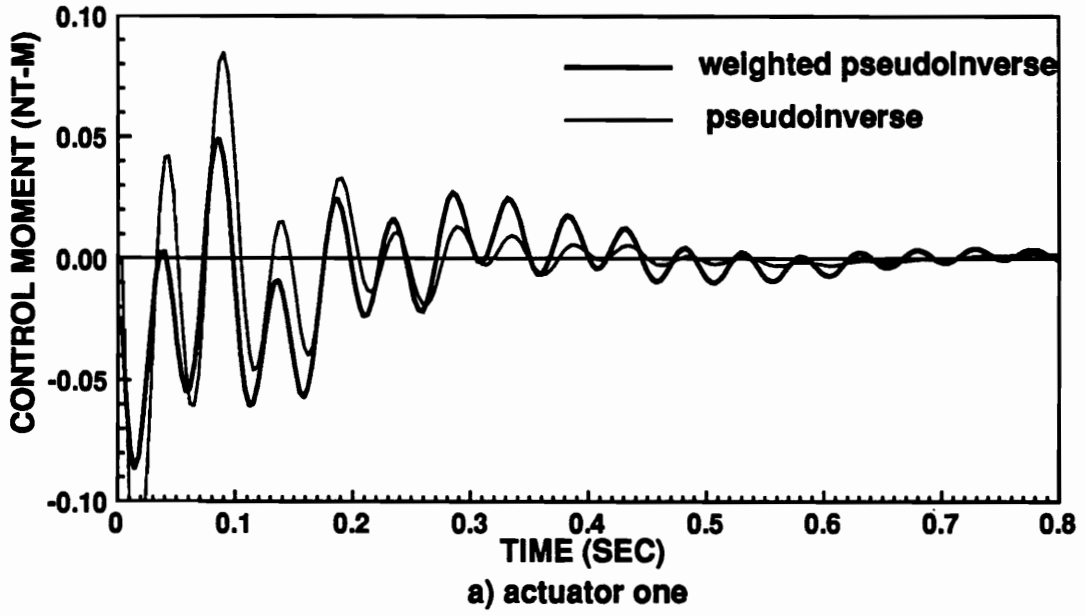


a) Weighted pseudoinverse method



b) Pseudoinverse method

Figure 5.13: Controlled modal vibrations when weighted pseudoinverse and pseudoinverse methods are used



actuator design:
 (0.249,0.176), (0.751,0.176)

$$Q = \begin{bmatrix} 33.1 & 0.00 & 0.00 \\ 0.00 & 23.4 & 0.00 \\ 0.00 & 0.00 & 1.00 \end{bmatrix}$$

Figure 5.14: Comparison of actuators applied moments according to weighted pseudoinverse and pseudoinverse method

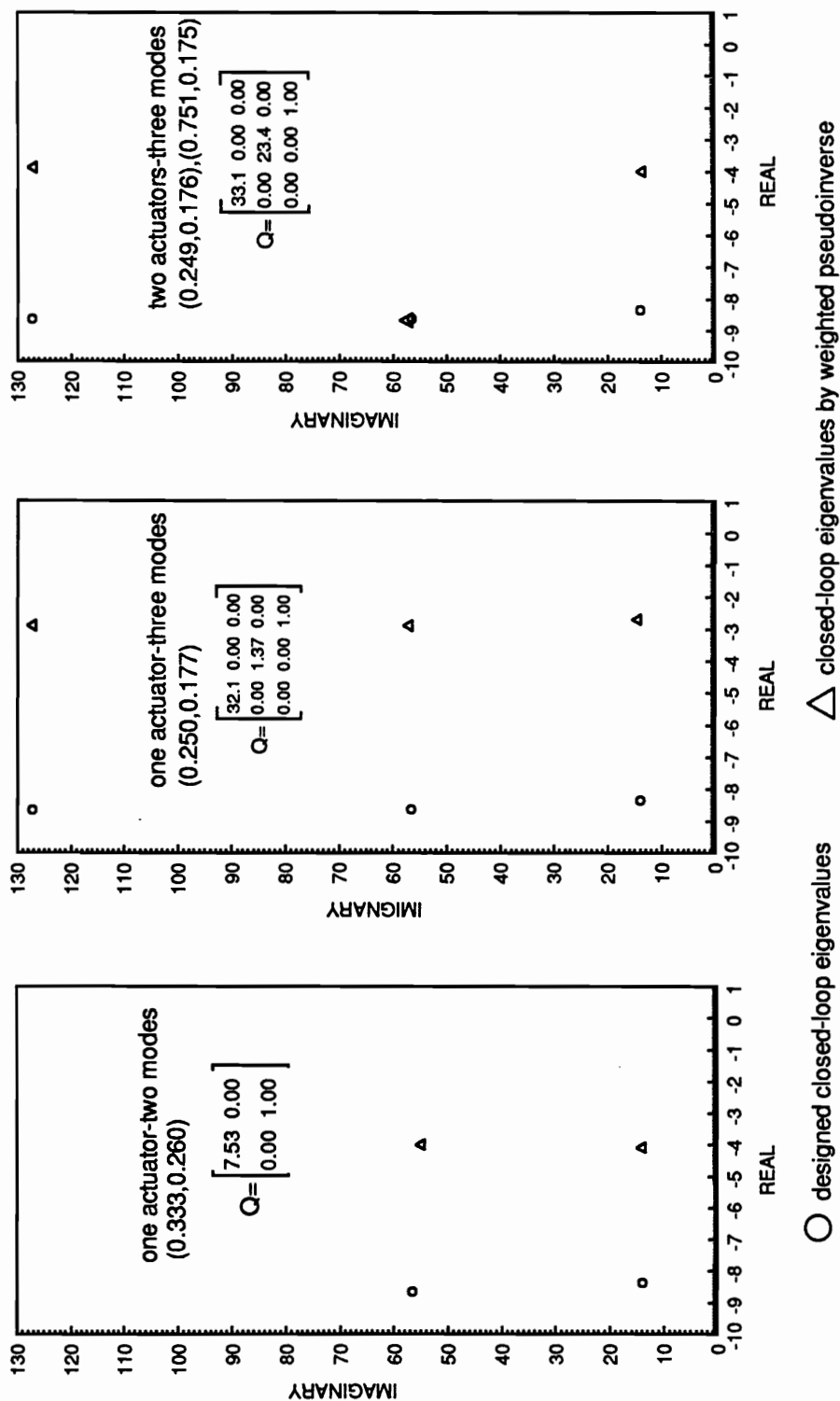


Figure 5.15: Comparison between the designed closed-loop eigenvalues and the closed-loop eigenvalues by using weighted pseudoinverse

distributed. The even deviations from the designed closed-loop eigenvalues guaranty the equal control over the control modes. In figure 5.15 (a) and (b), it can be observed that weighted pseudoinverse method does not change the imaginary value of the closed-loop eigenvalues. For one actuator controlling two modes, weighted pseudoinverse gives half of the designed value in the real axis. When controlling modes, one third of the designed value in real axis is given. In two actuator case, which is shown in figure 5.15 (c), second closed-eigenvalue is kept the same as the designed; the first and the third have the same imaginary value as the designed closed-eigenvalues and halve of the designed real value.

5.5.3 Modal Control Forces Domains

It has been pointed out that, when fewer actuators are used, the realized modal control forces constitute a subspace of the designed actuator control moments. The subspace has fewer dimensions than the original space. Figure 5.16 shows the designed modal control forces domain and the realized modal control force domains by using weighted pseudoinverse and pseudoinverse method, respectively. It can be observed that the realized modal control forces are tilted toward f_2 more, when pseudoinverse is used, than when weighted pseudoinverse method is used. The tilt angle demonstrates why first mode gets more control when weighted pseudoinverse method than when pseudoinverse method is used.

Utilizing the weighted pseudoinverse bears its disadvantages. Figure 5.17 shows that there will be control forces applied to the modes which are not vibrating. Rewrite

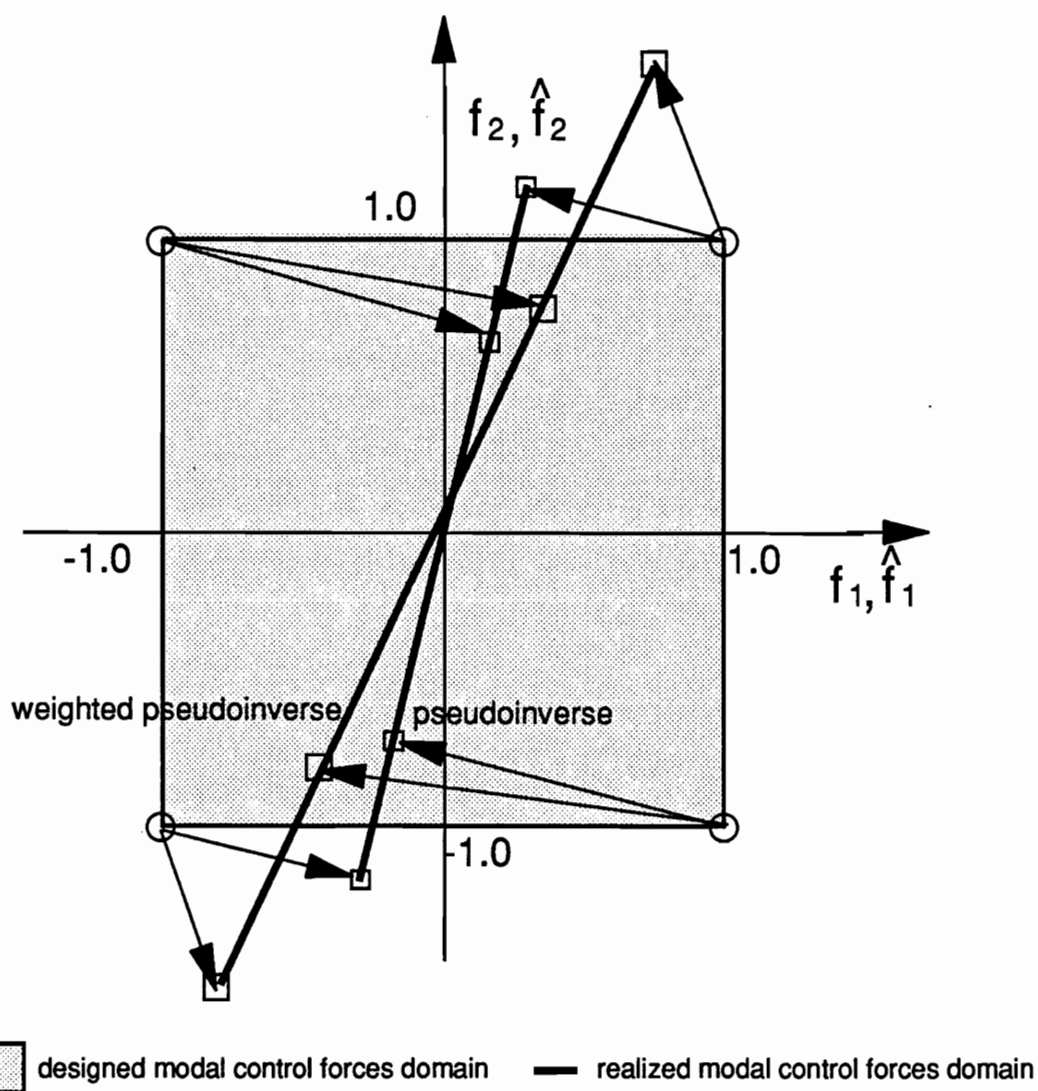
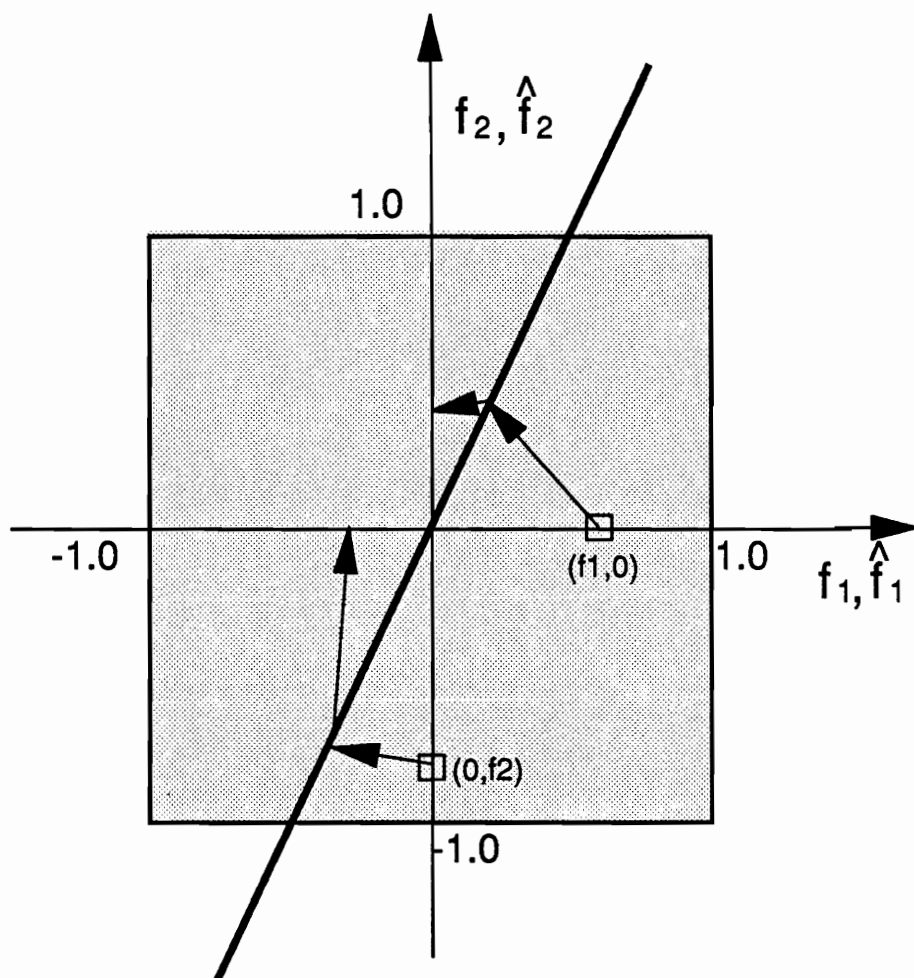


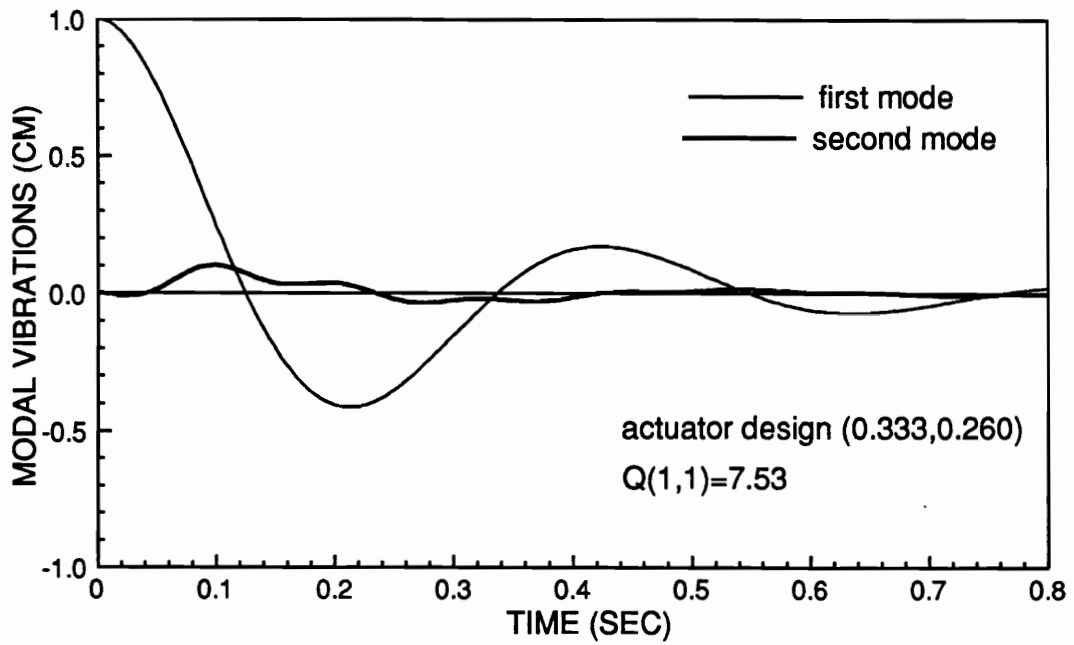
Figure 5.16: Designed modal control forces domain and the realized modal control forces domain by using pseudoinverse method one actuator, (0.177,0.177), controlling two modes



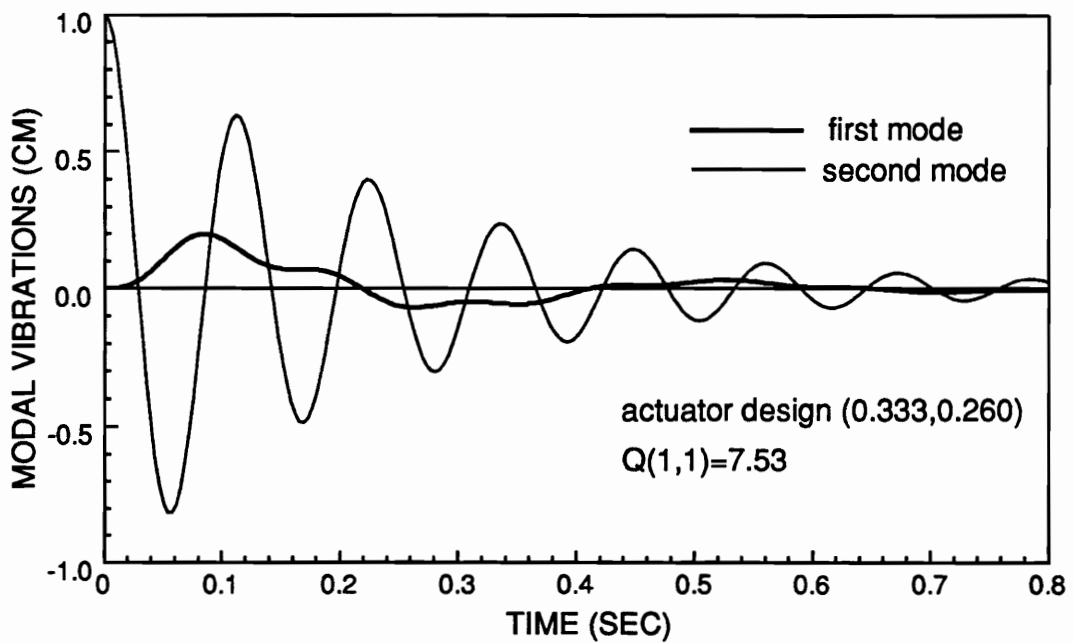
designed modal control forces domain

 realized modal control forces domain

Figure 5.17: The control over each of the modes will spillover into the other modes when pseudoinverse or weighted pseudoinverse method is used



a) spillover into the second mode



b) spillover into the first mode

Figure 5.18: The spillover problem when fewer actuators are used

Eq. (5.?)

$$\{\tilde{f}\} = \left\{ \sum_{j=1}^{nact} \sum_{k=1}^{modc} \frac{R_k}{R_i} U'_{ij} U'_{jk} f_k \right\}. \quad (5.65)$$

It can be observed that \tilde{f}_i will not be zero, even if f_i is zero. This is very much like a spillover problem, and more serious. Figure 5.18 demonstrates the control excited modal vibrations when the weighted pseudoinverse method is used. The excited vibrations have to be controlled, which needs extra control effort.

Chapter 6

CONCLUSIONS AND RECOMMENDATIONS

6.1 Conclusions

Two major conclusions can be drawn from this study:

- Approaches for optimally designing piezoelectric actuators in vibration control systems for flexible structures have been formulated; the results of using the proposed approaches both with or without spillover considerations are shown to be very effective by numerical simulation.
- The weighted pseudoinverse method has been proposed. Combined with optimization procedures for finding optimal Q matrix, this method can effectively alleviate the actuator number requirements by IMSC.

This study did some preliminary work to constitute the foundation for further investigation of optimal design of piezoelectric actuators in vibration control systems.

6.2 Discussions and Recommendations

An approach to optimizing the piezoelectric actuators has been presented in this study. This approach is suitable to the vibration suppression systems. The specific

cases of beam like structures has been used as example to demonstrate the results of the optimal designs. In more complex structures, what will be needed is approximate eigenfunctions from the discretized model of the structure. The approaches in this study will be appropriate in applications in any other systems. However, the computation time could be dramatically increased if the discretized structure mode are used. In the discretized model, the structure eigenfunctions needed to be solved for each optimization step. A great deal of efforts should be given to reach the least time consuming computation algorithm.

The mechanical model of piezoelectric actuators in this study has sufficient accuracy for many applications. For better precision, a more accurate nonlinear actuator model can be used.

Dealing with two dimensional structures may be one of the research tasks following this study. Expansion of the approach in this study into two dimensional structures, will require quite large amount of work in the optimization formulation. In two dimensional case, the characterization of the piezoelectric actuators needs dimensions, shapes, and orientations. Defining a set of appropriate parameters to describe the actuators will be the first step. The formulation of constraints on the actuators, such as non-overlay, within the structural boundaries, etc., is the second step in the optimization formulation. The actuators can be limited to be some specific shapes, such as squares, rectangular, etc., to simplify the problem.

The statistical model used in this study is relatively simple. A better way is to obtain the probability distribution with respect to the initial modal displacements and velocities by experiments under the working circumstances. The statistical derivation will

be base on the experimental data. Designs thus obtained will suit the real problem better.

Sensing system, which is an equal important part in the system, is not studied in this research. Piezoelectrics can also be used as sensors. The piezoelectric sensor designs are subject to optimization to yield best results. At the same time, there will be structural constraints applied on the piezoelectric sensors. Therefore, system designs need to optimized by taking into consideration of the piezoelectric actuators and sensors together.

REFERENCES

Anderson, E. H., and E. F. Crawley, 1989, "Piezoelectric Actuator of One- and Two-Dimensional Structures", MIT Report, SSL #5-89.

Bailey, T., and J. E. Hubbard Jr., 1985, "Distributed Piezo-electric Polymer Active Vibration Control of a Cantilever Beam", *Journal of Guidance and Control*, Vol. 8, Sept.-Oct., pp. 605-611.

Balas, M. J., 1982, "Trends in Large Space Structure Control Theory: Fondest Hopes, Wildest Dreams", *IEEE Transaction on Automatic Control*, Vol. AC-27, No. 3, pp. 522-535.

Baruh, H., and L. Meirovitch, "On the Placement of Actuators in the Control of Distributed-Parameter Systems", *AIAA Paper 81-0638*, pp. 611-620.

Baz, A., and S. Poh, 1988, "Performance of an Active Control System with Piezo-electric Actuators", *Journal of Sound and Vibration*, Vol. 126, No. 2, pp. 327-343.

Cady, W. G., 1964, **Piezoelectricity**, Dover, New York.

Cooper, L., and D. Steinberg, 1970, **Introduction to Method of Optimization**,

W. B. Saunders Company.

Cross, L. E., *et al.*, 1980, "Electrostrictive Behavior of Lead Magnesium Niobatebased Dielectrics", *Ferroelectrics*, 1980, Vol. 27.

Crawley, E. F., and J. de Luis, 1987, "Use of Piezoelectric Actuators as Elements of Intelligent Structures", *AIAA Journal*, Vol. 25, No. 10, pp.1373-1385.

Forward, R. L., 1981, "Electronic Damping of Orthogonal Bending Modes in a cylindrical mast-experiment", *Journal of Spacecraft*, Vol. 18, pp.11-17.

Foesythe, G. E., and C. B. Moler, 1967, "Today's Method of Linear Algebra", *SIAM Rev.*, pp.489-515.

Fuller, C. R., Rogers, C. A., and H. H. Robertshaw, 1989, "Active Structure Acoustic Control with Smart Structures", *Proceedings of SPIE Conference 1170 on Fiber Optical Smart structures and Skins II*.

Haftka, R. T., and M. P. Kamat, 1985, **Elements of Structural Optimization**, Martinus Nijhoff Publishers.

Halmos, P. R., 1974, **Finite-Dimensional Vector Spaces**, Springer-Verlag New York Inc.

Henry, E. C., 1969, **Electronic Ceramics**, Doubleday & Company, Inc.

Hohn, E. F., 1964, **Elementary Matrix Algebra**, The Macmilan Company, New York.

Im, S., and S. N. Atluri, 1989, "Effects of a Piezo-Actuators on a Finitely Deformed Beam Subjected to General Loading", *AIAA Journal*, Vol. 27, No. 12, pp. 1801-1807.

Jaffe, B., 1971, **Piezoelectric Ceramics**, Academic Press, New York.

Juang, J. N., and G. Rodriguez, 1979, "Formulations and and Applications of Large Structure Actuator Sensor Placements", *Proceedings of the Second VPI&SU Symposium on Dynamic and Control of Large Flexible Spacecraft*, pp.247-262.

Kavlie, D., and J. Moe, 1971, "Automated Design of Frame Structures", *ASCE Journal of Structure Div.*, 33-62.

Kirk, E. D., 1970, **An Introduction to Optimal Control Theory** Prentice-Hall.

Hissel, G. J., and J. G. Lin, 1982, "Spillover Prevention via Proper Synthesis/Placement of Actuators and Sensors", *Proceedings of 1982 A. C. C.*, Vol. 3, pp. 1213-1218.

Lawson, C. L., 1974, **Solving Least Squares Problems**, Prentice-Hall, Inc.

Liang, C. A., Rogers, C. A., and C. R. Fuller, 1989, "Acoustic transmission/Radiation Analysis of Shape Memory Alloy Reinforced Laminate Plates," accepted for publication by *Journal of Sound and Vibrations*.

Lindberg, R. E., Jr., 1982, "Optimization of Actuator Placement via Degree of Controllability Criteria Including Spillover Consideration", *AIAA-paper 82-1435*.

Longman, R. W., and K. T. Alfrend, 1981, "Actuator Placement from Degree of Controllability Criteria for Regular Slewing of Flexible Spacecraft", *AIAA-paper 82-1435*.

Mason, W. P., 1971, "Fifty Years of Ferroelectricity", *The Journal of the Acoustical Society of America*, Vol. 50, No. 5, pp.1281-1298.

Meirovitch, L., 1967, **Analytical Methods in Vibrations**, The Macmiclan Co., New York, NY.

Meirovitch, L., 1980, **Computational Methods in Structural Dynamics**, Sijthoff-Noordhoof Co., Alphen aan den Rijn, The Netherland.

Meirovitch, L., and H. F. Vanlandingham, 1977, "Control of Spinning Flexible Spacecraft by Modal Synthesis", *Acta Astronautica*, Vol. 4, No. 9-10, pp.985-1010.

Meirovitch, L., and H. Baruh, 1981a, "Optimal Control of Damped Flexible Gyroscopic Systems", *Journal of Guidance and Control*, Vol. 4, No. 2, pp.157-163.

Meirovitch, L., and H. Baruh, 1981b, "Control of Self-Adjoint Distributed-Parameter Systems", *Journal of Guidance*, Vol. 5, No. 1, pp.60-66.

Meirovitch, L., H. Baruh, and H. Oz, 1983, "A Comparison of Control Techniques dor Large Flexible Systems", *Journal of Guidance and Control*, Vol. 6, No. 4, pp.302-310.

Mendenhall, W., 1986, **Mathematical Statistics with Applications**, Duxbury Press, Boston.

Poh, S., and Baz, A., "Active Control of a Flexible Structure Using a Model Positive Position Feedback Controller", *To be published*.

Rogers, C. A., 1988, "Novel Design Concepts Utilizing Shape Memory Alloy Reinforced Composites," *Proceedings of the American Society for Composites 3rd Technical Conference on Composite materials*, Technomic Publishing Co., Seattle, September.

Rogers, C. A., Liang, C., and J. Jia, 1989, "Behavior of Shape Memory Alloy Reinforced Composites-Part I: Model Formulation and Concepts," *Proceedings of the 30th Structures, Structural Dynamics, and Materials Conference*, Mobile, AL, April 3-5, 1989.

Rogers, C. A., Liang, C., and J. Jia, 1989, "Behavior of Shape Memory Alloy Reinforced Composites-Part I: Results," *Proceedings of the 30th Structures, Structural Dynamics, and Materials Conference*, Mobile, AL, April 3-5, 1989.

Tharja, R., and R. T. Haftka, 1985, "NEWSUMT-A: A Modified Version of NEWSUMIT for Unequality and Equality Constraints", *VPI Report 148*.

Toda, M., 1978, "Electromotional Device Using PVF2 Multilayer Bimorph", *Transactions of the Institute of Control Engineers of Japan*, E61, pp.507-512.

Viswanathan, C. N., and R. W. Longman, 1979, "A definition of the Degree of Controllability - A Criterion for Actuator Placement", *Proceedings of 2nd VPI&SU/AIAA Symposium on Dynamics and Control of Flexible Spacecraft*, June, 1979, pp. 369-384.

Wilkinson, J.H., 1965, **The Algebraic Eigenvalues Problem**, Clarendon Press, Oxford.

APPENDIX A: EIGENVALUES OF DAMPED SYSTEMS

Let $\{x\}$ be a vector of dimension n . The equations of motion of n degrees of freedom system, with mass matrix M , damping matrix C , and stiffness matrix K , are:

$$M\{\ddot{x}\} + C\{\dot{x}\} + K\{x\} = \{0\} \quad (6.1)$$

Assume

$$\{x\} = \{X\}e^{\lambda t}, \quad (6.2)$$

where λ is a complex number. Differentiate Eq.(2),

$$\{\dot{x}\} = \lambda\{X\}e^{\lambda t} = \lambda\{x\} \quad (6.3)$$

Rewrite the equations of motion in the following form

$$-M^{-1}(C\{\dot{x}\} + K\{x\}) = \lambda\{\dot{x}\} \quad (6.4)$$

Combining the Eqs.(3) and (4), we have

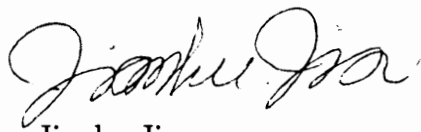
$$\begin{bmatrix} 0 & I \\ -M^{-1}K & -M^{-1}C \end{bmatrix} \begin{Bmatrix} x \\ \dot{x} \end{Bmatrix} = \lambda \begin{Bmatrix} x \\ \dot{x} \end{Bmatrix} \quad (6.5)$$

here I is unit matrix. The eigenvalues of the system can be solved from the matrix

$$\begin{bmatrix} 0 & I \\ -M^{-1}K & -M^{-1}C \end{bmatrix} \quad (6.6)$$

VITA

The author was born on November 15, 1962 in Hebei Province, China. He went to Nanjing Aeronautical Institute, Nanjing, China, where he received his BS in Mechanical Engineering in February, 1982. From February, 1982 to November of 1985, he worked as a research and reaching assistant in Nanjing Aeronautical Institute. He received his M.S. in Mechanical Engineering of Virginia Polytechnic Institute and State University in November of 1987 and then began his Ph.D program in the same department. His degree of Ph. D was completed in July of 1990, in Mechanical Engineering Department of Virginia Polytechnic Institute and State University.

A handwritten signature in cursive script, appearing to read 'Jianhu Jia'.

Jianhu Jia